POLITECNICO DI MILANO
Master's Degree in Computer Science Engineering
Department of Electronics and Computer Science Engineering

The Study of the Electromyographic Signal for the Control of a Prosthetic Hand

AI & R Lab
Artificial Intelligence and Robotics
Laboratory of Politecnico di Milano

Supervisor: Prof. Giuseppina Gini
Assistant supervisor: Ing. Dario Cattaneo

Master's thesis of:
Giuseppe Lisi, registration number 732932

Academic Year 2009-2010

To my family

Abstract

The design of a prosthetic device, able to reproduce the functions of a real human hand, is characterized by many challenges. The ideal prosthesis would be easy to control, comfortable to wear and aesthetically pleasing. This thesis is concerned with finding solutions to the first of the three objectives mentioned above.
The EMG control is the most used approach in todays prosthetic devices, because it is noninvasive compared with other methods. Its goal is to create an association between a predefined set of hand motion patterns and the corresponding EMG signals generated by the forearm muscles. In this way the classifier mounted on the prosthetic hand is able to recognize a muscle contraction and sends to the controller the command to reproduce the correspondent hand movement.
The system designed in the current work is composed by many modules, which process the signals detected by a 3-channel EMG acquisition board. The first one is the segmentation module, which is able to understand when a muscle contraction, also referred to as signal burst, starts and ends. The second module is the features extractor, which, applied to each individual burst, extracts from it some representative parameters in the time-frequency domain, by the application of the Continuous Wavelet Transform (CWT). This generates a large matrix, which must be reduced by applying the Singular Value Decomposition (SVD). The feature extractor also computes two temporal parameters which are then concatenated to the result of the SVD, to form the feature vector representing to the burst.
An Artificial Neural Network is then trained to associate each feature vector with the corresponding hand movement. In particular the system learns how to classify 7 different movements, with a performance of 98-100%.
Eventually, the influence of some factors on the performance of the system is discussed, namely the displacement of the electrodes from the original training position, the patient's fatigue, body structure, concentration, motivation and training level.

Sommario

La mano è la parte terminale dell'avambraccio e le sue funzioni la rendono un organo molto importante del corpo umano. Può essere utilizzata per adempiere ad una vasta quantità di compiti come afferrare oggetti, toccare, percepire stimoli, manipolare, comunicare e tanti altri.
E' facile comprendere come la perdita dell'arto superiore possa avere conseguenze significative nella vita di una persona, sia da un punto di vista funzionale che da quello psicologico: dopo l'evento traumatico essa non sarà più in grado di eseguire gesti e movimenti che prima erano un tramite naturale verso l'ambiente esterno.
Per aiutare una persona amputata a recuperare, in qualche modo, alcune delle funzionalità ormai perse, l'approccio più comune è quello di sostituire l'arto amputato con una protesi artificiale. Purtroppo al giorno d'oggi, gli impianti protesici, sia robotizzati che no, sono affetti da molti problemi, come bassa controllabilità, poche funzionalità e estetica scadente, il che li rende ben lontani dall'essere quegli oggetti biomimetici a cui tutti noi aspiriamo.
Questa tesi si prefissa una serie di obiettivi: il primo è quello di eseguire uno studio interdisciplinare dello stato dell'arte del mondo delle protesi di arto superiore, non solo da un punto di vista tecnologico, ma anche medico, psicologico e biologico in generale; tale studio è funzionale al secondo obiettivo, quello di progettare un sistema in grado di percepire la volontà dell'amputato e controllare una protesi robotica di conseguenza; terzo ed ultimo obiettivo è quello di capire come diversi fattori, fisiologici e no, possano influenzare le prestazioni del sistema progettato.

Il Sistema Biologico della Mano Come detto in precedenza, uno degli obiettivi di questo lavoro è quello di creare un sistema che sia in grado di percepire contrazioni muscolari a livello dell'avambraccio e di controllare una protesi robotica di conseguenza. Al fine di realizzare tale progetto è, prima, necessario comprendere il sistema mano, la sua anatomia, i muscoli

che lo movimentano e i relativi processi che ne regolano le contrazioni.
In secondo luogo si mostrano le principali qualità della mano reale, che la rendono un modello da imitare nella costruzione di una sua replica artificiale:

- la maggior parte dei muscoli che movimentano le dita e il polso sono posizionati fuori dalla mano stessa, il che la rende leggera e non ingombrante;
- è dotata di un gran numero di sensori estero e propriocettivi, più sensibili rispetto a quelli nel resto del corpo, in tal modo il cervello è in grado di mappare costantemente lo stato della mano e dell'ambiente che la circonda;
- il suo controllo viene eseguito in maniera gerarchica dal cervello, nel senso che la pianificazione dei gesti rimane ad un livello di gerarchia più alto ed è generalmente sotto il controllo della persona, mentre il coordinamento di tutte le contrazioni muscolari al fine di eseguire quei determinati movimenti avviene a livello più basso (inconscio).

Protesi di Mano: lo Stato dell'Arte I ricercatori che lavorano nel campo delle protesi pongono le necessità degli amputati al primo posto. È importante capire quali sono le priorità di una persona durante la sua giornata, in quanto non tutti gli schemi motori possono essere riprodotti dalle tecnologie allo stato dell'arte.
Innanzitutto, l'impatto psicologico è uno degli aspetti più importanti da considerare quando si tratta di protesi. Gli amputati di arto superiore tendono a rifiutare qualsiasi tipo di impianto protesico, soprattutto se questo non viene applicato nei primi trenta giorni dall'amputazione. Questo rende necessario l'affiancamento di uno psicologo che permetta di tenere sotto controllo il recupero del paziente. Inoltre, per far si che i tempi di applicazione della protesi siano i più brevi possibile è necessario che i medici che eseguono le operazioni chirurgiche post traumatiche, procedano secondo un protocollo ben definito.
La mano artificiale ideale dovrebbe essere facile da controllare, comoda da indossare ed esteticamente piacevole, tutte caratteristiche che le protesi commerciali allo stato dell'arte non posseggono o posseggono solo in parte. Prendendo a modello la mano reale, la ricerca scientifica si sta concentrando su interfacce uomo-protesi più intuitive, che permettano anche di fornire un certo feedback all'utente. Altri campi d'interesse riguardano l'affidabilità nel controllo, la destrezza, l'antropomorfismo e la cosmetica della mano.
La tesi si concentra sulla prima delle aree di ricerca menzionate in preceden-

za, l'interfaccia uomo-protesi. Il controllo delle protesi robotiche moderne è comunemente basato sull'analisi del segnale elettromiografico, in quanto si tratta di un approccio poco invasivo rispetto ad altri metodi. Quello che viene fatto è progettare dei classificatori in grado di imparare associazioni tra un insieme predefinito di schemi motori della mano e i corrispondenti segnali elettrici generati dalla contrazione dei muscoli dell'avambraccio. In questo modo il classificatore montato sulla protesi è in grado di riconoscere una contrazione muscolare e di mandare al controllore il movimento corrispondente da eseguire. Questo obiettivo viene normalmente raggiunto con l'applicazione di metodi statistici e di analisi nel dominio tempo-frequenza, accoppiati con potenti classificatori come le Reti Neurali Artificiali o le Support Vector Machines. Allo stato dell'arte i migliori approcci di classificazione hanno ottenuto performance del 99.5% sul riconoscimento di 4 schemi motori, del 98% su 6 schemi motori, e del 93.54% su 8, utilizzando più di tre canali di acquisizione.

Il Segnale Elettromiografico La comprensione del segnale elettromiografico, delle sue caratteristiche principali e dei metodi di analisi comunemente applicati ad esso, è molto importante, in quanto gran parte di tali aspetti sono funzionali alla fase di progetto.
L'unità funzionale elementare del muscolo è chiamata Unità Motoria ed è composta da un α-motoneurone e le fibre muscolari corrispondenti che esso innerva. Nel momento in cui il cervello comanda una contrazione muscolare, gli α-motoneuroni inviano degli impulsi nervosi alle fibre muscolari sotto il loro diretto controllo.
Degli elettrodi posizionati sulla cute dell'avambraccio sono in grado di rilevare il potenziale di questi impulsi, che sommandosi danno vita al segnale elettromiografico (EMG). Essendo la somma di impulsi che avvengono in istanti di tempo leggermente diversi l'uno dall'altro, il segnale EMG è da considerarsi come un processo stocastico.
L'acquisizione di questo segnale biologico, le cui componenti in frequenza primarie variano tra i 10 e 200 Hz , può essere contaminata principalmente in tre modi: gli elettrodi si muovono generando dei disturbi in bassa frequenza; l'attivazione di altri muscoli interferisce con quella che vogliamo rilevare (cross-talk); fonti esterne come la frequenza di rete si sommano al segnale. Per superare il primo dei problemi elencati è sufficiente applicare un filtro passa alto (10 Hz), il secondo problema invece viene affrontato basandosi sulla reiezione al modo comune fornita dagli elettrodi in configurazione bipolare, mentre il terzo problema non è risolvibile in quanto la frequenza

di rete (50 Hz) è anche una importante componente spettrale del segnale stesso.
Un altro fattore notevole è l'affaticamento muscolare, infatti quando un muscolo viene sforzato nel tempo lo spettro si sposta verso le basse frequenze e aumenta la sua ampiezza. Questo rende il segnale non-stazionario, il che ha delle ripercussioni importanti nella scelta dei metodi di analisi da applicare in fase di elaborazione.
Possibili metodi per comprendere quando una contrazione muscolare inizia e finisce ed analizzarne la forza corrispondente, consistono nella rettificazione e l'inviluppo lineare del segnale EMG.

Il Progetto Il sistema progettato nel presente lavoro, acquisisce il segnale EMG per mezzo di tre canali (6 elettrodi), posizionati in modo distribuito attorno all'avambraccio. Una volta che queste coppie di elettrodi (configurazione bipolare) hanno rilevato i segnali dai rispettivi muscoli, una scheda di acquisizione EMG si occupa della loro amplificazione e filtraggio.
Il prossimo passo è quello di capire quando ogni contrazione (burst) inizia e finisce, per fare questo viene applicato un particolare metodo di segmentazione. Infatti, dal momento che i segnali provengono da tre fonti diverse, la segmentazione della contrazione è caratterizzata da problemi di parallelismo. L'approccio seguito è quello di rettificare e inviluppare il segnale originale, per estrarne il contorno. In seguito si applica un sistema di sogliatura dinamica che permette di suddividere ogni burst secondo le direttive del canale che, per quella determinata contrazione, ha rilevato la forza più elevata.
Dopo la segmentazione, ogni singolo burst viene analizzato utilizzando la Continuous Wavelet Transform (CWT) che ne estrae una grande matrice rappresentativa, composta da valori nel dominio tempo-frequenza. Questa matrice viene poi elaborata con il metodo della Singular Value Decomposition, al fine di estrarne le informazioni principali e quindi di ridurne le dimensioni. Il vettore ottenuto viene poi concatenato a due parametri temporali, che sono l'integrale e la media del segnale EMG rettificato, ottenendo così il vettore definitivo rappresentante il burst.
Tenendo presente che ogni movimento viene rilevato da tre canali, il vettore di feature che lo rappresenterà sarà costituito dalla concatenazione dei vettori rappresentativi dei tre burst provenienti dai tre canali. Quindi per ogni schema motorio della mano, si acquisiscono i segnali EMG, che vengono segmentati ed elaborati con i metodi descritti in precedenza per ottenere il vettore di feature corrispondente. L'obiettivo è insegnare ad una Rete Neurale Artificiale a riconoscere 7 diversi movimenti della mano e questo viene

fatto allenandola ad associare ad ognuno di essi il corrispondente vettore di feature.

Risultati Per poter analizzare la capacità di adattamento del sistema, esso è stato testato su più di una persona: 4 soggetti sani sono stati sottoposti a delle sedute di acquisizione e i dati di ognuno sono stati utilizzati per personalizzare differenti Reti Neurali Artificiali. Per due di loro, si sono rilevate percentuali di riconoscimento che variano dal 98% al 100% (69 movimenti riconosciuti su 70), mentre per i restanti due si sono riscontrate alcune difficoltà determinate della loro struttura corporea.
Anche i test "fallimentari" sono stati molto utili perchè ci hanno permesso di comprendere come certi fattori influenzino l'analisi del segnale. Abbiamo notato, per esempio, che un maggiore volume tra il muscolo e la pelle dell'avambraccio produce una forte attenuazione dell'ampiezza del segnale. Inoltre è stato possibile identificare una forte influenza sulle prestazioni da parte di altri fattori come l'affaticamento muscolare, la concentrazione, la motivazione e il livello di allenamento del paziente.

Conclusioni Perchè il sistema funzioni con alti livelli di prestazione, il paziente deve essere ben addestrato e motivato, oltre ad avere un buon tono muscolare. Un possibile modo per estendere questo lavoro di tesi potrebbe essere lo sviluppo di software grafici (videogiochi), che rendano meno noioso l'addestramento del paziente, motivandolo nel percorso di riabilitazione.
Inoltre, si tenga presente che durante le prime fasi di acquisizione, un amputato non può vedere se ha compiuto in modo corretto una contrazione che gli è stato chiesto di eseguire. Quindi sarebbe utile un software che permetta di farsi una idea iniziale riguardo alla bontà dei movimenti eseguiti dal paziente.
Altri possibili lavori futuri potrebbero potrebbero ruotare attorno al progetto di una protesi di mano e del rispettivo controllore di basso livello.

Acknowledgements

I wish to express my sincere gratitude to my advisor, Prof. Giuseppina Gini and to my assistant supervisor Dario Cattaneo for their guidance and kindness. Their support was crucial to the development and success of the entire work of thesis.
I also thank Paolo Belluco, who supported this project with the EMG board, and people of the AIR Lab, who were helpful in solving some electronics issues. A tribute also goes to Brandon Kuczenski and Florian Knorn, for publishing their respective codes with BSD license.
Thanks to all my friends, who endured me and with whom I spent those necessary relaxing times, which allowed me to lucidly develop this thesis.
Eventually, my deepest gratitude goes to my family, for their unflagging support throughout my life, without them this dissertation would have been impossible.

Ringraziamenti Desidero esprimere la mia sincera gratitudine alla mia relatrice, la Professoressa Giuseppina Gini e al mio correlatore Dario Cattaneo per la loro disponibilità e gentilezza. Il loro supporto è stato fondamentale ai fini dello sviluppo e della buona riuscita dell'intero lavoro di tesi.
Ringrazio anche Paolo Belluco, che ha supportato questo progetto con la scheda EMG e le persone dell'AIR Lab, che sono state di grande aiuto nella risoluzione di alcuni problemi dovuti all'elettronica.
Un omaggio va anche a Brandon Kuczenski e Florian Knorn per aver pubblicato con licenza BSD i loro rispettivi codici.
Grazie a tutti i miei amici, che mi hanno sopportato e con i quali ho trascorso quei momenti di riposo necessari per far si che questa tesi venisse sviluppata in modo lucido.
Infine il ringraziamento più grande va alla mia famiglia, che mi ha supportato instancabilmente ogni giorno della mia vita, senza di loro questa tesi sarebbe stata impossibile.

Contents

Introduction

The hand is the terminal part of the forearm and its functions make it an important organ of the human body: people can use it to grasp objects, touch, sense, manipulate and communicate. Therefore it has a primary role also in social activities, which makes its cosmetics even more important.
It is easy to understand how the loss of the hand has significant consequences both from a psychological and functional point of view, in a person's life. After the traumatic event he will not be able to perform gestures that before were a natural way towards the external environment.
Prosthetic implants are the most common solution for the upper limb replacement, but since todays commercial devices suffer of low controllability, low functionality and low cosmetics, they are far away from being the biomimetic artificial hand we are looking for.
This thesis has many goals: the first is to make a detailed interdisciplinary study of the state of the art prosthetic solutions, not only from a technological point of view but also from a medical, psychological and, more in general, biological angle; this study is functional to the second goal, the design of a system able to perceive the amputee's will and to control a robotic prosthesis accordingly; the third, and last, goal is to understand how different factors can influence the performances of the designed system.
The EMG control is the most used approach in todays prosthetic devices, because it is noninvasive compared with other methods. During a muscle contraction, nerve impulses are sent by the motoneurons to the muscle fibers, these impulses are detected and collected by electrodes placed on the skin of the forearm. The resulting signal is of stochastic nature and is called electromyographic (EMG) signal.
The goal of the EMG control is, therefore, to create an association between a predefined set of hand motion patterns and the corresponding EMG signals generated by the forearm muscles. In this way the classifier mounted on the prosthetic hand is able to recognize a muscle contraction and sends to the controller the command to reproduce the correspondent hand movement.

This goal is normally achieved by statistical and time-frequency domain methods coupled with a powerful classifier.
Many works have been carried out on this subject before this thesis, but the inspiring ones were few. Therefore, since the the majority of the papers faces this topic just from the engineering point of view, the decision was to carry out a more detailed interdisciplinary discussion.
The most inspiring work, in the scope of the design of a new control system, was of course the thesis written by Matteo Arvetti [1], who designed a classifier able to detect five different hand motion patterns with a performance of 90%, using just two electrodes (one channel) in opposite configuration. After a careful study of the pros and cons of the methods applied in the thesis mentioned above, its main concepts were used as a landmark to create a new system from scratch.
In the current work the recording of the EMG signal is carried out by means of three different channels (6 electrodes) positioned in a distributed fashion around the forearm, sending the detected signals to a brand new acquisition board. In this way, the whole muscle activity is recorded, therefore we need to extract just the part of the signal (burst) related to the muscle contraction. Since the signals come from three different sources, the segmentation of the contraction is characterized by parallelism issues. Our system addresses this problem by dynamically selecting the leading channel for the detection of each contraction.
After the segmentation, each single burst is analyzed using the Continuous Wavelet Transform which extracts from it a large representative matrix composed by values in the time-frequency domain. This big matrix is then processed using the Singular Value Decomposition to reduce its dimensionality and obtain a little vector. This is then concatenated with other two temporal parameters, the integral EMG and the Mean Absolute Value, to form the feature vector representing the burst.
After the design of the feature extractor, four sound subjects were asked to attend some acquisition sessions, in which they had to perform 7 different movement types. The recorded data were used to train more than one Artificial Neural Network for each subject. Once the ANN has been trained, it was used to recognize different movements, leading to performances ranging between 98% and 100%.
Since the subjects used to test the system performances had different body structures it was also possible to analyze the influence of many varying factors. For example we could notice that a large volume between the muscle and the forearm skin, can attenuate the signal and modify its spectral composition. The system is able to easily overcome the second issue, but

since some bursts are very attenuated in amplitude, many weak muscle contraction are not even detected. The influence of other factors, like muscle fatigue, patient's concentration, motivation and training level was also analyzed. Leading to the conclusion that a patient needs to be well trained and prepared before the customization of his own prosthetic controller, as well as motivated and assisted.
The thesis is divided into six chapters: *Chapter 1* discusses the biologic system of the hand, in order to give to the reader the basic terminology; it shows the structure of the muscles, their contraction process and their functions, all aspects that are functional to the project phase; eventually, it proposes a sort of parallelism between the real and the artificial hand. *Chapter 2* gives an overview about the psychological and medical issues concerning the hand amputation and, then, presents in detail the technological state of the art related to modern prosthetics. *Chapter 3* presents the electromyographic signal in all its aspects. *Chapter 4* is one of the most important parts of this thesis and discusses in detail the logic design of the implemented system. *Chapter 5* presents the results obtained and, eventually, *Chapter 6* draws some conclusions and gives some hits for future expansion of the current work.

Chapter 1

The Biological System of The Hand

This chapter presents an overview of the complex biologic system of the human forearm and hand. The first section introduces the possible movements of the hand, the second its anatomy, then, the third section, focuses on the control system and the fourth on the muscular contraction. This chapter aims at providing the reader with the basic terminology related to the hand system and at showing the structure of the muscles, their contraction process and their functions, all aspects that are functional to the project phase. Moreover we want to show how well implemented is the "natural project" of the hand and to start a parallelism with the artificial limb to be concluded in the next chapter.

1.1 The Hand Movements

The upper limb is anatomically divided into three subparts, the arm, the forearm and the hand. The first ranges from the shoulder to the elbow, the second is the portion from the elbow to the wrist and the third and terminal part is located below the forearm [2]. The hand is used for grasping and holding and consists of the wrist, palm, four fingers, and an opposable thumb.
Before treating the complex subject of the hand's anatomy, an overview of the functions of the hand's joints is presented. This is done in order for the reader to master the terms that will often be used during the thesis. All the functions have to be considered with respect to a starting landmark, namely the neutral position. This varies from function to function, thus it is presented in each subsection.

1.1.1 Hand Pronation and Supination

The neutral configuration is the one in which the elbow is fixed at side in 90 degrees of flexion, and the axis of the hand's palm is perpendicular to the floor.
From this position, the pronation consists of a rotation of the forearm that moves the palm of the hand face down. On the other hand, starting from the neutral position, the pronation consists of a rotation of the forearm that moves the palm of the hand face up.(Figure 1.1).

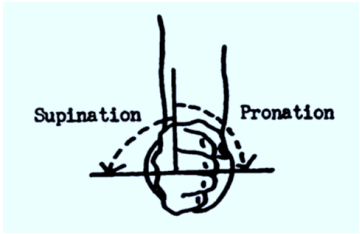

Figure 1.1: Hand pronation and supination [3].

1.1.2 Wrist Extension and Flexion

The neutral configuration is the one in which the elbow is fixed at side in 90 degrees of flexion, and the palm of the hand is face down (Figure 1.2) . The

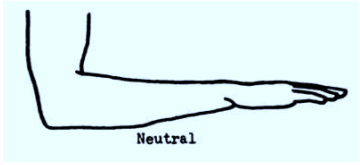

Figure 1.2: The neutral position of the wrist extension and flexion [3].

extension is also called dorsiflexion and consists of an upward rotation of the wrist, with respect to the neutral position. Vice versa, the wrist flexion or palmar flexion, consists of a downward rotation of the wrist (Figure 1.3).

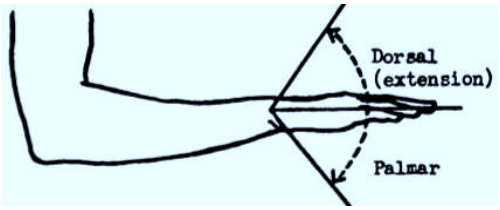

Figure 1.3: Wrist extension and flexion [3].

1.1.3 Wrist Adduction and Abduction

In this case the neutral position is the same as the one of the wrist extension and flexion (Figure 1.2). The abduction of the wrist is also called radial deviation and consists of a wrist rotation towards the thumb side. The adduction is the rotation of the wrist towards the opposite side and is called ulnar deviation (Figure 1.4).

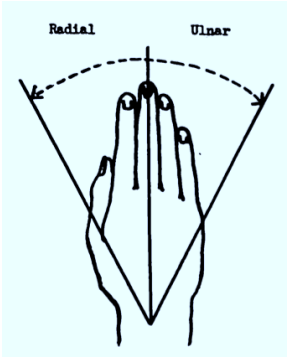

Figure 1.4: Wrist radial deviation (abduction) and ulnar deviation (adduction) [3].

1.1.4 Finger Hyperextension and Flexion

The neutral position is the one in which the finger are all extended. The hyperextension of the fingers consists of a larger extension than the normal extended posture, while the flexion consists of a bending of the fingertips towards the palm (Figure 1.5). The hyperextension should be easily noted if present, because it is an unnatural movement.

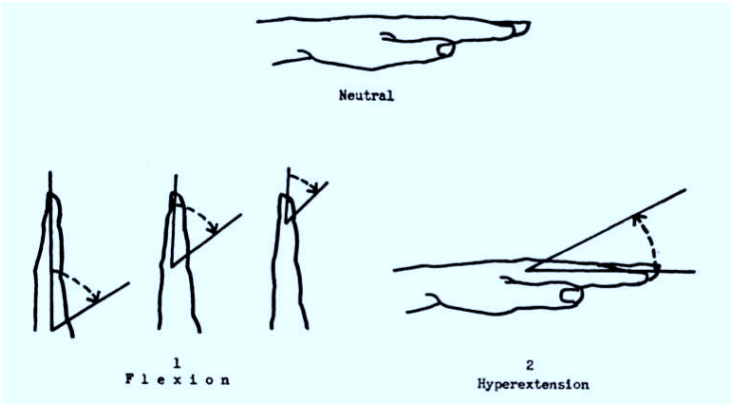

Figure 1.5: Fingers' neutral position, hyperextension and flexion [3].

1.1.5 Thumb Abduction and Opposition

The neutral position is with the thumb alongside the forefinger and extended. The abduction is the motion that pulls the thumb part away from the midline of the hand. It is measured by the angle that the thumb makes with the forefinger, which can reach 90 degrees of aperture. The opposition consists of the flexion of the tip of the thumb on the palm of the hand. (Figure 1.6) [3].

Figure 1.6: Thumb abduction and opposition [3].

1.2 The Anatomy of the Hand

1.2.1 The Bones

1.2.1.1 The Bones of the Forearm

The ulna is a long bone, prismatic in shape, placed at the medial side of the forearm, parallel with the radius. It is divisible into a body and two extremities. Its upper extremity, of great thickness and strength, forms a large part of the elbow-joint. The bone diminishes in size from above downward, becoming very small at its lower extremity, which is excluded from the wrist-joint by the interposition of an articular disk.
The radius is situated on the lateral side of the ulna, which exceeds it in length and size. Its upper end is small, and forms only a small part of the elbow-joint; but its lower end is large, and forms the chief part of the wrist-joint. It is a long bone, prismatic in form and slightly curved longitudinally. It has a body and two extremities (Figure 1.7).

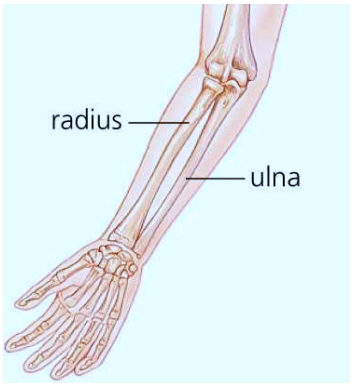

Figure 1.7: Radius and ulna.

1.2.1.2 The Bones of the Hand

The skeleton of the hand has 27 bones and is subdivided into three segments: the *carpus* or wrist bones; the *metacarpus* or bones of the palm; and the *phalanges* or bones of the digits. The front and the back of the hand are respectively called *palm* and *dorsum*, while their relative adjectives are *volar* and *dorsal*
The *carpal bones*, eight in number, are arranged in two rows. Those of the proximal row, from the radial to the ulnar side, are named the navicular (scaphoid), lunate, triangular, and pisiform; those of the distal row, in the

same order, are named the greater multangular (also called trapezium and attached to the thumb), lesser multangular (trapezoid), capitate, and hamate.

The *metacarpus* consists of five cylindrical bones which are numbered from the lateral side (ossa metacarpalia I-V); each consists of a body and two extremities and is coupled with a finger.

The *phalanges* are fourteen in number, three for each finger, and two for the thumb. Each consists of a body and two extremities. The body tapers from above downward; its sides are marked by rough edges, which give attachment to the fibrous sheaths of the Flexor tendons (Figure 1.8).

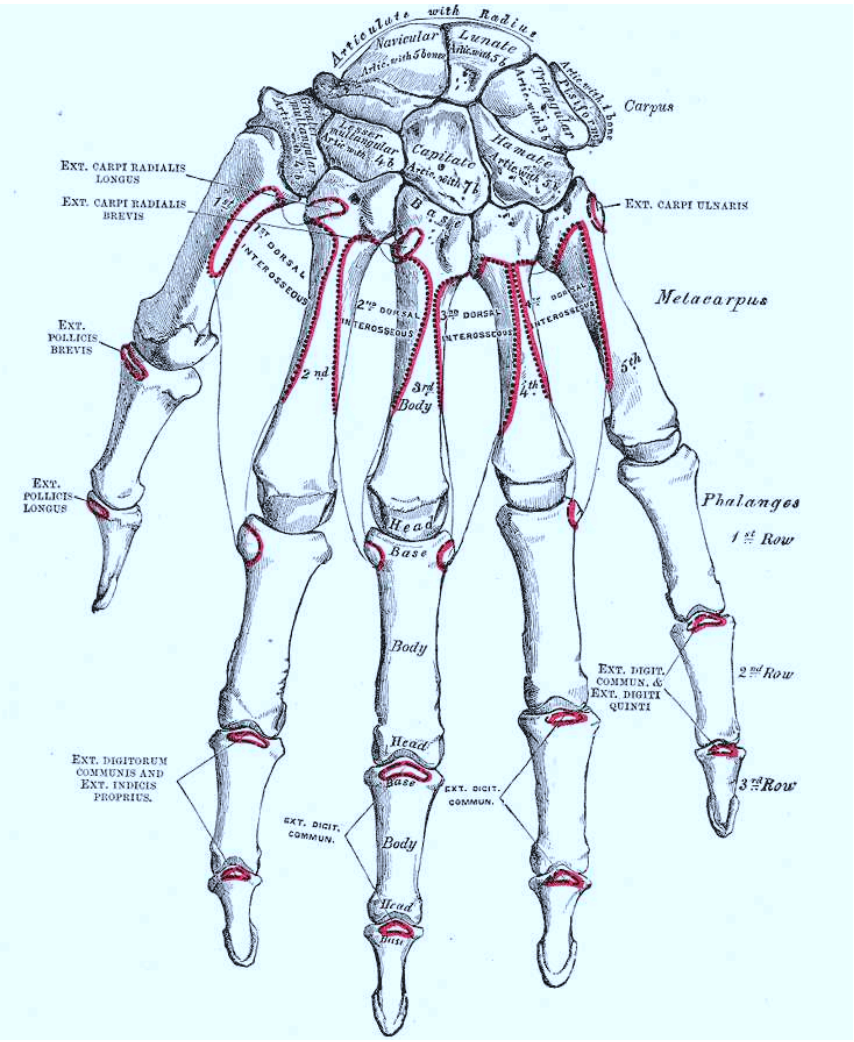

Figure 1.8: Bones of the left hand [4].

1.2.2 The Articulations

1.2.2.1 The Articulations of the Forearm

The articulation of the radius with the ulna is effected by ligaments which connect together the extremities as well as the bodies of these bones. The ligaments can be subdivided into three sets:

1. those of the proximal radioulnar articulation;
2. the middle radioulnar ligaments;
3. those of the distal radioulnar articulation.

The movements in the distal radioulnar articulation consist of rotation of the lower end of the radius around an axis which passes through the center of the head of the ulna. To obtain the *pronation* of the forearm and hand, the radius has to rotate forward, while the *supination* is achieved by its backward rotation.

1.2.2.2 The Articulations of the Hand

The wrist joint is a condyloid articulation: which means that an ovoid articular surface, or condyle, is received into an elliptical cavity. The lower end of the radius and the under surface of the articular disk compose the half of the articulation which stands above, while the navicular, lunate, and triangular bones form the complementary part which stays below. The articular surface of the radius and the under surface of the articular disk form together a concave surface, the receiving cavity. The superior articular surfaces of the navicular, lunate, and triangular form a smooth convex surface, the condyle, which is received into the concavity.
The joint is surrounded by a capsule, strengthened by the following ligaments:

- the Volar Radiocarpal;
- the Ulnar Collateral;
- the Dorsal Radiocarpal;
- the Radial Collateral.

The movements permitted in this joint are flexion, extension, abduction, adduction, and circumduction.

The Mid-carpal joint is the joint between the two rows of carpal joints. The chief movements which it permits are flexion and extension and a slight amount of rotation.

The Trapezometacarpal articulation of the thumb (articulatio carpo metacarpea pollicis) is the joint between the first metacarpal and the greater multangular (trapezium). It has great freedom of movement thanks to the configuration of its articular surfaces, which are saddle-shaped. In this articulation the movements permitted are flexion and extension, abduction and adduction, circumduction and opposition.

The Carpometacarpal is the articulation of the other four metacarpal bones with the carpus (articulationes carpometacarpeae). The bones are united by dorsal, volar, and interosseous ligaments. The movements allowed in the carpometacarpal articulations are limited to slight gliding of the articular surfaces upon each other. The extent of this movements varies from finger to finger: the metacarpal bone of the little finger is the most movable and that of the ring finger is the latter, while the metacarpal bones of the index and middle fingers are almost immovable.

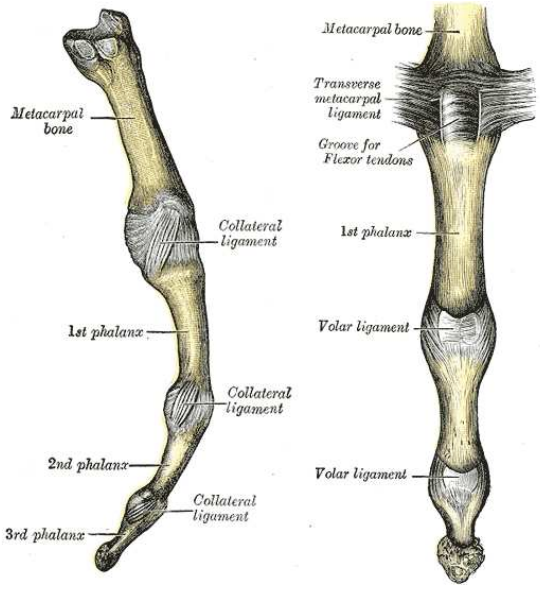

Figure 1.9: Metacarpophalangeal articulation and articulations of digit [4].

The Metacarpophalangeal joints are of the condyloid kind, formed by the reception of the rounded heads of the metacarpal bones into shallow cavities on the proximal ends of the first phalanges. The only exception is the thumb, which presents more of the characters of a ginglymoid joint: a freely moving joint that allows extensive movement in one plane. Each joint has a volar and two collateral ligaments. The movements achieved by these joints are adduction, abduction, flexion, extension and circumduction; though the first two of them are very limited because they cannot be performed when the fingers are flexed (Figure 1.9).

The interphalangeal articulations are hinge-joints; each has a volar and two collateral ligaments. The only movements allowed are flexion and extension and they are more extensive between the first and second phalanges than between the second and third. The amount of flexion is very considerable, but extension is limited by the volar and collateral ligaments (Figure 1.9) [4].

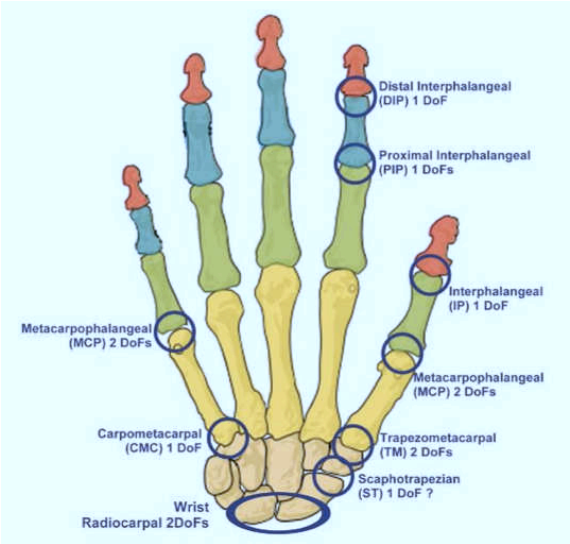

Figure 1.10: Joints of the hand and relative degrees of freedom [5].

The Degrees Of Freedom of the Hand: in total we can count 22 degrees of freedom in the hand and two more in the wrist (adduction/abduction and flexion/extension) (Figure 1.10) [5].

1.2.3 The Muscles

The muscle is a contractile organ, which function is to generate force. This force results in motion thanks to the leverage exerted on the bones by tendons attached to muscles.
The muscles moving the human hand can be divided in two groups: the extrinsic and intrinsic muscles. The former are the long flexor and extensors located in the forearm, while the latter are located in the palm.

1.2.3.1 The Muscles in the Forearm (Extrinsic)

The forearm muscular structure is organized into anterior and posterior compartments, separated by the interosseous membrane that connects the radius and ulna. The anterior compartment is the one that a person can see when the arm is supine. It contains the flexor muscles, together with the median nerve (and branches), the ulnar nerve, and accompanying vessels. The posterior compartment contains the extensor muscles (with the exception of the brachioradialis, which is an elbow flexor), the radial nerve, and its branches.
The forearm contains nineteen muscles. Within both the posterior and anterior compartments there are two and three layers of muscle groups, respectively. It is possible to sort the muscles by function, remembering that for each one there exist a tendon that actuates a particular part of the hand (Figure 1.11) [6]:

Flexor division:

- muscles which rotate the radius on the ulna:
  - pronator teres (superficial group, anterior compartment - pronates)
  - pronator quadratus (deep group, anterior compartment - pronates)
  - supinator (deep group, posterior compartment - supinates)
- muscles which flex the hand at the wrist:
  - flexor carpi radialis (superficial group, anterior compartment)
  - flexor carpi ulnaris (superficial group, anterior compartment)
  - palmaris longus (superficial group, anterior compartment)

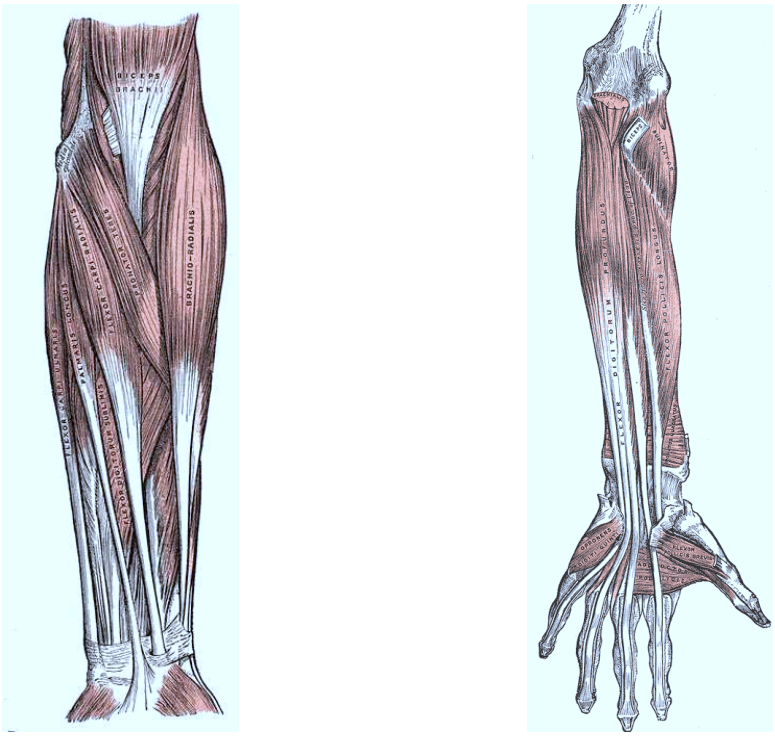

(a) Front of the left forearm. Superficial muscles. (b) Front of the left forearm. Deep muscles.

Figure 1.11: Figures taken from [4]

- muscles which flex the digits:
  - flexor digitorum superficialis (intermediate group, anterior compartment)
  - flexor digitorum profundus (deep group, anterior compartment)
  - flexor pollicis longus (deep group, anterior compartment)

Extensor division:

- muscles which extend the hand at the wrist:
  - extensor carpi radialis longus (superficial group, posterior compartment)
  - extensor carpi radialis brevis (superficial group, posterior compartment)
  - extensor carpi ulnaris (superficial group, posterior compartment)

- muscles which extend the digits, except the thumb:
  - extensor digitorum (superficial group, posterior compartment)
  - extensor indicis (deep group, posterior compartment)
  - extensor digiti minimi (superficial group, posterior compartment)
- muscles which operate in extension or abduction of the thumb:
  - abductor pollicis longus (deep group, posterior compartment - abducts thumb)
  - extensor pollicis brevis (deep group, posterior compartment)
  - extensor pollicis longus (deep group, posterior compartment)

1.2.3.2 The Muscles in the Hand (Intrinsic)

The intrinsics muscles are situated totally within the hand. They are divided into 4 groups (Figure 1.12):

1. thenar group: moves the thumb and occupies the radial side. It is composed by the abductor pollicis brevis, flexor pollicis brevis, opponens pollicis, and adductor pollicis muscles. All are innervated by the median nerve except for the adductor pollicis and the deep head of the flexor pollicis brevis, which are innervated by the ulnar nerve. They originate from the flexor retinaculum and carpal bones and insert at the proximal phalanx of the thumb.
2. hypothenar group: moves the little finger and occupies the ulnar side. It consists of the palmaris brevis, abductor digiti minimi, flexor digiti minimi, and opponens digiti minimi. They are all innervated by the ulnar nerve. This group of muscles originates at the flexor retinaculum and carpal bones and inserts at the base of the proximal phalanx of the small finger.
3. lumbrical group: contributes to the flexion of the metacarpophalangeal joints and to the extension of the interphalangeal joints. They originate from the flexor digitorum profundus tendons at the palm and insert on the radial aspect of the extensor tendons at the digits. The index and long finger lumbricals are innervated by the median nerve, and the small and ring finger lumbricals are innervated by the ulnar nerve.

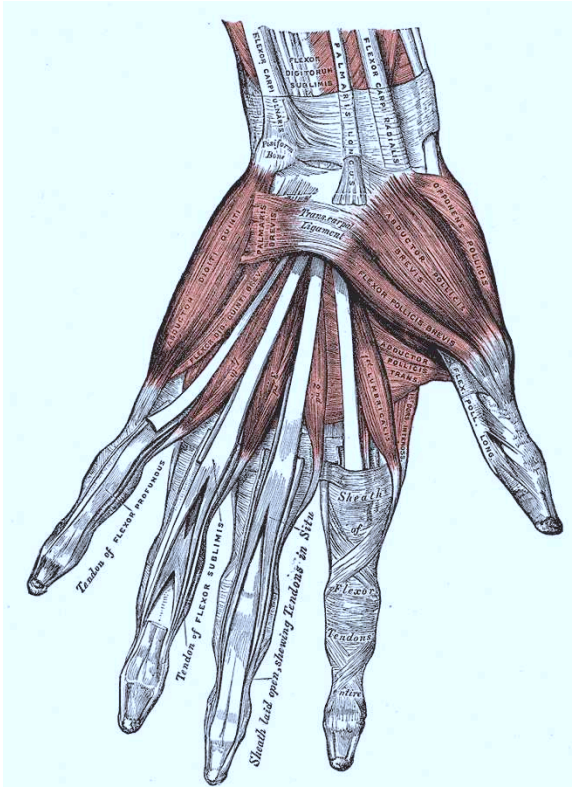

Figure 1.12: The muscles of the left hand. Palmar surface. [4].

4. interossei group: the interossei group consists of 3 volar and 4 dorsal muscles, which are all innervated by the ulnar nerve. They originate at the metacarpals and form the lateral bands with the lumbricals. The dorsal interossei abduct the fingers, whereas the volar interossei adduct the fingers to the hand axis.

1.2.3.3 The Tendons

Normal finger flexion is a complex fine motor action that requires the integrity and orchestration of a number of delicate structures that are centered around the flexor tendon system [7].
The tendon is the tissue by which a muscle attaches to bone. Tendons are somewhat flexible, but fibrous and tough. They are like ligaments in being tough, flexible cords. But tendons differ from ligaments in that tendons extend from muscle to bone, whereas ligaments go from bone to bone as at

a joint. Despite their tough fibrous nature, tendons and ligaments are both considered "soft tissue," that is soft as compared to cartilage or bone. The tendons of wrist and hand pass through bony and ligamentous guide systems. Flexor tendons pass through a "tunnel" bounded dorsally by carpal bones, laterally by the greater multangular and the projection of the hamate, and volarly by the tough transverse carpal ligament. Similarly, the dorsal carpal ligament guides the extensor tendons, and a system of sheaths serves as a guide for flexor and extensor tendons through the metacarpal and phalangeal regions [8].

1.2.3.4 The Pulley System

The pulley system is composed of focal thickened areas of the flexor tendon sheaths, and is one of the most important biomechanical structures used in flexion. Not only for accurate tracking of the tendon but also to maintain its apposition. Thanks to the pulley system the bone is maintained across the joint and a fulcrum to elicit flexion and extension is provided.
At anatomic inspection, these retinacular structures result in focal, well-defined areas of thickening of the tendon sheath that are referred to as the annular pulley system. Additional crisscrossing fibers between the components of the annular pulley system are referred to as the cruciate pulley system. The *retinacular system* in the thumb is composed of 2 annular and 1 oblique pulleys, while, each of the other fingers contains 5 annular and 4 cruciate pulleys. [9].
In general, the length of each pulley varies in direct proportion to the length of the digit, and the thickness, in turn, is directly proportional to the length of the pulley. The first annular pulley (A1) begins in the region of the palmar plate of the metacarpophalangeal joint and extends to the level of the base of the proximal phalanx. The second annular pulley (A2) arises from the volar aspect of the proximal part of the proximal phalanx and extends to the two thirds of the proximal phalanx. The third pulley (A3) is small and extends over the region of the proximal interphalangeal joint. The fourth pulley (A4) is in the midportion of the middle phalanx, and the fifth pulley (A5) is in the region of the distal interphalangeal joint. To complete the structure, the three cruciate pulleys C1, C2, and C3, which are respectively behind A3, A4 and A5 (Figure 1.13b).
The primary function of the flexor pulley system in the fingers is to convert the available linear translation and force in the muscle-tendon unit into rotation and torque at the finger joints (Figure 1.13a) [7].
Moreover the annular pulleys are of biomechanical importance in preventing

tendon excursion during digital flexion, whereas the cruciate pulleys provide the necessary flexibility for approximation of the annular pulleys at flexion, while maintaining the integrity of the flexor sheath.

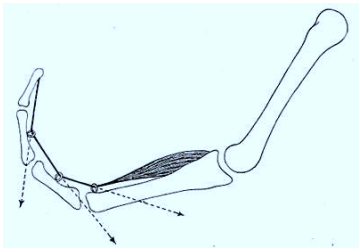

(a) The pulley mechanism in action [3].

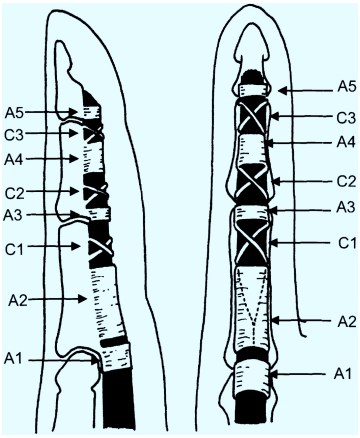

(b) Sagittal (left) and coronal (right) representations of the pulley system of a typical flexor tendon (black areas) of the finger. Dotted lines represent the division of the flexor digitorum superficialis tendon into two bands at this level [7].

Figure 1.13

1.2.4 The Nervous and Sensory Systems

1.2.4.1 The Nervous System

The peripheral nervous system conveys electrical commands from the central nervous system to the organs of the body. The neuron is the elementary nerve cell and it is responsible of the nervous conduction. It consists of several dendrites, forming the input of the neuron, a nucleus and a cell body, called soma, from which originates the axon. The latter has a more or less pronounced tree structure, and forms the output of the neuron.

1.2.4.2 The Nerves of the Hand

The hand is innervated by 3 nerves: the median, ulnar, and radial nerves. Each has both sensory and motor components. An overview about the nerve

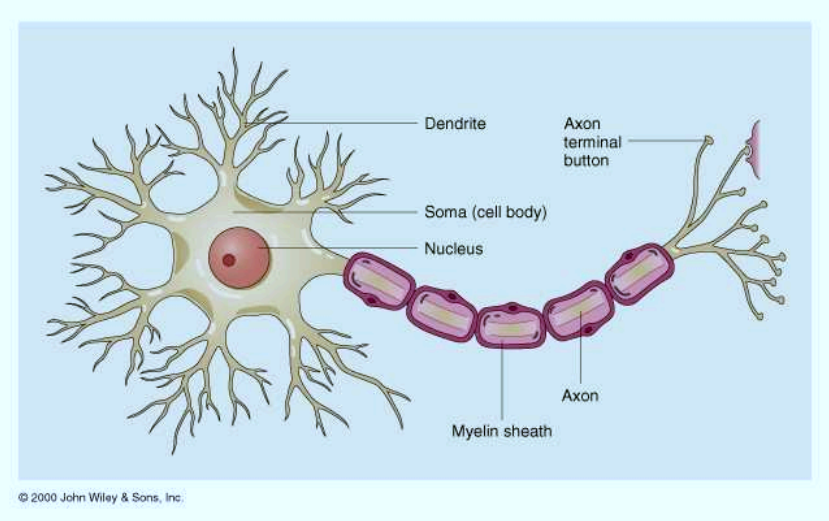

Figure 1.14: The neuron

supply is presented, except for minor variations and exceptions [9] [8]:

- The median nerve is responsible for innervating the muscles involved in the fine precision and pinch function of the hand. In particular the flexor muscles of the wrist and fingers, the abductors, opponens and flexor of the thumb and the lumbricals I and II.
- The ulnar nerve is responsible for innervating the muscles involved in the power grasping function of the hand. All the intrinsic muscles of the hand are innervated by the ulnar nerve, including all the interossei, lumbricals III and IV.
- The radial nerve is responsible for innervating the wrist extensors, which control the position of the hand and stabilizes the fixed unit. The thumb and finger extensors are innervated as well.

1.2.4.3 The Somatosensory System

Each of the major nerve trunks mentioned above, diverges into countless smaller branches ending in the papillae of the palmar pads and dorsal skin. The whole neuromuscular system is so coordinated in the brain, whose motor response to stimuli is ordinarily subconscious and reflex. Thus an object slipping from the grasp is automatically gripped more firmly, but not so

firmly as to damage the hand itself. Noxious stimuli are rejected automatically, as when the fingers are withdrawn from an object uncomfortably hot [8].
The somatic sensory system has two major components: a subsystem for the detection of *mechanical stimuli* (e.g., light touch, vibration, pressure, and cutaneous tension), and a subsystem for the detection of *painful stimuli and temperature*. Together, these two subsystems give humans and other animals the ability to identify the shapes and textures of objects, to monitor the internal and external forces acting on the body at any moment, and to detect potentially harmful circumstances [10].
The specialized sensory receptors in the cutaneous and subcutaneous tissues are of various nature. They include free nerve endings in the skin, nerve endings associated with specializations that act as amplifiers or filters, and sensory terminals associated with specialized transducing cells that influence the ending by virtue of synapse-like contacts. Based on function, this variety of receptors can be divided into three groups: *mechanoreceptors, nociceptors, and thermoceptors.*
On the basis of their morphology, the receptors near the body surface can also be divided into *free and encapsulated types.* Nociceptor and thermoceptor specializations are referred to as free nerve endings because the unmyelinated terminal branches of these neurons ramify widely in the upper regions of the dermis and epidermis; their function is to transmit pain and temperature sensations. Most other cutaneous receptors show some degree of encapsulation, which helps determine the nature of the stimuli to which they respond.
Despite their variety, all somatic sensory receptors work mainly in the same way: stimuli applied to the skin (receptive field of a neuron) deform or otherwise change the nerve endings, which in turn affects the ionic permeability of the receptor membrane. Changes in permeability generate a depolarizing current in the nerve ending, thus producing a receptor potential that triggers action potentials. This overall process, in which the energy of a stimulus is converted into an electrical signal in the sensory neuron, is called sensory transduction and is the critical first step in all sensory processing.

Tactile Information - Mechanosensory processing of external stimuli is initiated by the activation of a diverse population of cutaneous and subcutaneous mechanoreceptors at the body surface that relays information to the central nervous system for interpretation. Mechanosensory information is carried to the brain by several ascending pathways that run in parallel through the spinal cord, brainstem, and thalamus to reach the primary so-

matic sensory cortex. The latter projects in turn to higher-order association cortices in the parietal lobe, and back to the subcortical structures involved in mechanosensory information processing.

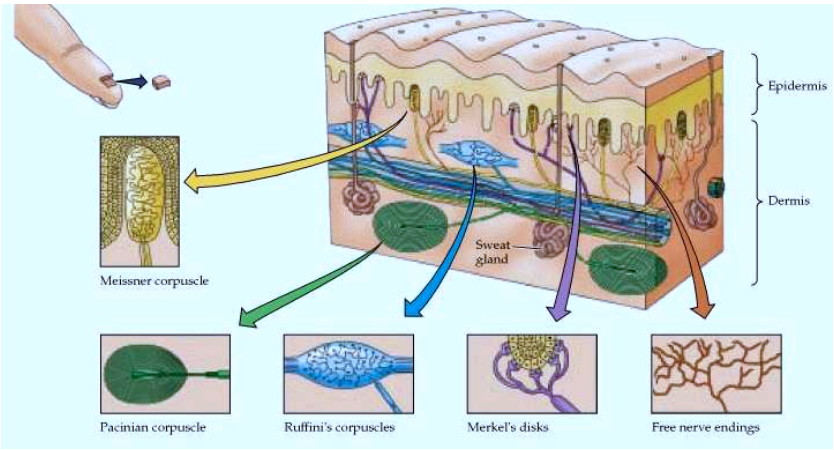

Figure 1.15: The skin harbors a variety of morphologically distinct mechanoreceptors. This diagram represents the smooth, hairless (also called glabrous) skin of the fingertip. [10].

Four major types of encapsulated mechanoreceptors are specialized to provide information to the central nervous system about touch, pressure, vibration, and cutaneous tension: respectively the Meissner's corpuscles, Pacinian corpuscles, Merkel's disks, and Ruffini's corpuscles. These receptors are referred to collectively as low-threshold (or high-sensitivity) mechanoreceptors because even weak mechanical stimulation of the skin induces them to produce action potentials. All low-threshold mechanoreceptors are innervated by relatively large myelinated axons, ensuring the rapid central transmission of tactile information.
An overview of the major characteristics of the receptors mentioned above is now presented:

- *Meissner's corpuscles*, which lie between the dermal papillae just beneath the epidermis of the fingers, palms, and soles, are elongated receptors formed by a connective tissue capsule. The center of the capsule contains one or more afferent nerve fibers that generate rapidly adapting action potentials following minimal skin depression.

Meissner's corpuscles are the most common mechanoreceptors of glabrous (hairless) skin (the fingertips, for instance), and their afferent fibers account for about 40% of the sensory innervation of the human hand. These corpuscles are particularly efficient in transducing information about the relatively low-frequency vibrations (30-50 Hz) that occur when textured objects are moved across the skin. In summary they provide information primarily about the dynamic qualities of mechanical stimuli.

- *Pacinian corpuscles* are large encapsulated endings located in the subcutaneous tissue. One or more rapidly adapting afferent axons lie at the center of an onion-like capsule, which acts as a filter, allowing only transient disturbances at high frequencies (250-350 Hz) to activate the nerve endings. Pacinian corpuscles adapt more rapidly than Meissner's corpuscles and have a lower response threshold. These attributes suggest that Pacinian corpuscles are involved in the discrimination of fine surface textures or other moving stimuli that produce high-frequency vibration of the skin. They make up 10-15% of the cutaneous receptors in the hand. Pacinian corpuscles are also located in interosseous membranes and they probably detect vibrations transmitted to the skeleton. Together with the Meissner's corpuscles, they provide information primarily about the dynamic qualities of mechanical stimuli.

- *Merkel's disks* are located in the epidermis. They account for about 25% of the mechanoreceptors of the hand and are particularly dense in the fingertips, lips, and external genitalia. Selective stimulation of these receptors in humans produces a sensation of light pressure. These several properties have led to the supposition that Merkel's disks play a major role in the static discrimination of shapes, edges, and rough textures.

- *Ruffini's corpuscles* are located deep in the skin, as well as in ligaments and tendons. The long axis of the corpuscle is usually oriented parallel to the stretch lines in skin; thus, Ruffini's corpuscles are particularly sensitive to the cutaneous stretching produced by digit or limb movements. They account for about 20% of the receptors in the human hand contributing to the kinesthetic sense and control of finger position and movement. They are believed to be useful for monitoring slippage of objects along the surface of the skin, allowing modulation of grip on an object.

The receptive fields of the neurons innervating the surface layers are smaller than that of the neurons in depth. The density of the surface receptors varies with the body map: they are more dense on the fingertip and on the lips. The dimensions of the receptive fields varies with position of the receptor as well. For example, on the fingertip the receptive field of the Meissner's corpuscles have a diameter of 2mm, while on the palm of the hand they are of 10mm.
A high receptor density is reflected by a high density of innervation. The skin areas with the highest density of innervation are the the fingertips, which hold up to 300 tactile afferent fibers per cm^2. The spatial discrimination ability that we have thanks to the fingertips, based on the smallness of the local receptive fields, allows us to discriminate the surface roughness and to read Braille.
Based on the above, it is not surprising that the tactile acuity greatly varies in different skin districts. For each area of the skin, the minimum distance between two raised points, which are still perceived as separate, is about 2 mm at the tip of the fingers (maximum resolution), about 4 mm on the lips, 10 mm in the palm of hand and more than 40 mm on the skin of the thigh and calf [11].

Pain and Temperature sensations - The relatively unspecialized nerve cell endings that initiate the sensation of pain are called nociceptors (noci- is derived from the Latin for "hurt"). Like other cutaneous and subcutaneous receptors, they transduce a variety of stimuli into receptor potentials, which in turn trigger afferent action potentials.
Because peripheral nociceptive axons terminate in unspecialized "free endings," it is conventional to categorize nociceptors according to the properties of the axons associated with them. There are three major classes of nociceptors in the skin: *mechanosensitive nociceptors, mechanothermal nociceptors, and polymodal nociceptors.*
In general, the faster-conducting nociceptors respond either to dangerously intense mechanical or to mechanothermal stimuli, and have receptive fields that consist of clusters of sensitive spots. Other unmyelinated nociceptors tend to respond to thermal, mechanical, and chemical stimuli, and are therefore said to be polymodal.
The thermoreceptors are of four different kinds. Two of these, known as cool and warmth receptors, are regarded as sensory receptors that respond to innocuous stimulation. The two others, known as heat and cold receptors, are nociceptors [12].
The receptive fields of all pain-sensitive neurons are relatively large, par-

ticularly at the level of the thalamus and cortex, presumably because the detection of pain is more important than its precise localization.

Proprioception - Whereas cutaneous mechanoreceptors provide information derived from external stimuli, another major class of receptors provides information about mechanical forces arising from the body itself, the musculoskeletal system in particular. These are called proprioceptors, roughly meaning "receptors for self". The purpose of proprioceptors is primarily to give detailed and continuous information about the position of the limbs and other body parts in space. Low-threshold mechanoreceptors, including muscle spindles, Golgi tendon organs, and joint receptors, provide this kind of sensory information, which is essential to the accurate performance of complex movements.

The most detailed knowledge about proprioception derives from studies of *muscle spindles*, which are found in all but a few striated (skeletal) muscles. The major function of muscle spindles is to provide information about *muscle length* (that is, the degree to which they are being stretched). The density of spindles in human muscles varies. Large muscles that generate coarse movements have relatively few spindles; in contrast, extraocular muscles and the intrinsic muscles of the hand and neck are richly supplied with spindles, reflecting the importance of accurate eye movements, the need to manipulate objects with great precision, and the continuous demand for precise positioning of the head. This relationship between receptor density and muscle size is consistent with the generalization that the sensory motor apparatus at all levels of the nervous system is much richer for the hands, head, speech organs, and other parts of the body that are used to perform especially important and demanding tasks.

Whereas muscle spindles are specialized to signal changes in muscle length, low-threshold mechanoreceptors in tendons inform the central nervous system about changes in *muscle tension*. These mechanoreceptors, called *Golgi tendon organs*, are distributed among the collagen fibers that form the tendons.

Finally, rapidly adapting mechanoreceptors, called *joint receptors*, in and around joints, gather dynamic information about limb position and joint movement [10].

1.3 The Control System

1.3.1 The Anatomy of the Brain

1.3.1.1 The Motor Cortex

The motor cortex is a region of the cerebral cortex involved in the planning, control, and execution of voluntary motor functions. It is situated in the *frontal lobe* (Figure 1.16), and contains the representation of the somatotopic mapping.
The surface area devoted to controlling the movements of each body part varies in direct proportion to the precision of the movements that can be

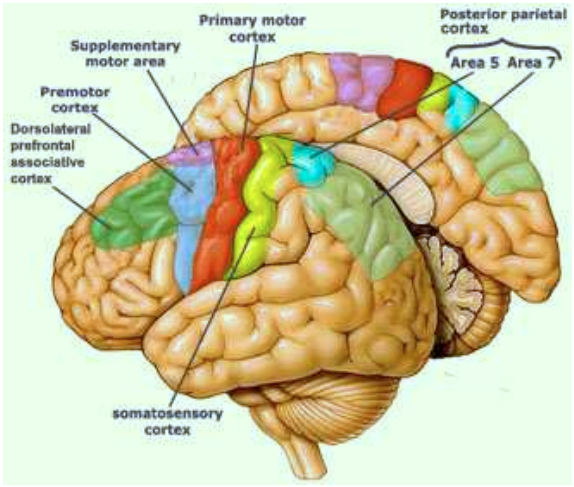

Figure 1.16: The motor cortex [13].

made by that part (Figure 1.17).
This regions of the motor cortex can be anatomically organized in:

- *primary motor cortex*: focal stimulations in this region elicit highly localized muscle contractions at various locations in the body; it is located in the Area 4;
- *premotor area*: is believed to help regulate posture by dictating an optimal position to the motor cortex for any given movement; it is located in the Area 6;
- *supplementary motor area*: influence the planning and initiation of movements on the basis of past experience; it is located in the Area 6;

- *posterior parietal cortex*: assesses the context in which a movement is being made. The parietal cortex receives somatosensory, proprioreceptive, and visual inputs, then uses them to determine such things as the positions of the body and the target in space. It thereby produces internal models of the movement to be made, prior to the involvement of the premotor and motor cortices. It is situated in the *parietal lobe*;

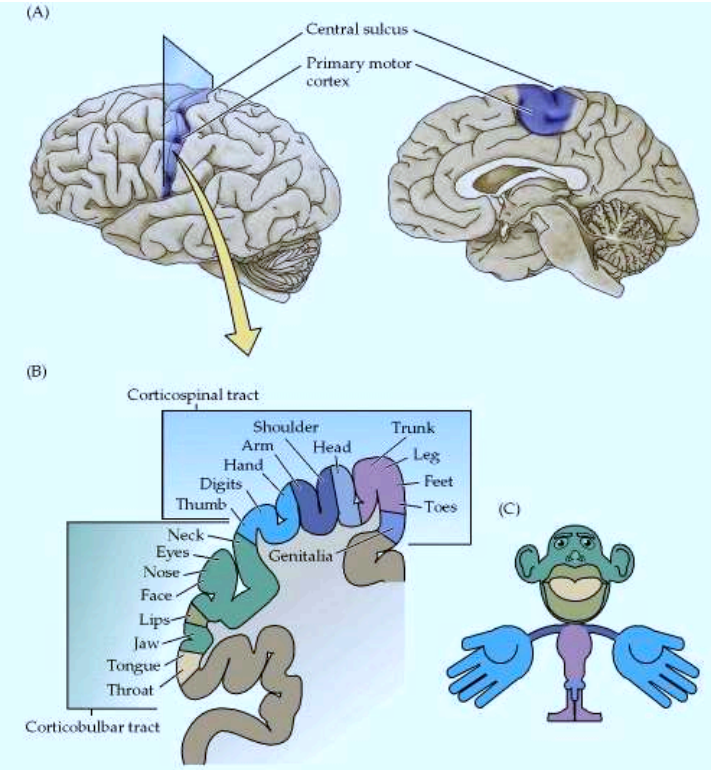

Figure 1.17: Topographic map of the body musculature in the primary motor cortex. (A) Location of primary motor cortex. (B) Section of the brain, illustrating the somatotopic organization of the motor cortex. (C) Representation of various portions of the body musculature in the motor cortex. Fine motor control capabilities (such as the hands and face) occupy a greater amount of space than those that exhibit less precise motor control (such as the trunk). [10].

1.3.1.2 The Basal Ganglia

The basal ganglia plays an indirect role in the motor system. By projecting to the motor cortex, the premotor cortex, and the supplementary motor area simultaneously, they form part of the cortobasal ganglia motor loop, which determines and controls what movements will be performed.

1.3.1.3 The Cerebellum

For the body to make any given gesture, the sequence and duration of each of the basic movements of each body segment involved must be controlled in a very precise manner. One of the cerebellum's jobs is to provide this control over the timing of the body's movements. It does so by means of a loop circuit that connects it to the motor cortex, modulating the signals that the motor cortex sends to the motor neurons.
In humans, the cerebellum also analyzes the visual signals associated with movement. These signals may come either from the movement of objects within the field of vision or from the sight of the moving body segments themselves. The cerebellum appears to calculate the speed of these movements and adjust the motor commands accordingly.

1.3.2 Movement planning

Any voluntary movement can be accurately described as an intentional effort undertaken jointly by the motor cortex and numerous other neural systems acting cooperatively. This effort is organized hierarchically.

1. The top level of the hierarchy takes care of defining the motor strategies: *the objectives of the movement and the behaviours to be applied* to achieve these objectives. The prefrontal cortex prepares the plans for the movement. Meanwhile, the frontal cortex receives information from a large number of axons projecting from the parietal cortex, which is involved in spatial perception.

2. The secondary motor areas work with the cerebellum to specify the *precise time sequence of contractions* of the various muscles that will be required to carry out the selected motor action. The brain also needs to convert the coordinates of the external environment into a set of intrinsic coordinates. This conversion allows a person to adjust the angles of the various joints that are involved in the movement.

3. The primary motor cortex, the brainstem, and the spinal cord come into play to *produce the contractions of all the muscles needed* for the

chosen movement. The primary motor cortex determines how much force each muscle group must exert, and then sends this information to the spinal motor neurons and interneurons that generate the movement itself, as well as the postural adjustments that accompany it.

The operation of each hierarchical level in the motor control system is extremely dependent on the sensory information that it receives. In the determining of motor strategies, sensory information helps to generate a mental image of the body and its position in its environment. The decisions on how to apply motor controls (for example, the duration and amplitude of each contraction) are based on memories of sensory information about past movements. And in the actual execution of a movement, sensory feedback enables the brain to maintain the body's posture and helps it to determine the length and tension of the muscles before and after every voluntary movement [13].

1.4 The Muscle Contraction

1.4.1 The Muscle Structure

The muscle is a tissue able to generate and transmit force. In particular, a *striated muscle* is a hierarchical material made up of a large amount of parallel fibers, whose diameters are about 1 micrometer and yet with a length of several centimeters. The adjective "striated" depends on the fact that the fibers, composing this type of muscle, are actually bundles of thinner structures known as fibrils. These little structures have repeating cross striations throughout their length known as Z-bands. The area between these striations is called sarcomere and contains thick and thin filaments bound together by a system of molecular cross-linkages. During contraction cycle, conformational changes in the cross-linkages lead to only very slight changes in the length of the filaments but cause substantial changes in the distance between Z-bands as the thick filaments slide in between the thin filaments (Figure 1.18).

1.4.2 The Muscle Innervation

Each striated muscle is innervated by a single motor nerve. In particular the traveling of the nerve to the muscle consists of axons of numerous individual α-motoneurons, which as a collective are referred to as a motoneuron pool. Each α-motoneuron axons divides into a number of small branches, termed

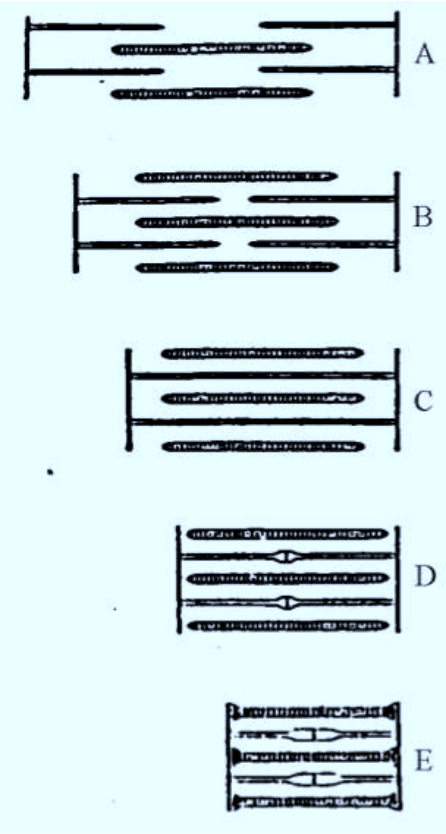

Figure 1.18: The contraction cycle [14]. Thick filaments are the ones in the center, while the thin ones start from the lateral positions.

axon fibrils, which form neuromuscular junctions. Each α-motoneuron innervates a number of interspersed muscle fibers within a muscle, and each muscle fiber is usually innervated by only one α-motoneuron. The spatial distribution of the neuromuscular junctions on the muscle surface is not random, but forms at most a few clusters (typically only one) called innervation zones. An important functional consequence of this structure is that muscle fibers do not contract individually but rather the entire set of muscle fibers innervated by a single α-motoneuron contracts in consonance. Therefore, the most elementary functional unit is composed by the α-motoneuron cell body, its axon, its axon fibrils and the individual muscle fibers innervated by these axon fibrils. This entity is called motor unit (Figure 1.19).

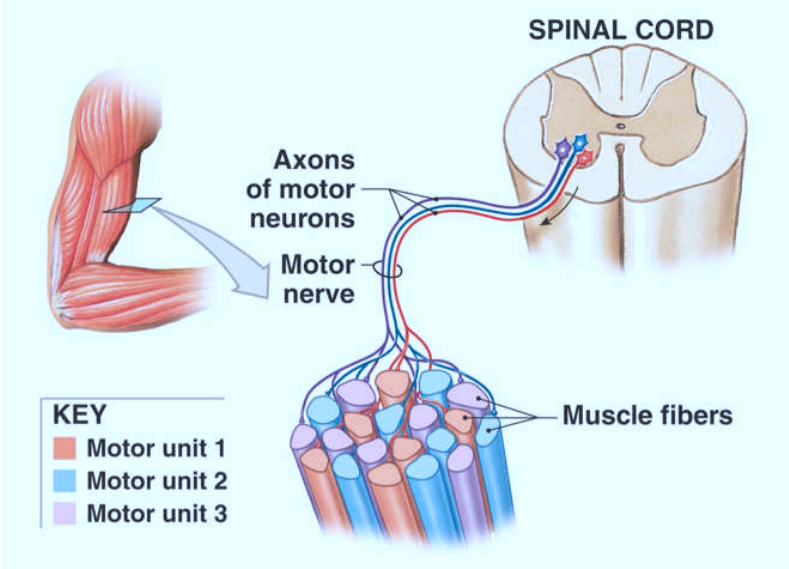

Figure 1.19: Motor units schematic representation [15].

1.4.3 The Size Principle

The axons of the motoneurons within a motoneuron pool vary in diameter. Therefore the smaller the diameter of a motoneuronal axon, the smaller the amount of axon fibrils, the smaller the number of muscle fibers it innervates and the smaller the size of its cell body.
Hence, the activation of a muscle by small motoneurons produces smaller and more precise actions than the activation of the same muscle by larger motoneurons. Moreover if the diameter of the motoneuron is small, the critical firing threshold of its cell body is consequently low, thus the muscle it innervates is more fatigue resistant.
These relationships constitute the "size principle" and contribute to our ability to control force in a smooth and graded fashion. More specifically, the initial force contraction produced by a muscle is attributable to small α-motoneurons discharging intermittently and then discharging more frequently [16] . Stronger muscle contractions are due to the depolarization of increasingly large α-motoneurons within the motoneuron pool, concurrent with increases in the firing rates of the smaller α-motoneurons already active. The maximal levels contraction and force are reached thanks to a further increase in the rapidity of the motoneuron pool firings.
Another consequence of the size principle is that muscles with a low innerva-

tion ratio, which is the number of muscle fibers innervated per motoneuron, are capable of producing more rapid and precise actions than muscles with a higher ratio.

1.4.4 The Contraction

The contraction of a motor unit is initiated by an action potential traveling from the cell body of the α-motoneuron, along its axon fibrils to the muscle motor unit fibers. Subsequently, *depolarization* of the muscle fiber membrane occurs, triggering the muscle contraction. The physiochemical mechanism responsible for the contraction involves a complex yet well characterized self-regulating calcium-dependent interaction between actin and myosin molecules. The membrane depolarization thus causes a time-varying transmembrane electric current field that evokes potential changes in the extracellular tissue, which can be measured invasively or intramuscularly by means of needle or wire electrodes, as well as non-invasively from the surface of the skin above the muscle [17][18][14].

1.4.5 Muscle fatigue

Muscles that are used intensively show a progressive decline of performance which largely recovers after a period of rest. This reversible phenomenon is called muscle fatigue. This is particularly clear when maximum isometric

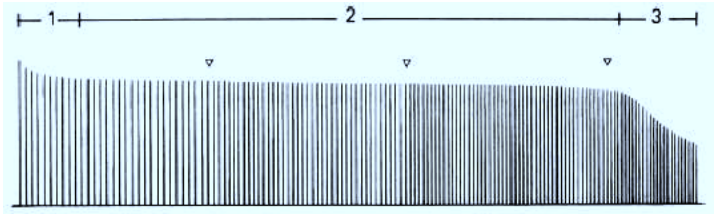

Figure 1.20: Force records during fatigue produced by repeated short tetani in an isolated mouse flexor digitorum brevis fiber; each tetanus appears as a vertical line. Stimulation protocol: 350-ms, 70-Hz tetani repeated every 4 s for 2 min, and the interval was decreased by approximately 20% every 2 min (interval changes indicated by open triangles). [19].

force is measured in repeated tetanic contractions, which occur when a motor unit has been maximally stimulated by its motor neuron. This happens

due to multiple impulses stimulating the motor unit and not giving it time to relax between contractions. Therefore the strength of impulse is increased as it is added to the previous impulse, creating a maximal contraction. During the repetitions of the contractions, a progressive force decline is visible even on the second tetanus of the series (Figure 1.20).
Other aspects of muscle performance also change during fatigue, in particular shortening velocity is reduced and the time course of relaxation slows down. Most practical activities are dependent on the power output of the muscles involved and, since power output is the product of both force and shortening velocity, the decline in performance can be larger than the decrease in isometric force. Of course, the decline in performance is not immediately apparent if a submaximal activity is performed, and in this situation fatigue manifests itself eventually as a failure to be able to continue the activity at the original intensity, often called exhaustion. In such an activity, the progress of fatigue can be estimated by occasionally interpolating a maximal contraction [20][19].

Chapter 2

Hand prosthesis: the state of the art

This chapter presents the state of the art technologies applied to the prosthetics of the upper-limb: the most important projects all around the world are shown in detail. The goal is to understand how the commercial devices can be improved in order to satisfy the needs of the amputees and to increase the know how for a future design of our own prosthetic hand. In particular, this study focuses on the trend followed by the scientific research in the field of the EMG control, and on the results obtained. Eventually, it is concluded the parallelism between the artificial and the real limbs.

2.1 Introduction

The loss of a limb is a traumatic event in a person's life and even more when it comes to the hand: its functionalities are necessary not only in prehensile tasks, but also when one wants to sense the surface conformation, the temperature of an object or receive a proprioceptive feedback. Moreover, the hand is one of the body parts most used in communication: humans are used to perform a lot of gestures to express feelings and concepts. Not least comes the aesthetic function: the hand is used to interact with other people and usually their opinion about its appearance is very important for the amputee.
Thus the study of a prosthetic hand is a complex problem, from a functional to a psychological point of view, indeed it has being studied along the years by medics, engineers and psychologists. The focus of the modern research on this field has been put on the priorities of the amputees. It is important to understand what are the needs of a person during his lifetime, because

not every movement or prehensile pattern can be reproduced with the state of the art technology [21].

2.2 Upper-limb amputation: statistics

In order to understand the extent of the upper-limb amputation phenomenon, a deep analysis on the statistical data from the two National Health Interview Survey made in United States in 1988 and 1996 is presented. At that time, there was an average of 133,735 hospital discharges for amputation per year: in contrast with lower extremities amputations, which were mainly due to dysvascular causes, upper-limb amputations had been mostly trauma-related (68% out of all the trauma-related). The second reason for an upper-limb amputation is cancer (23.9% out of all the cancer cases), then the dysvascular one (3% out of all the dysvascular cases). More than half of the trauma-related upper-limb amputations occurred at the lowest level (the finger), then at the thumb (12%), at the transradial level (2% - between elbow and wrist) and finally at the transhumeral one (1.5% - between shoulder and elbow). Moreover, considering the congenital losses, in 1996 the incidence is of 1,500 over 10,000 live births: the 58% out of all the discharges is related to the upper-limb, of which the 27% is at the longitudinal hand level [22].
Currently it has been estimated that in the U.S.A., there are approximately 1.7 million people living without a limb: one out of every 200 people has had an amputation [23] [24].
The main idea to keep in mind from the previous set of percentages and numbers is that *the most part of the upper-limb amputations are caused by a traumatic event.* This fact has an important impact on the psychology of the amputee, which will be further explored in the next section.
The latest important data on which to reflect is that there are approximately 1,908 upper-limb amputations a year versus 56,912 lower-limb amputations: the upper-limb amputees population is much smaller. Therefore, it is often noted that *upper-limb amputees feel isolated from their peers*[25].

2.3 Upper-limb amputation: psychological impact

The psychological repercussions of a traumatic event, like losing a hand, are many and of various nature. Each one has to be addressed in order to help the patient to overcome the worst moment of his life.
The previous section highlighted two problems that mainly upper-limb am-

putees have to cope with: the traumatic event that upsets their life and the fact of being a smaller amount of people with respect to the lower-limb amputees.
The upper-limb amputation causes are proved to be more related to a traumatic event in comparison to the lower-limb ones, which mainly are the effect of tumors or disease. Therefore, as with any other progressive disease, the patient often has some time to psychologically prepare himself for the possibility of amputation. The traumatic injury presents one more issue: the unpredictability. Overnight, a person loses his hand and, with it, his self-esteem, starting to encounter body-image concerns and to feel isolated. The upper-limb amputees population is long way less numerous than the lower-limb one, which makes the upper-limb amputee feel isolated even from people dealing with other type of amputations. Moreover, for the reason mentioned above, the literature and resources available are unintentionally focused on lower-limb concerns, with the possibility to bring more discouragement to the already difficult situation.
The upper-limb amputee must cohabit with his own disability all day long for his entire life: the hand is constantly exposed to the patient sight. Other psychological concerns may arise because of the loss of the dominant hand functionality: some habits that identified the patient must be changed, as handwriting, playing an instrument, drawing, painting or cooking. This causes a slower rehabilitation.
Furthermore, an amputee shares with other patients, affected by other kind of amputations, problems like post-traumatic stress disorders and other psychological concerns:

- nightmares or flashbacks of the accident;
- avoidance of the topic;
- emotional numbing;
- hyperarousal;
- phantom limb pain that could inhibit the rehabilitation;
- feeling of a decreased ability to defend themselves;
- depression caused by the loss of the job [26].

The upper-limb amputees are famous for rejecting prosthetic devices at a high rate, therefore researchers are questioning about the resources needed to enable the patients to cope with their limb loss and eventually with their

prosthesis. It has been found that individuals with upper-limb loss who are fitted within 30 days of amputation are more likely to accept prostheses than those fitted after 30 days. Moreover, differences between unilateral and bilateral amputees have an important consequence on acceptance. Unilateral amputees tend to master tasks with one hand, rejecting prostheses, as opposed to bilateral amputees, who require prostheses for some prehensile activities [27]. The findings of several studies led to the conclusion that mental health professionals need to be involved in the care of this population in addition to a screening tool being available to routinely address psychological adjustment [25].

2.4 From the surgeon point of view

The surgical amputation has evolved significantly since the days in which the limb was severed from the unanesthetized patient and the stump dipped in boiling oil to achieve hemostasis: the modern procedures of amputation have greatly developed after the two World Wars. In particular, within the last three decades, prosthetic research and rehabilitation engineering centers, supported by federal funding, have spread the results of their studies, promoting the enhancement of the know how.
Surgeons have the patient's life in their hands: when they have to face an injury caused by a traumatic event, they have to think and act in a very small time. This is the case of the amputation surgery, therefore the doctor must be aware of all the possible procedures to apply in each particular situation, in order not to lose time.
Each site throughout the upper or lower limbs has individualized characteristics of bone shape, nerves, musculature and blood vessels, as well as particular muscle, skin and soft tissue envelope structures available for padding, protecting, and reconstruction. A deep understanding of the anatomy of each site mentioned above would help the healing and the prosthetic rehabilitation, when deciding where and how to amputate.
A particular consideration can be made about the upper-limb case, deciding wether to salvage or amputate. The upper extremity doesn't have to support the whole body, in contrast with the lower extremity, therefore, even if the salvage will keep minimal assistive functions, it is often better than the prosthetic substitutes available on the market.
The surgeon has to go through important decisions before acting. He has to chose between amputation versus salvage and determine the most distal level of amputation still compatible with wound healing and subsequent satisfactory prosthetic fitting: in upper-limb amputations the transradial

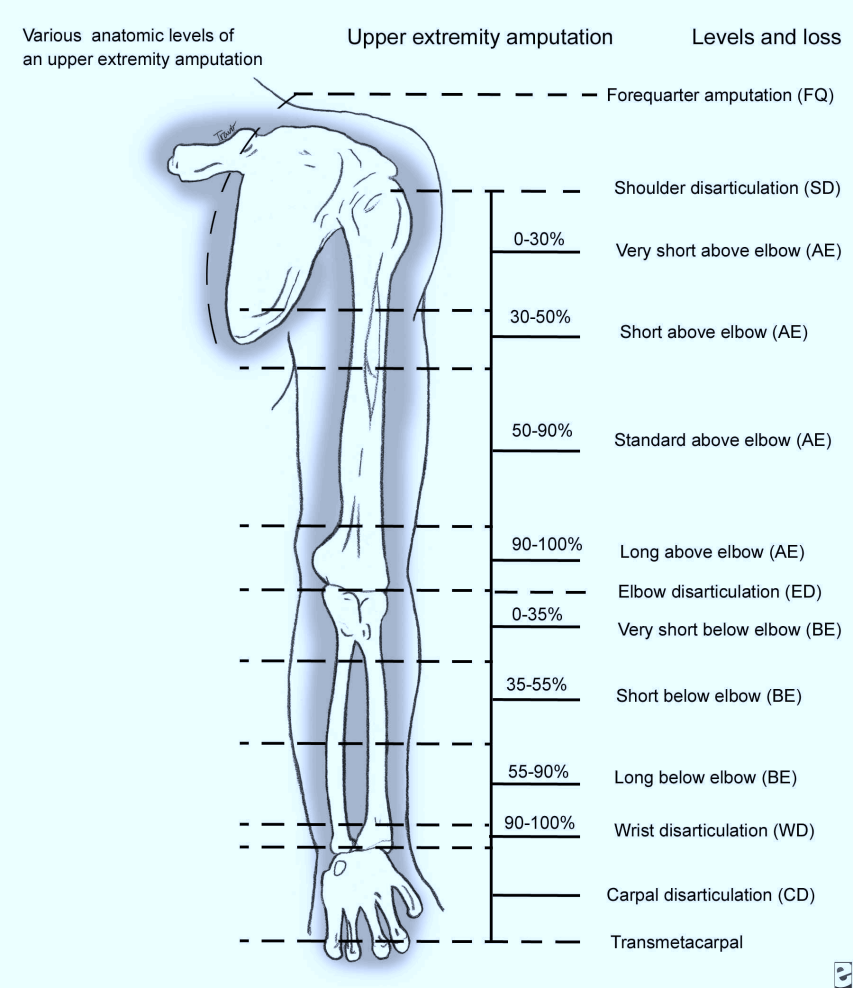

Figure 2.1: Amputation levels: the percentages represent the standard length of amputation at a given zone [28].

(elbow-wrist) one is preferred. The goal in modern amputation surgery is to conserve the length of the stump and obtain a well-healed, non-tender physiologic residual limb: in this way the prosthetic suspension and force transmission from the residual limb to the socket is improved [5]. Of course this surgical operation has important risks like joint contractures, phantom limb pain, neuroma formation, stump breakdown and, in children, bony overgrowth: all aspects that have to be prevented [29].
Doctors assert that immediately applying a prosthesis, brings astonishing physical and psychological rehabilitative advantages: the patient avoids a limbless period so that he can straight start to cope with the functional

restoration and accept the new extraneous device. Support and encouragement offered by the hospital environment are essential in order to return to a regular activity level.
We have to think not of artificial limbs, but instead of replacement limbs. The surgeon capable of making an amputation successful, can indeed help make the patient whole[30].

2.5 Hand prosthesis: functional classification

At present the choice in the prosthetic upper-limb market can be divided in two main groups, the *passive* and the *active* ones:

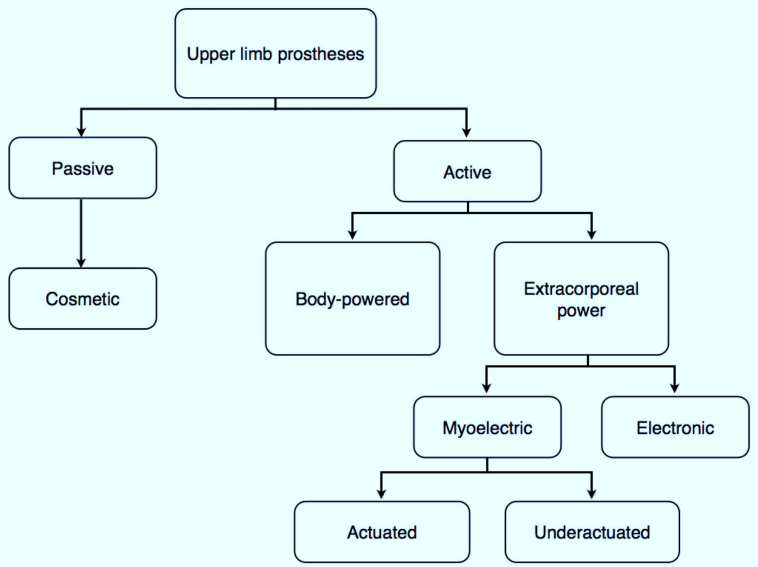

Figure 2.2: upper-limb prostheses classification.

- The upper-limb *passive* proshtesis (Figure 2.3) cannot be actively controlled, but it can be considered as a realistic reproduction of the amputee hand. Laboratories specialized in this field can customize the device depending on the patient's skin color and on the conformation of the healthy hand, achieving astonishing results. The drawback of this kind of prostheses is that it only provides an aesthetic functionality and doesn't restore any kind of dexterity to the amputated limb, even if the amputee can use it to push objects or help the healthy hand for simple manipulations.

Figure 2.3: Passive aesthetic prosthesis

- The *active* devices can be further divided into two groups, the *body-powered* and *extracorporeal powered prostheses*:

  - The *body-powered* (Figure 2.4), upper-limb prosthesis is sustained by a harness and actuated through relative body motion: a control cable is routed through a housing so that the tension is transmitted to the prosthesis. In this way the prehensors can be operated in either a voluntary opening or voluntary closing mode. The low cost, high reliability, light weight and simplicity of body-powered systems make them a reasonable choice, even if we have to consider as a drawback the presence of the cable that make them uncomfortable [31][32][33].

  - The *extracorporeal power prostheses* are classified in *myoelectric control* and *electronic control prostheses*:

    * The electric signal associated to the muscular contraction and more precisely to the ionic currents, flowing along the muscular fibers causing the muscle shortening, is called electromyographic signal (EMG). The *myoelectric prostheses* (Figure 2.5) use this signal, recorded form the amputees stump using a surface electrode and an electromyograph, to interpret the will of the amputee and reproduce the movement that he would do if he had his own limb [34]. Due to the difficulties in the electromyographic signal interpretation, the most of the commercial hands just recognize two kinds of movements: the opening and closing

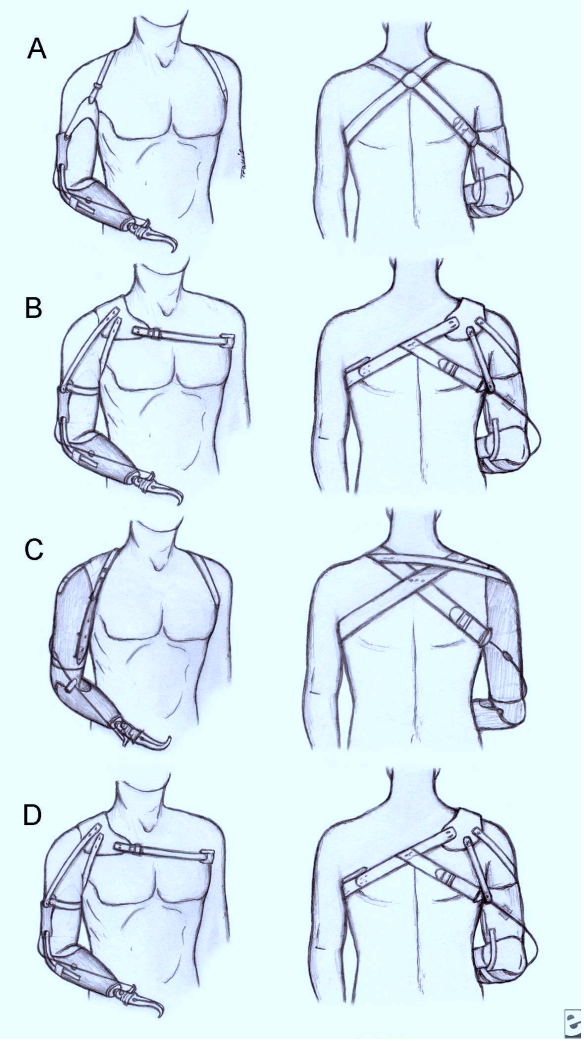

Figure 2.4: Harness of a body-powered prosthesis [28]

ones. This is achieved by recording the signal from two antagonist muscles, inasmuch the signal is stronger when recorded from a nearby muscular area, allowing the system to manage two very distinct signals.
Current commercially available prosthetic hands don't provide any kind of feedback except the visual one [35][36].
Myoelectric prostheses can be further divided in two subgroups: the *undercatuated* and *actuated* ones. The difference between the two is that the underactuated

prosthetic hands provide less actuators than the number of the hand's degrees of freedom(DoF). This means that not every joint has a motor, but there are some mechanical devices, like artificial tendons, attached to a smaller amount of motors that allow to flex and extend the fingers, like in a real hand [36].

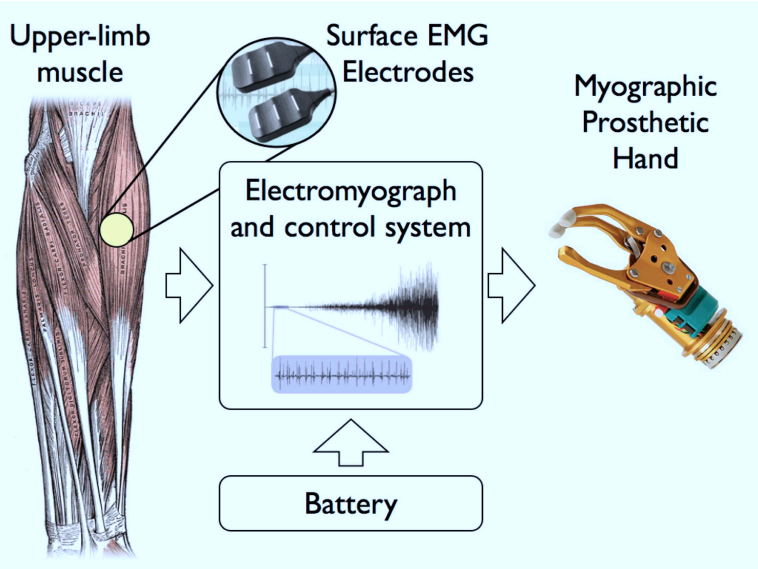

Figure 2.5: Myoelectric prosthesis functional schema

* Another noteworthy type of extracorporeal power prosthesis, is the *electronic control* one. This is less common than the myoelectric device but still in use. In this group are included servo controls, electronic switch controls, electronic touch controls and sometimes these features are merged together to constitute an hybrid system [37]. The *electronic control prostheses* are more useful than the myoelectric ones in particular situations. For example in case of congenital pathologies to the shoulder, where the muscular situation is anomalous and moreover there are protuberances, or even small fingers, that the patient can move. The amputee can use them to control the electronic switches in order to actuate the prosthesis [38].

2.6 Amputee's needs

In September 1992, The Institute for Rehabilitation and Research (TIRR) in Houston was awarded a two-year grant from the National Institutes of Health/ National Center for Medical Rehabilitation Research (NIH/NCMRR). More than 6,600 one-page surveys were sent to individuals with upper-limb loss or absence, throughout the United States.
The results of the surveys indicated necessary improvements in the design of a better upper-limb prosthesis. These qualities include additional wrist movement, better control mechanisms that require less visual attention, greater finger movement, the ability to make coordinated motions of two joints, better gloving material, better batteries and charging units, and improved reliability for the hand and its electrodes [39].
In the scope of another survey (2002), seventy Australian upper limb amputees responded to a detailed postal questionnaire asking how often they wore their prostheses and their level of satisfaction with both their prostheses and their functional abilities.
Only 44% of amputees reported wearing their prosthetic limbs half the time or more. These low levels of use might be partly due to dissatisfaction with the prostheses regarding the sweating, cosmesis, discomfort of the harness and strong pain.
The individual activities with which respondents recorded the greatest dissatisfaction were "using a knife and fork", "peeling vegetables", "tying shoelaces", "tying necktie", "buttoning shirt sleeves", "cutting nails", "carrying tray", "using a hammer and nail", "rewiring a plug" and "carrying multiple packages at once". Prostheses were rarely used for dressing tasks, while they were used more frequently in domestic activities such as food preparation, handy work, gardening, and work activities.
Many survey respondents were able to be independent and return to work without using prostheses, and many were quite satisfied with their functional abilities, regardless their level of prosthesis use.
Amputees need not only prosthesis rehabilitation, but also a program to assist them in their return to vocational, psychological, functional, and social wellness [40].

2.7 Commercial prostheses

The most common commercial electromyographic prostheses aim more at the reliability of the movement than at the complexity of the grasping patterns. Furthermore, the effort required to simultaneously control many

EMG inputs, leads to commercial prostheses that support only simple single DoF[41]. The ideal prosthetic hand is a cheap, visually appealing, lightweight, long running, highly dexterous and easily controlled devices. Moreover the sensorial feedback would be the feature that makes it the sensible replacement of the lost hand.
Unfortunately the state-of-the-art commercially available prosthetic hands are far from this ideal target: the current best devices are the SensorHand Otto Bock (2008b) by Otto Bock, and iLimb by Touch Bionics. At the time of writing two more advanced prosthesis are entering the market, but the there are very little informations about them: the MichelAngelo by Otto Bock and the BeBionic by RSL Steeper[42].

2.7.1 SensorHand by Otto Bock

The SensorHand (Figure 2.6) is a classical prosthetic "claw", endowed with one degree of freedom, which is typically proportionally controlled by one or two electromyography electrodes.

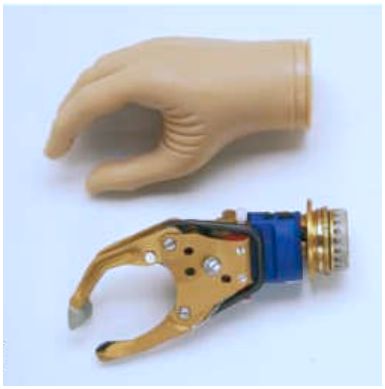

Figure 2.6: The SensorHand by Otto Bock

While the external glove is composed by five non-articulated fingers, the actual support has three extremities. The thumb in the support is matched with the thumb in the glove, the second finger in the support is matched with the index and middle finger in the glove and eventually the third support's extremity is matched with the glove's ring and little fingers. The single degree of freedom of the hand just allows the opening and closing movements

around the metacarpal joint: the thumb is in opposition to the index/middle finger, reproducing a claw.
The proportional speed range is 15-300 millimeters per second, which is twice the speed of other myoelectric hands. Furthermore a proportional grip force of 100N can be reached, despite the weight of 460 grams. In addition, the system can recognize when an object starts to slip from the hand and automatically increase the grip force, thanks to the AutoGrasp feature: this is one of the most important characteristics of the device and is achieved with the SUVA sensory system.
During the gripping phase, the SUVA sensors measure the vector force at the extremities of the hand, therefore when the object starts to slip the control system increase the grip force. This algorithm works in background without the intervention of the amputee, who is relieved by the fact that he doesn't have to schedule the whole prehension process. A clarifier example is the situation in which the hand is holding an empty glass: while water is poured, the hand automatically tunes the force to apply, without the help of the patient [5].
According to the analysis of the state-of-the-art of the Otto Bock hand, the main problems to be solved are [43]:

1. lack of sensory information given to the amputee;
2. lack of a "natural command" interface;
3. limited grasping capabilities;
4. unnatural movements of fingers during grasping;
5. low cosmetics.

2.7.2 iLimb by Touch Bionics

The iLimb hand is the first prosthesis in the market with five individually powered fingers. Each one is composed by two articulated phalanx, driven by a tendon which is connected to a DC motor. All the motors are activated together by the EMG signal, but different configurations can be achieved by individually stopping the fingers, by means of mechanical friction.
Actually there isn't any official technical paper available, but Touch Bionic asserts that the hand has a built-in stall detection feature, which tells each individual finger when it has sufficient grip on an object, thus when to stop powering. Individual fingers lock into position until the patient triggers an open signal through the muscle.

The thumb is fixed to a passive joint, which can be manually operated in order to achieve different prehensile patterns (Figure 2.7) [44]:

- key grip: the thumb closes down onto the side of the index finger. This grip is used to hold items such as a plate or a business card. The addition of wrist rotation enables the patient to turn a key in a lock in a totally "human" way;
- power grip: all fingers and the thumb close down together to create a full-wrap grip. This grip would be used to hold a can of drink whilst opening the ring-pull, for example, and for carrying large objects such as a briefcase or shopping bag;
- precision grip: the index finger and thumb meet (or index finger, middle finger and thumb meet) in order to pick-up small objects and to hold objects when performing finer control tasks;
- index point: the thumb and fingers close, but the index finger remains extended. Patients have found this grip very useful for operating computer keyboards, telephone dial pads, ATM cash machines and a host of other everyday requirements.

Figure 2.7: The prehensile patterns allowed by the mobility of the thumb.

The iLimb prosthesis is better than the other commercial devices from different points of view:

- five independent fingers available: the hand is capable of different grasping patterns;
- multiple contact points with the grasped object: more secure grip;
- opposable thumb;
- the hand is much more realistic;

The drawbacks are the cost and the lack of any kind of feedback to the user, except the visual one, of course.

2.7.3 The hands of the near future

In the time of writing, Otto Bock and RSL Steeper are refining their last creations: the informations about these new products are very few for obvious reasons, however a little presentation of their features is going to be shown

2.7.3.1 MichelAngelo by Otto Bock

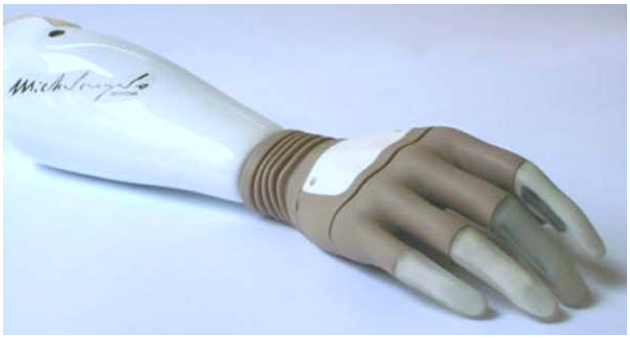

Figure 2.8: MichelAngelo by Otto Bock

The MichelAngelo prosthetic hand (Figure 2.8) is clearly inspired by the Touch Bionic's iLimb, it is endowed with two electrodes and five independent fingers: therefore it is guessable that only the opening and the closing movements are available. This means that it doesn't bring any new grasping abilities, compared with iLimb, even if Otto Bock asserts that it has six DoF which is new in the prosthetic hand market.
The engineers working on the project assert that the MichelAngelo hand provides proportional control for multi-axial movements, but a complexity reduction had to be achieved by controlling movement synergies rather than the individual DoF[45]. This means that we can expect that the hand is underactuated in order to simplify the movement patterns and reduce its weight.
Moreover they say that even if high-bandwidth signal transduction from the subject to the device is in sight, the information flow in the reverse direction will retain severe limitations. In order to exploit recent advances in robotics in prosthetic devices, appropriate feedback signals must be reconstructed from an optimal combination of local sensors and efficient data

analysis [45]. It looks like the engineers at Bnft-Goettingen are working to achieve some sort of feedback, which is still not available in any commercial prosthetic device.
The drawback of this new prototype is the cost, even if the hope is that the increasing competition in this field will make these objects more affordable.

2.7.3.2 BeBionic by RSL Steeper

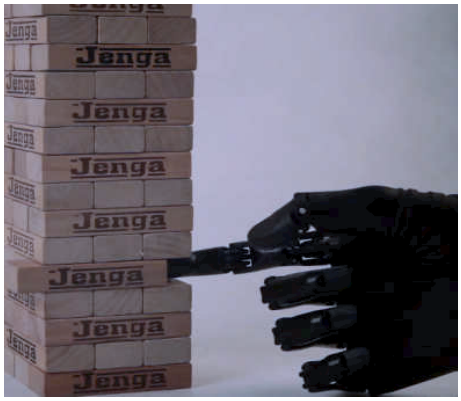

Figure 2.9: BeBionic by RSL Steeper

Looking at the previews of the BeBionic (Figure 2.9), the expectations are very high. RSL Steeper presents it this way: "Bebionic hands feature naturally compliant grip patterns combining innovative technology with life-like appearance. Functions of the hand such as speed, grip force and grip patterns may be custom programmed to suit individual user requirements through smart software and wireless technology. Lighter than existing products, it will be available to the market at an affordable price.
The bebionic range will also include the world's first powered wrist with rotation as well as flexion/extension. Completing the range is an advanced silicone skin available in 19 skin shades."[46]
From this little presentation we can understand that the most important feature will be a higher mobility of the wrist, which is very important for the patient: unnatural movements will be avoided thanks to the two DoF of the wrist. Another noteworthy characteristic is the reprogrammability of the device in order to accomplish customized task depending on the patient.

2.8 Scientific research

In the last decades, classical robotic knowledge has been introduced in the myographic prosthetic hand field, in order to investigate new and more complex systems, aimed at matching users' desires and expectation.
The scientific research is focusing on new intuitive human-prosthesis interfaces, in order to allow the control of more DoF. Moreover the bidirectional data exchange with the device has gained much importance: the aim is to give some kind of feedback from the prosthesis to the user.
Other fields of interest are the improvement of the performances, the dexterity, the anthropomorphism and the cosmetics of the prosthetic hand [47].

2.8.1 Mechanical design

Due to the need of aesthetic and light solutions, in the last two decades the common choice has been to use less actuators than the actual number of DoF of the hand. This approach allows to install less motors, thus reducing the bulk and inertia of the manipulator system. Underactuation is achieved by linking together the motion of the joints of a finger, or even of two whole fingers. The problem of this approach is that the hand's DoF would actually be the same number as the actuators in the device, which leads to a poor adaptation to the object geometry. This problem can be overtaken using tendons transmission between consecutive joints in order to use few actuators, while maintaining the joints mobility.

2.8.1.1 Tendon driven hands

The MARCUS, Hokkaido, RTR II and CyberHand hands[5] are examples of devices endowed with tendon driven fingers (Figure 2.10). Each distal phalanx is connected to its respective actuator by a lever based on a cable. In this way the fingers can wrap the objects around and spread the force over multiple contact points. Being the grip well distributed, it is much more stable [48].

2.8.1.2 Bar mechanism

The Southampton REMEDI hand is based on a different kind of phalanx linking. It has six DoF, consisting of six small electrical motors: two are used in the extension/flexion and rotation movements of the thumb, while

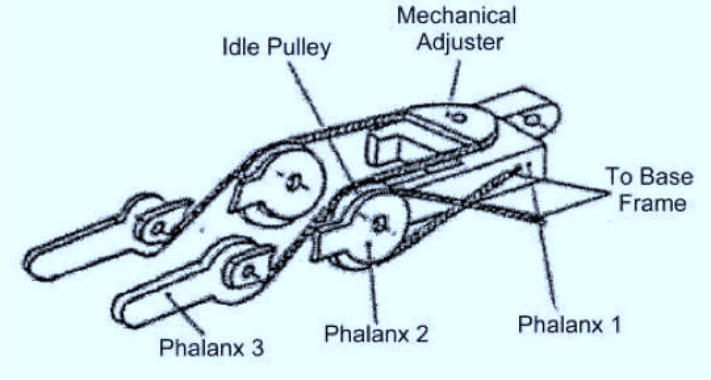

Figure 2.10: MARCUS finger's leverage system [48].

the four remaining motors are assigned to the remaining individual fingers [49]. Each finger is driven by its own worm wheel, which is linked to a system of six independently moving bars, composing the finger. This particular design is mechanical efficient and avoids backlash, which is characteristic of the tendon driven links (Figure 2.11)[50].

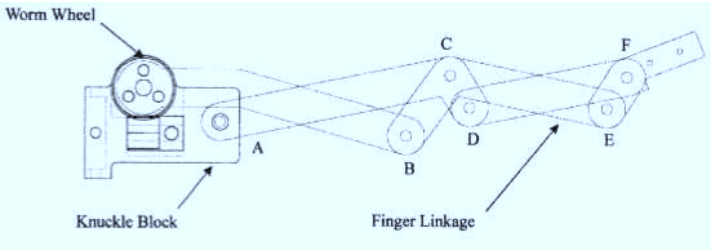

Figure 2.11: Bar mechanism design schematic [50].

2.8.1.3 Wrist and thumb actuation

What makes the MANUS-HAND special, compared to the previous hands, is of course the wrist and thumb mechanisms. This hand is provided with ten joints, of which three are independently driven (Figure 2.12):

1. the finger mechanism: a crossed-tendon mechanism is used in the fingers instead of the more traditional bar mechanism in the field of

robotics;

2. the thumb mechanism: the thumb movements are coupled by means of a Geneva-wheel based mechanism, which makes it possible to use one actuator for thumb movements in two planes(cylindrical and lateral grasps). To the MANUS' designers knowledge, this is an innovative aspect of this hand;

3. the wrist mechanism: commercial Ultrasonic motors have been used to drive the wrist pronation-suppination;

The fourth and fifth fingers of the MANUS-HAND are provided with a martensitic structure. These fingers can be manually shaped for long-term grasps [51].

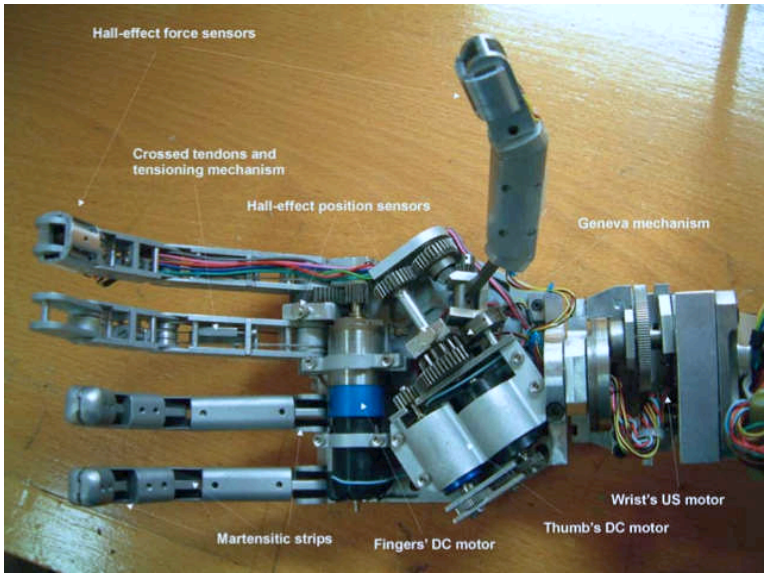

Figure 2.12: The MANUS-HAND [51]

2.8.1.4 Fluid actuation

In 2007 the Ultralight Hand has been presented: it is a very lightweight artificial hand endowed with five fingers and 13 DoF driven by a new type of powerful small size flexible fluidic actuator. The actuators are completely integrated in the fingers which allowed the design of a very compact hand. Because of the elastic properties of the actuators the contact force is spread

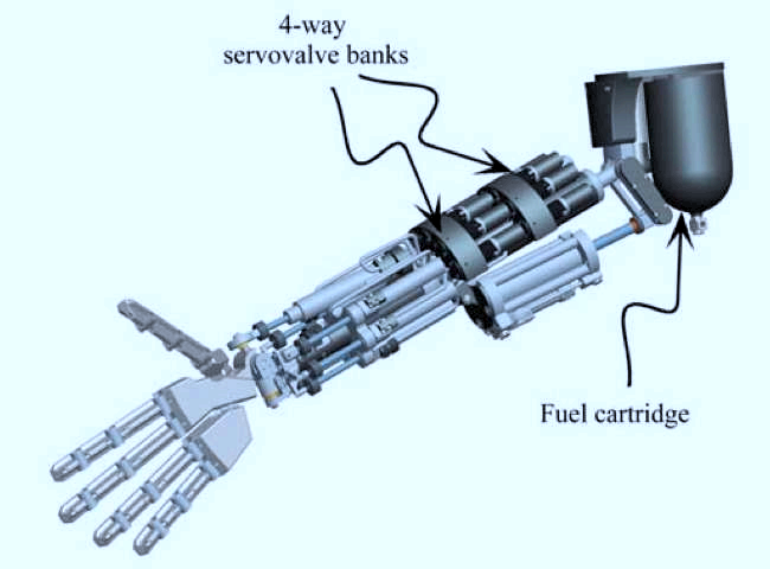

Figure 2.13: Pneumatic arm by the Vanderbilt University [52].

over a greater contact area. Additionally the surface of the fingers is soft and the friction coefficient is increased by the silicone-rubber glove, that covers the artificial hand. The result is that a reduced grip force is needed to hold an object.
Because of the self adapting properties of the fingers many different objects can be grasped without sensory information from the hand. This enables the developement of a low-mass prosthetic hand with high functionality. The wrist is also flexible and a rotation of 30 degrees in each direction can be achieved [53].
In the same year an anthropomorphic 21 DoF, 9 degrees of actuations arm prosthesis for use by transhumeral amputees was presented by the Vanderbilt University (Figure 2.13). The energy demand of the system is satisfied by the catalytic decomposition of the monopropellant hydrogen peroxide, which has recently been shown to provide better performances than state-of-the-art batteries and electromagnetic motors. The catalytic reaction upon which the approach is based is strongly exothermic, and the resultant thermal energy is transduced to mechanical works via the expansion of the gaseous reaction products. This system allows the presence of five pneumatic actuators in the hand which can drive 17 DoF: the actuators forces are applied through a series of cables and cable sheaths, which are equivalent to the tendons. The qualities of this hand are that no power consumption is required for isometric

contractions, liquid propellant is nonflammable and insensitive to shock and the low temperature benign exhaust is projected to be both visually and audibly insignificant [52].

2.8.2 Sensory systems

2.8.2.1 Proprioceptive systems

The proprioceptive sensors are used to detect the state relative to an internal reference system. In the next paragraphs the most common ones are presented.

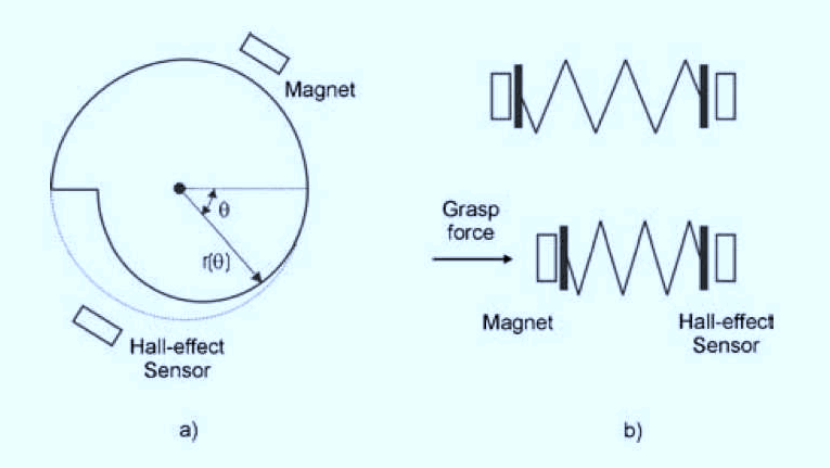

Figure 2.14: MANUS-Hand Hall effect: (a) Position sensor, (b) Force sensor [51]

Position sensors: the Hall effect is the principle behind position and force sensors mounted on the MARCUS, RTR II, CyberHand and MANUS-Hand hands prototypes [5][48].
Position sensors were developed by placing a permanent magnet opposite to the Hall effect sensor. In between, a cam made of ferromagnetic steel modifies the reluctance of the magnetic circuit resulting in a linear relation between cam rotation and output voltage. In the MARCUS hand, for example, the magnetic plate is fixed to the first phalanx structure and rotates with respect to the joint rotation axis, while the Hall effect sensor is fixed to the metacarpus phalangeal joint [48]. Therefore it is possible to sense

the rotation of the joint of each disarticulation of the hand and compute the actual configuration of the finger. The force sensors are embedded in the fingertips and based on Hall effect pick-ups as well. In this case, the permanent magnet is spring mounted and the resulting magnetic field at the Hall effect sensor location results in a linear relationship between force exerted and output voltage (Figure 2.14)[51].

Magnetic encoders: the Southampton REMEDI and CyberHand hands motors are endowed with digital magnetic encoders and motor-current sensors, which respectively provide finger position and the force applied to the manipulated objects. The advantage of this system is that the sensors are an integral part of the electronic hardware interface. This is crucial to the minimization of lead length between the analogue sensor and signal processing components (thereby limiting noise interference from the motors), as well as eliminating the need for externally mounted devices which are susceptible to reliability problems.

The cable tension sensor is based on a micromechanical structure which can continuously monitor the cable tension applied by the motors of the fingers. It is mounted in some tendon driven underactuated hands like the RTR II and CyberHand hands [5]. This sensor is obtained from a cantilever which is elastically strained by the cable and is fundamental for the low-level control algorithms of the grasping force.

2.8.2.2 Exteroceptive systems

The exteroceptive sensors are used to detect the state of the environment in which the agent is operating. In the next paragraphs the most common ones are presented.

Piezoresistive and piezoelectric materials: an array of thick-film sensors is located on each fingertip cantilever of the Southampton REMEDI hand: it is endowed with a static force sensor and a dynamic force sensor.
The static force sensor exploits the piezoresistive effect exhibited by thick-film resistors. In this effect, the resistance of a thick-film resistor changes in a linear manner with the strain experienced by the resistor.
The dynamic force sensors are essentially vibration sensors which are made of piezoelectric material: it generates an electric charge on its surface when mechanically deformed. They are used to detect any rapid variations in the

force over the fingertip surface, or vibration, which could be indicative of an object slipping from grasp.

Temperature sensor: is a part of the thick-film array mounted on the Southampton REMEDI hand. The temperature of an object held within the prosthetic hand is determined by monitoring the change in the resistance of a thick-film thermistor paste printed in the space between the two force sensors in the fingertip cantilever. This paste demonstrates a highly linear relationship between resistance and temperature [54].

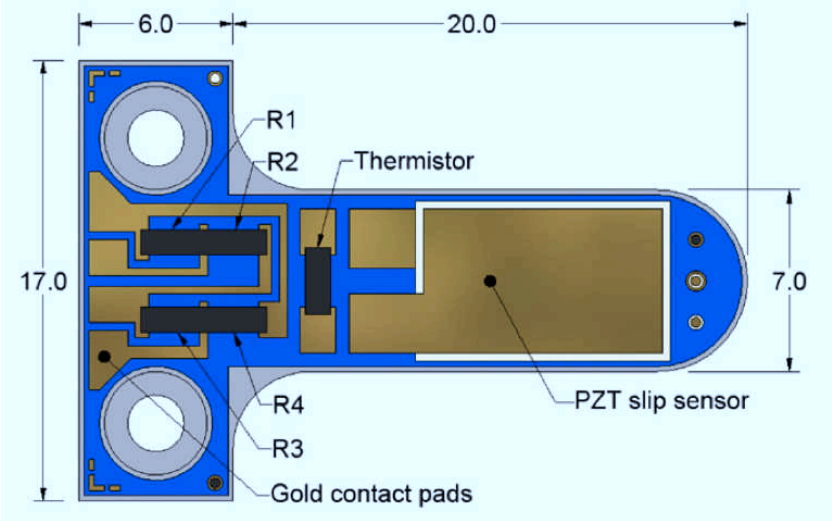

Figure 2.15: Dimensions of the fingertip cantilever (mm) and the location of sensors [54].

Contact sensors: a flexible layer, made of contact sensor arrays, which covers the CyberHand is designed to emulate the sensitivity of the mechanoreceptors of the human hand with pressure thresholds of $< 15mN/mm^2$, that is sensitive enough to be compared with the human receptors.

The triaxial force sensor is integrated in the fingertips of the CyberHand. It is based on an aluminum alloy 3D flexible structure: six semiconductor strain gauges are mounted, three for the sensor itself and the remaining three for temperature compensation. The force sensor can be

used to detect slippage at digit-object interfaces. Moreover it is able to detect object contact as well as object lift-off and replacement, events known to be crucial for the sequential coordination of the grasp-and-lift task in humans.

Force microsensors: the Soft and Compliant Tactile Microsensor (SCTM) system, shows a high sensitivity and robustness and can detect the onset of slippage with an average latency of about 7 ms. These results are very important if compared with the human reactivity, which has a time delay an order of magnitude higher than the SCTM system [5].

Slip sensor: An acoustic slip sensor used in the MARCUS hand provides feedback if an object starts to slide from the hand during the holding phase. The sensor consists of a microphone sealed within a rubber tube, and is capable of detecting air movement which is highly coupled to fluctuations at the finger surface. Hence the signal resulting from an object sliding across the surface of the tube is much greater than any extraneous noise. This device has been improved and integrated into the tips of the thumb, index and middle digits of the Southampton REMEDI hand, as only three slip sensors are required to determine if an object is slipping in any prehensile configuration [55].

2.8.3 Control

The control system is one of the most important aspects of a prosthetic hand because patients have to rely on it, and on its performances. The most common choice among researchers is the use of a two level architecture. The first and higher level is the one under the patient's will. Given that today's devices are endowed with just two electrodes, the control patterns available to the user are few. The second and more sophisticated level is the one that works in background: the prosthetic hand built-in sensory system provides the microprocessor with a lot of useful information during the grasp planning phase.

2.8.3.1 Southampton Adaptive Manipulation Scheme

The Southampton REMEDI (2000) and MARCUS (1995) hands control system, following the idea presented above, are based on the Southampton Adaptive Manipulation Scheme (SAMS), which coordinates all the different DoF to achieve a stable grip. When the user wants to execute a task, like

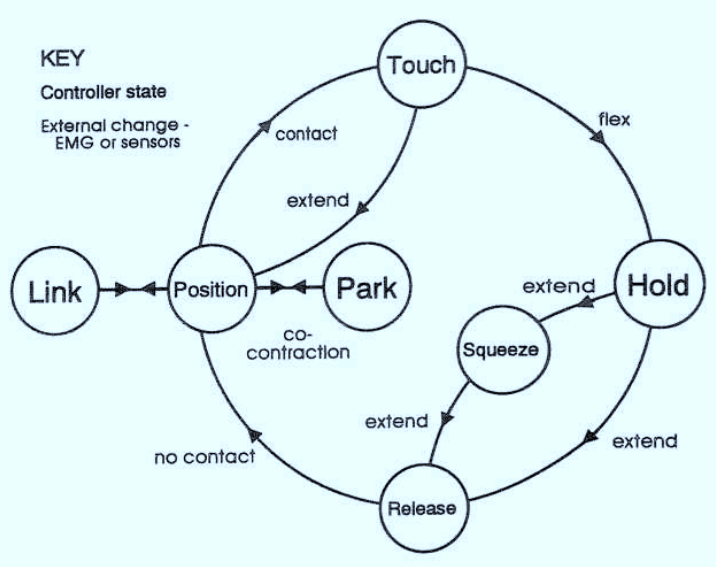

Figure 2.16: State diagram of the SAMS hands. Control is mediated by electromyographic input or contact with sensors on the palmar surface of the hand [56].

moving an object, he just has to produce the EMG signal corresponding to the hand opening and then to bring the device near to the object to grab (POSITION - Figure 2.16). At this point the SAMS system detects the object's shape thanks to the sensors on the palmar surface of the hand and a computer controller selects from a small repertoire the most similar shape. Corrections are made in order to maximize the contact area and minimize the applied force, while the touch is maintained light so that the operator can obtain the best attitude (TOUCH - Figure 2.16). Then the user takes the control back and produce a closing EMG signal (HOLD - Figure 2.16). While the object is held, the system detects the slippage of the objects and adjust the force applied. When the final position is reached the user can produce another opening EMG signal and release the object in the desired spot (RELEASE - Figure 2.16). It is important to set higher threshold when the hand's opening occurs while an object is held, so that it wouldn't be that easy to drop an object (Figure 2.17) [56][57].

2.8.3.2 Spring modeling

The MANUS hand (1998) is endowed with another kind of hierarchical control strategy. Given that the hand has just two active fingers, namely the

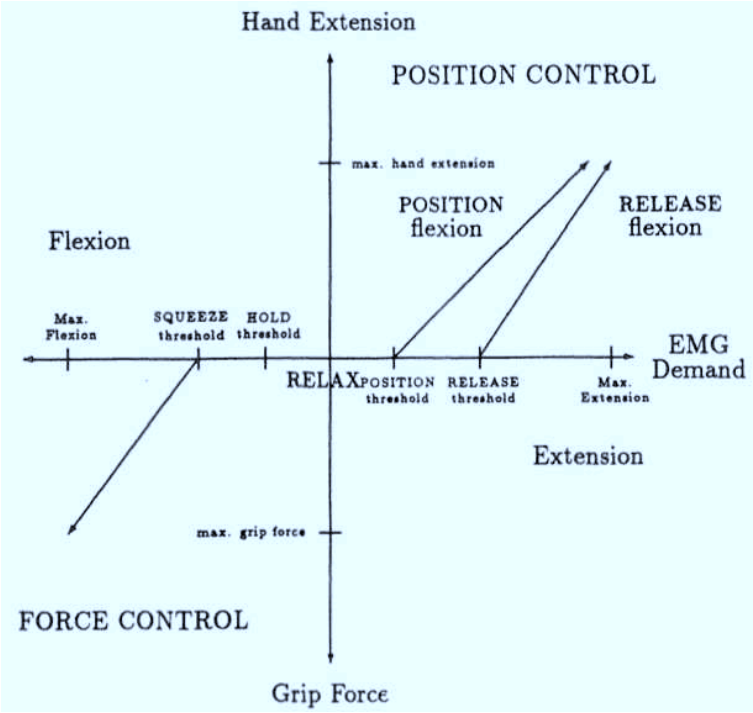

Figure 2.17: EMG control of the SAMS. The flexor and extensor signals are arranged as a continuous range from full flexion to full extension, the vertical axis is hand position or grip for demand, depending on controller state [56].

index and middle fingers, both of them implement the underactuated principle and just one actuator is used. Each finger has a its own low level micro-controller, so that for every grasping mode the finger's performance is determined by a set o desired positions and fingers' stiffness. For instance if cylindrical grasps are considered, the set point would be the full flexion for index and middle fingers and full flexion in opposition for the thumb. The force exerted by each finger during the grasp obeys to Hooke's law, thus behaving as the spring's one (impedance control). When a finger touches the object to grasp and starts applying force on it, if this too high, the finger will move the object against the opposite thumb, but the exerted force will decrease because the finger is closer to the desired position. The procedure presented above recalls a sort of adaption to the object stiffness. Eventually equilibrium is reached when the finger and thumb forces match each other [51].

2.8.3.3 CyberHand Hierarchical Control

The CyberHand control architecture takes inspiration from natural grasping. Grasps are triggered by a higher level unit that is able to recognize the user's intentions and invoke appropriate grasping primitives. In the first implementation of the high level controller a reduced set of primitive grasps has been chosen (cylindrical, spherical,tri-digital and lateral grasp). The grasping task is composed of two subsequent and different phases: the pre-shaping and the grasping (closure) phase. The pre-shaping phase is performed by a PID controller to control the position and select the tendons force, by means of cable tension sensors. During the second phase the prosthetic hand closes the fingers until the desired grasp force is reached. The final grip consists of a bio-inspired balanced distribution of the forces within the hand: each finger has to grip the object with the same force. This is done to increase the grasp stability and to reduce the slippage risk [5].

2.8.4 Bidirectional interfaces

The commercial prosthetic hands don't provide any sensory feedback to the user, so that he has to drive the device relying only on his vision. No tactile or proprioceptive feedback is delivered to the amputee. The most recent scientific researches have tried to overcome this limit mainly focusing on vibrotactile or electrotactile interfaces: the Ultralight [58], the MANUS [51], the Southampton [59], the CyberHand[60][47] and the Yokoi[61] projects have been developing such feedback systems during the last decade.
Vibrotactile stimulation is defined as a tactile sensation evoked by mechanical vibration of the skin, typically at frequencies of 10 to 500 Hz, whereas with electrotactile stimulation a local electric current is passed trough the skin [60]. Eventually, the approaches of the future are presented, namely the surgical implanted peripheral neural interfaces and reinnervation procedures.

The vibrotactile approach is based on the simple intuition that a vibratory response, varying contiguously with a sensory stimulus such as grasping pressure, can be a useful feedback to the patient in the moment in which he has to control his grip force. Typically, vibrations are applied in discrete frequencies to the ventral skin of the forearm. The patient's frequency discrimination ability is determined by the correct recognition of unambiguous frequency steps.
The vibrotactile feedback system implemented by the Johns Hopkins University [62], employed a C2 tactor (Engineering Acoustics, Inc.) that was

mounted to the upper arm with an elastic band. The stimulation protocol was a square wave amplitude modulated signal that produced a train of discrete vibratory pulses. The waveform was modulated in two ways: variations of the envelope frequency as well as variations of the vibratory carrier frequency (Figure 2.18). The envelope frequency conveyed grasping force information. Slower pulsations represented a weaker force and rapid pulsations represented a stronger force. This stimulation protocol was chosen because the intensity of a vibrotactile sensation does not grade well with the vibration amplitude or frequency. Rather, the repeated stimulation of rapidly adapting receptors at different envelope frequencies can provide a suitable impression of varying intensities. In the scope of the Johns Hopkins University project, a subject was asked to reach preset force levels with the vibrotactile feedback. The force information measured by the strain gauge was related to the envelope frequency delivered to the subject. Higher envelope frequency correlated with higher grasping force. The carrier frequency

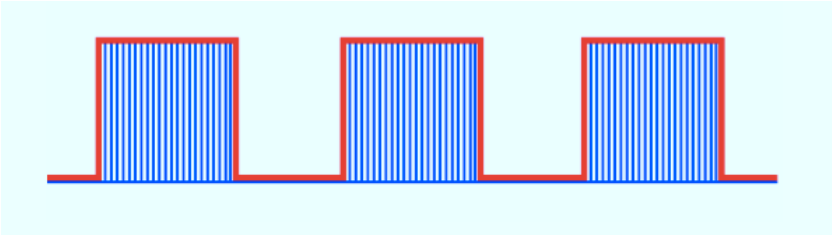

Figure 2.18: Envelope frequency shown in red, carrier frequency in blue [62].

was varied from 100 Hz to 230 Hz to correspond to the position of the hand as reported by the position sensor. This modulation conveyed some proprioceptive information which could be useful for determining object stiffness in situations where the user loses vision of the prosthetic hand. Of the different principles of force feedback, a vibrotactile system was chosen, because acceptance among patients is high.

A group of german researchers tested thirty persons without amputation, two female and two male persons with an upper limb amputation [58], in order to understand their degree of acceptance and of satisfaction regarding the vibrotactile system. The exercise consisted in grasping a soft ball, first with and then without visual control. During the phase in which they could see, all the patients were surprised at the beginning of the grasp, because, even though they had thought that they had not yet touched the ball, the vibrotactile feedback was active. After few minutes, the tested persons already reduced the visual control of their prosthesis. The users have shown considerable interest in a force feedback system and they supposed that its application will clearly raise the acceptance of the prosthesis. This feedback system looks particularly helpful when grasping soft or fragile objects and can also be used for learning to control the hand via myoelectrodes [58].

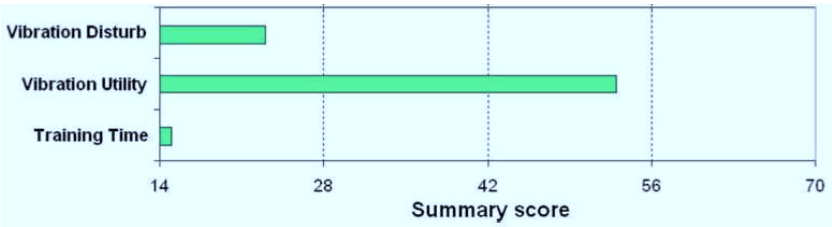

Figure 2.19: Summary score graph on the vibrotactile feedback system and on the duration of the training time [47].

Subjective opinions have also been collected during the testing phase of the CyberHand project. The question referred to the system benefits during the selection of the force closure and about the discomfort caused by its wearing. The opinion on the vibrotactile feedback system is summarized in Figure 2.19. According to all the subjects, the vibrotactile system does not disturb at all and is helpful during the grasp tasks. The analysis of training duration is also shown in Figure 2.19: subjects feel that a very short training

time is required in order to correctly use the prosthesis [47].

The electrotactile approach is used in the Yokoi hand [61], in order to provide the human body with more feedback channels. Two different types of stimulation have been tested, surface stimulation and interferential current stimulation. Interest was also posed on their influence over the EMG acquisition process, in order to determine the best approach to provide tactile feedback in the prosthetic application. Even though the EMG signal obtained from the user body is contaminated by the electrical stimulation, the error in the pattern recognition process is considerable low. The researchers working on the Yokoi hand state that the surface stimulation method gives promises to be a suitable method, while the interferential based method, whether easier to discriminate, produces a SNR of 90%, rendering the pattern recognition process unusable.

Neural Signal Control and Direct Neural Sensory Feedback: the nervous system has plasticity, which makes it capable of adaption and functional recovery. Nerve signals accurately reflect the motor nerve command from the brain, moreover they are highly stable, reproducible, and exportable. Interfacing peripheral nerve electrical signal from the nerve stump is becoming the focus of the research into the control of prosthesis. The voluntary motor control of nerve activity has not been completely defined yet. Interfacing intrafascicular electrodes with severed fascicule of proximal nerve stumps in radial, ulnar and median nerves is an important way to explore residual motor signaling and intrinsic relationships. This approach could be preferred to the classic EMG one, because it provides higher open and closed-loop stability, muscle fatigue detection, and multiple movement patterns. On the other hand, potential impediments could come from long-term limb amputation issues, like neural pathways degeneration, differential atrophy, decreased conduction velocity and the loss of effective neuromuscular contact or central connections. Current experiments [63] show that the subject was able to generate motor neuron activity related to phantom limb movements, and intrafascicular electrodes were able to export the real-time electrical signal of nerves 29 months after amputation, without any nerve rehabilitation training before the clinical trial. This confirms that either the neural pathways for control of missing limb motions remain intact or dynamic and adaptive motor cortical plasticity quickly comes into play.
From the amputee point of view, the neural interface with the prosthesis is not only useful for a more natural control of the device but also for receiving important informations directly to the brain. Appropriate, graded,

distally referred sensations can be provided through stimulation of amputee nerve stumps with intrafascicular electrodes and these sensations can be used to provide feedback information about grip strength and limb position [64]. Another important project has been carried on by the researchers of the Biomedical Campus University of Rome, jointly with the University Scuola Superiore Sant'Anna of Pisa. They have been able to connect the CyberHand to the patient's brain, with neural electrodes interfaced to the median and ulnar nerves of the amputee. After one month of experimentation, the patient was able to move the hand only thanks to his cerebral impulse, achieving the movements prefixed in the research program: the thumb opposition, the fist closing and the movement of the little finger.

Reinnervation procedures: the reinnervation technique consist in nerve transfers to muscle, to develop new electromyogram control signals and nerve transfers to skin, to provide a pathway for cutaneous sensory feedback to the missing hand. Professor Kuikek [65] did targeted reinnervation surgery

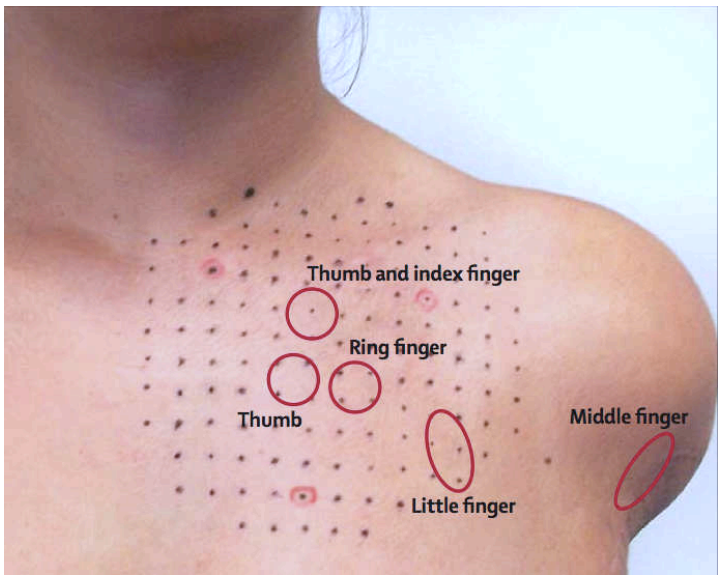

Figure 2.20: Map of areas that the patient perceived as distinctly different fingers in response to touch [65]

on a woman with a left arm amputation at the humeral neck. The ulnar, median, musculocutaneous, and distal radial nerves were transferred to separate segments of her pectoral and serratus muscles. Two sensory nerves were cut and the distal ends were anastomosed to the ulnar and median

nerves. After full recovery the patient was fit with a new prosthesis using the additional targeted muscle reinnervation sites. Functional testing was done and sensation in the reinnervated skin was quantified. The patient described the control as intuitive and the reactivity of the prosthesis as appropriately. Functional testing showed substantial improvement and both motor and process skills increased. The denervated anterior chest skin was reinnervated by both the ulnar and median nerves. The patient felt that her hand was being touched when the chest skin was touched.
Targeted reinnervation improved prosthetic function and ease of use in the patient, moreover targeted sensory reinnervation provides a potential pathway for meaningful sensory feedback.

2.8.5 EMG signal analysis

The common approach for the control of a powered hand prosthesis is based on the surface myoelectric signal, which is used as the input of the system. The myoelectric control is achieved by extracting particular parameters from the signals issued by the stump's muscles, which are then classified with the respective hand movement. Surface EMG electrodes are used to detect the muscular activity: the modern sensors are intrinsically differential, therefore each one represents a channel. Each channel applied to the amputee's skin provides a time series representing the activity of the muscle on which it is posed.
The myoelectric signal has several advantages over other control inputs:

- no harnesses are needed to control the prosthesis unlike the body-powered ones;
- the signal is detected by means of non invasive sEMG electrodes, which are applied to the surface of the skin;
- the muscle activity required to provide control signals is relatively small, almost like the one needed for the real hand;
- electronics behind the control system is continuously improved and miniaturized.

Electronics and control algorithms have been complementary in their development, particularly in this field. This is due to the fact that in a prosthetic hand all the components have to be miniaturized and, at the same time, they have to provide lot of computational power to satisfy the algorithm's needs. Therefore the hardware improvements of the last years have allowed

researchers to focus on better algorithms, in order to provide more functionalities to the prosthetic devices.

2.8.5.1 Single-function systems

During the 1960s and 1970s the development of semiconductor device technology and the associated decrease in device size and power requirements, allowed researchers to improve the prosthesis state of the art. The single-function (one DoF) classification consisted of the ability of the prosthesis to recognize the opening and the closing movement from the muscular activity. In particular, the approach was to use two double-state channels to control the activity of two different muscles, the flexor and extensor digitorum: in this way when the electrode applied on the extensor digitorum detected activity over a certain threshold, the fingers started to open and, viceversa, when the flexor electrode sensed its muscle's signal overcoming a threshold, the fingers started to close. This system was the first to appear in commercial devices like the ones by Otto Bock and Hugh Steeper [66]. The goodness of such approach was that the signals needed for the control of the prosthesis were the ones that the amputee would have used with his real hand. Unfortunately, if the level of amputation is too high the muscles in the stumps are no more available, thus a different method was developed in the late 1960s. A three-state channel was used, it was able to detect the signal level with respect of two thresholds:

- if signal was under the first threshold, there was no activity;
- if the signal was above the first and under the second threshold, the prosthesis opened;
- if the signal was above the second threshold, the prosthesis closed.

This method overcame the previous problems, because with just one channel the signal could be detected even from high level amputation stumps. The problem in this case was that the control was no more natural nor physiologic, because two movements were controlled by one muscle. These systems are well developed, reasonably reliable, and for the most part provide the performance that clients require from the commercially available prostheses.

2.8.5.2 Multifunction systems

With the recent developments in multifunction prostheses hardware there has been considerable effort towards providing improved multifunction control. Since 1975 to the present there were large improvements in the perfor-

mance of multifunction prostheses : more than 90% of recognized movements for hands able to perform more than the opening and the closing functions. This is due to a new kind of classification approach: the pattern recognition. To classify each type of signal, a set of features has to be extracted from it, for example time-domain statistics, short-time Fourier transform (STFT) values, wavelet transform, model parameters and others more. In general, this feature vector can be highly dimensional, therefore dimension reduction techniques have to be applied in order to reduce the classification complexity. After reducing the feature vector dimensions, the next step is to train a classifier in order for it to be able to match each signal's feature vector with a particular hand movement. Possible classifiers include Bayes, linear discriminant analyzer, multilayer perceptron neural network, and Support Vector Machines.

Multifunction single-channel systems are able to recognize more than one function by means of just one channel. The first approach to this issue, dating 1977, was to extract the feature vector of the bipolar myoelectric signal by means of a model which provided information about relevant signal parameters and statistics [67]. Then the feature vector was used to derive a Bayes minimum probability of error receiver (classifier). Other studies carried on in 1980 used a combination of state-space methods and statistical decision theory which are applicable to a broad class of nonlinear estimation problems [68]. In 1975 a new feature extraction process was proposed, which consisted in the application of the ARMA model and the Kalman filter to the EMG time series [69]. This method was able to recognize four different movements with a performance of 95% [70].
The year 1993 saw for the first time the application of Artificial Neural Networks in this field. This approach relied on the fact that the structure of the EMG signal is distinct for contractions which produce different limb functions. So that the actual structure of the myoelectric signal over time could be used to discriminate limb functions. To represent the above mentioned structure, five statistic features were used: the mean absolute value, the mean absolute value slope, the zero crossing, the slope sign changes and the waveform length. These feature vector was used to train an Artificial Neural Network which had performances ranging between 80% and 98% depending on the subject performing the movement [71].

Multifunction multi-channel systems: the previous paragraph presented the single-channel approach, in which the possible improvements can be achieved thanks to novel feature vector extraction methods. Another

way of enhancing the EMG control systems can be the addition of more channels: other electrodes have to be positioned on the forearm.
A two-channel system able to recognize six different functions with 85% of performance was presented in 1982: this approach required the extraction of just two features, namely the zero-crossing and variances which were inputted in a *linear-discriminant* classifier [72]. In 1983 a performance of 95% was obtained thanks to a four channels system, extracting four ARMA coefficients per channel, which was able to classify four functions using a *nearest neighbor* classifier [73].
In 1995 two channels were used to extract five time-domain features per channel, in order to train an Artificial Neural Network to classify four functions: this method obtained a performance of 90% movements recognized [74]. Performances of 98% on six functions and 99.5% on four functions were reached using wavelet coefficient features extracted from four channels. They were reduced in dimension by principal components analysis and classified by an Artificial Neural Network [75].
In 2004 an investigation was carried on about the extent of increase in classification performance with number of channels. The performance in classifying 10 functions with a linear discriminant classifier increased with number of channels, reaching 94% at 16 channels. However, the performances at eight and four channels drop to only 93% and 87% respectively [70].
An interesting comparison study was issued in the same year to understand which was the best approach between the temporal and the spectral ones. The results of this investigation are interesting: the inexpensive and simple multiple trapezoidal windowing, which is a temporal method, has offered much better time efficiency and lower dimension of the feature vector than the expensive method based on the short time Thompson transform, with just a slightly smaller classification hit rate [76].
In 2005 a motion pattern classifier which combines Levenberg-Marquardt based neural network, with parametric Autoregressive model as feature vector, was presented. This motion pattern classifier can successfully (performances higher than 90%) identify three types of motion of thumb, index finger and middle finger, by measuring the surface EMG through two channels [36]. Another system was proposed in the same year: singular value decomposition features (SVD) extracted from wavelet coefficients were used as inputs for a neural network classifier to predict amputee's movement intentions [77]. Similar works presented in 2007 and 2009 use similar concepts on different biosignals [78][79].
In 2006 a method based on Support Vector Machines was introduced: the system is endowed with ten electrodes and is able to recognize the open-

ing and closing actions of the index finger, thumb and other fingers. This approach is shown to be robust across sessions and can be used independently of the position of the arm. With these stability criteria, the method is ideally suited for the control of active prosthesis with a high number of active DoF [80]. In the same year an interesting method was proposed: a motion pattern classifier which combines Variable Learning Rate based neural network with wavelet transform and nonlinearity analysis method. This classifier can successfully identify the flexion and extension of the thumb, the index finger and the middle finger (6 functions overall), by measuring the surface EMG signals through only three channels. In this case the performance varies between 90% and 95% [81].
The year 2007 saw an intense research activity, which led to very interesting results. The cascaded kernel learning machine (CKLM) was introduced as a novel classifier in this field, in order to achieve high-accuracy EMG recognition. The CKLM is trained with a 13-dimensional feature vector, composed by autoregressive model parameters and EMG histogram, which are extracted from each of the three channels of the system. This approach led to a recognition rate of 93.54% on eight different postures [82].
Another system composed of a Wavelet Packet Transform (WPT), a Linear Discriminant Analysis (LDA), and a Multilayer Perceptron (MLP) is able to recognize nine kinds of hand motion from four-channel EMG signals. The features are first extracted by using a WPT, thereafter, an LDA is used for linear supervised feature projection to reduce the dimensionality of the WPT features and improve the class separability. Finally, the LDA-projected features are applied to an MLP. The experimental results confirmed that the proposed method achieved a high recognition accuracy, and the subject could control the myoelectric hand without any perceived operation time delay [83].
Not less important have been the results obtained by the application of the TDSEP. This approach is based on the decomposition of the signal into components originating from different muscles. The processing requires the decomposition of the surface EMG by temporal decorrelation source separation (TDSEP) based blind source separation technique. Pattern classification of the separated signal is performed in a second step with a back propagation neural network. The experimental results, show that the system was able to reliably recognize different subtle hand gesture (4 hand actions) with an overall accuracy of 97% [84].
In 2008 a new learning method was proposed, which can detect opening (extension) and closing (flexion) actions of all human fingers, as well as sideways movements (abduction/adduction) using lower arm surface EMG

(10 channels). The classifier proposed is a Support Vector Machine, which is shown to be able to classify independently of the position of the arm. The authors of this research say that with ten electrodes, successful classification of ten or more classes depends on several, mostly human factors which have to be eliminated in future works [85].
In 2009 a system based on fuzzy inference was adducted: this study designs the membership function and the fuzzy rules from the average value and the standard deviation of the root mean square of the myoelectric potential for every channel of each motion. Four channels were able to classify six different functions with a performance near to 98% [86]. In the same year an Artificial Neural Network with a recurrent structure and a time-delay factor for input has been trained on continuous finger joint angles. The target hand motions were four, and the relative angles were detected by a data glove. Then the moving average of the signals coming from each of the eight channels were used to train the above mentioned network, leading to a good classification reliability [87].
Another approach has been used to classify not only the functions but the also the forces applied in the movement as well: ten channels detect the muscle activity, which is matched to the force/torque sensors output, to train the classifier. Thus four different functions and their relative force can be recognized by both an Artificial Neural Networks and a Support Vector Machine with performances higher than 90% [88][89].
There are a number of research directions towards meeting the goal of simultaneous, independent, and proportional control of multiple DoF with acceptable performance (classification rate and active daily living) and near "normal" control complexity and response time.
To reach simultaneous, independent, and proportional control, there are two possible approaches: direct control and motion pattern classification. The first is based on a one-to-one mapping between a given channel activity and a given function. This requires a signal detection method that is immune to crosstalk between muscles. Most promising in this regard is the targeted reinnervation to which are applied signal telemetry implants. An implantable system can be placed in the reinnervated muscle providing a control source that is both physiologic and immune to crosstalk [65]. This allows a direct proportional control of each function [70].
On the other hand, the future on the pattern recognition approach would be characterized by the electrode array. A vector of electrodes posed all around the forearm, detecting signals from a group of muscles. This means that the feature patterns depend on the group co-activity. The feature set will, then, be used to train classifiers ranging from Artificial Neural Networks to Sup-

port Vector Machines.
An interesting and potentially effective approach to independent simultaneous control is independent component analysis (ICA - TDSEP) and blind source separation. Applied to the signals generated by a group of muscles and detected by an array of electrodes, it is theoretically possible, under certain conditions, to recover the individual muscle signals for control purposes [84].

2.8.6 Defense Advanced Research Projects Agency

The Revolutionizing Prosthetics program of the Defense Advanced Research Projects Agency (DARPA) will create, within this decade, a fully functional (motor and sensory) upper limb that responds to direct neural control. The DARPA researchers has recently decoded the brain's motor signals with such fidelity that motor movements of a robotic arm can be achieved entirely by direct brain control.
In two years, they have delivered a prosthetic for pre-clinical trials (Prototype 1: two-year project) that is far more advanced than any device currently available. This prosthetic enables many DoF for grasping and other hand functions, and will be rugged and resilient to environmental factors. By 2010, is going to be delivered a prosthetic for clinical trials (Prototype 2: four-year project) that has function almost identical to a natural limb in terms of motor control and dexterity, sensory feedback (including proprioception), weight, and environmental resilience. The four-year device will be directly controlled by neural signals [90].
Prototype 1 consists of a 7 independent DoFs upper limb prosthetic arm, to be used for targeted reinnervation patients. It serves as a test bed for evaluation of haptic feedback, indirect sensory perception approaches and to demonstrate advanced prosthetic function with non-invasive and low invasive classification algorithm.
Prototype 2 consists in a fully actuated 27 DoFs prosthetic arm to be used as platform for testing neural control and sensory feedback, since it integrates pressure, temperature, and vibration sensors. The objective of the second phase is to produce a fully neurally integrated upper extremity prosthetic.
Two arms, inspired by the Prototype 2, but with different architectures will be produced. One with an extrinsic actuated hand (as in the natural model), and one with an intrinsic actuated hand. The first will be tendon driven, whereas the second will use custom brushless DC motors [5]. The intrinsic actuated hand (Figure 2.21) will be endowed with 18 DoF, which, as in Prototype 2, will be driven by intrinsic actuators, 3 of which are housed in the

Figure 2.21: Rendered images of the 50% Female and 50% male 18 DOF Intrinsic hands and 3 DOF Intrinsic Wrists [91].

wrist. The idea is to use custom brushless DC electric motors capable of providing high torque at physiological hand speed. These motors are small enough to be fitted into the volume of a female hand, yet capable of providing the sufficient torque and speed of a male hand. These motors, coupled with high torque capacity Wolfrom transmissions, form the drivetrains for each of the DoF's in the hand.
Each finger has 3 articulations with 2 motors. The distal and medial phalanges are driven by 1 motor and coupled by a differential drive mechanism, while the proximal phalange has its own actuator. Index, ring and little fingers have abduction/adduction motors in the palm. The thumb has 4 DoFs, each with its own motor. The wrist does flexion-extension, radial-ulnar deviation and wrist rotation.
The designers of the hand think that inherently compliant DC electric motor drivetrain architectures, such as series elastic actuators, are a good choice to withstand shock loads . Such drives will enable the hand system to have better impact resistance and possibly more biomimetic operation.
Force or position sensors are being integrated into each finger tip and joint axis. All these sensors and motor controller are coupled to a single large hand control module mounted in the back of the hand [91].
The results of this program will allow upper limb amputees to have as normal life as possible, despite their severe injuries. Currently, prototypes from the two-year and four-year efforts are undergoing human testing. [90]

2.9 Imitation of the Biologic System

Since both the artificial and biologic systems have been discussed, this the right time to conclude the parallelism previously started. Looking at the state of the art prosthetic devices it is impressive how the design of these systems has been positively influenced by the biologic model:

- the biologic system of pulleys, tendons and extrinsic muscles suggested that, in order to reduce the weight and the size of the hand, it is important to adopt an underactuated approach. Therefore all the DC motors are out of the hand and the torque is transmitted by artificial tendons;
- the human body is provided with different types of sensor, each one specialized for a particular task. This allows the somatosensory system to have a comprehensive knowledge of the state of the hand. For the same reason, the artificial hands are endowed with many proprioceptive and exteroceptive sensors, bringing each one a particular information.
- as stated in Chapter 1, the control of the hand is performed in a hierarchical fashion by the brain. The same approach is chosen in the state of the art prosthetic, in which the control system is divided into a high and a low levels. The first is under the the person's will, while the second basing on the informations coming from the sensors, determines the forces and the adjustments to perform in order to achieve the task requested by the high level controller.

2.10 Amputee's training

The importance of the prosthetic training was analized in a Canadian study involving 26 upper-limb amputees. It was found that in a group of individuals who received training, 90% used their prosthesis in a functional way. On the other hand, in an untrained group of patients only 50% used the prosthesis functionally. Therefore prosthetic training, as well as duration after amputation and counseling, influence the overall acceptance of the prosthesis. The literature advises the immediate management of the amputee in order to obtain high acceptance. In the first days after the amputation the amputee might be more willing to try a prosthesis. A proper rehabilitation program is as important as a properly fitting prosthesis. The quality of training will determine how the amputee uses the prosthesis for the rest of

his or her life. For these reasons, training should be prescribed nearly to every new upper-extremity amputee [27].
In the scope of patients rehabilitation, there are mainly three different steps to follow to obtain good results in controlling the prosthesis: the pre-prosthetic training, the basic prosthetic training and advanced prosthetic training.

2.10.1 Pre-prosthetic training

The training, executed for the application of commercial devices, is always aided with a computer-based software. Ottobock for example provides its patients with MyoBoy (Figure 2.22). On the computer screen the patient can visualize each signal detected by each electrode applied to the patient forearm. Initially, the focus of the training is on the independent activation of each muscle. Once the amputee demonstrates the ability to separate each muscle signal the concept of proportional control is introduced. The proportional control is the relationship between the force developed by the selected muscle contraction and the speed and grip force of the prosthesis. Each electrode is endowed with a dial that can be manually adjusted to increase or decrease the sensor's gain. This allows the therapist to dampen the amplitude of the signal once the patient develops mastery of control and increases the muscle strength. The MyoBoy software is very motivating

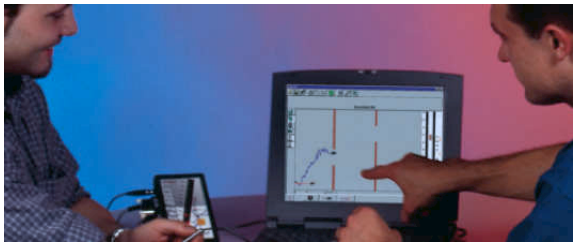

Figure 2.22: Snapshot of the MyoBoy system by Ottobock.

for patients: a virtual hand responds to the muscle signal as a myoelectric prothesis would. Moreover this tool provides a car game that is very useful to train and test the accuracy of the patient's control.
Thereafter, the electrodes can be attached to the patient's actual terminal device, before the fabrication of the preparatory prosthesis. This step provides three-dimensional perception of the prosthesis. Which means that new concepts can be introduced for a more advanced training. For instance,

the prepositioning for the most efficient grasp patterns and the appropriate force control with different densities of objects.
The skills and knowledge that the patient gains with pre-prosthetic training are critical to motivation and success with his prosthesis. Patients that receive pre-prosthetic training demonstrate some amount of immediate success at first fitting [92].

2.10.2 Basic training

Learning to use a prosthesis is similar to learning the operation to control other complex mechanical devices: a daily life example is the task of learning to drive a car. In the same way, when an amputee starts his prosthetic training, the first step is to learn how to control the individual components to operate the prosthesis. The individual motion patterns are then combined together to accomplish complex tasks. The goal is to achieve smooth movement of the prosthesis with the minimal amount of delays and awkward situations in daily activities.
The creativity of the therapist is very important in order to achieve the mastery of the movement control. Media appropriate for training include objects of various shape, texture, density, and weight, such as one-inch wood square blocks, round blocks, cotton balls, Styrofoam cups, or a cup filled with water. Moreover if verbal, tactile and visual feedback is given to the patient, a faster training is more likely.
The amputee is trained to apply the skills learned during the control training phase, to start actual functional use of the prosthesis. This may cause increased user frustration due to the awkward and the artificial nature of a prothesis. The level of difficulty in training and the amount of training time needed may vary from one prosthetic user to the other.

2.10.3 Advanced training

The advanced training is aimed to achieve a natural motor pattern. The patient, after this phase, has to be able to save body energy, decrease biomechanical stress to the intact limb, and learn the most efficient approach to tasks without extraneous body movements.
There are five characteristics of advanced prosthetic rehabilitation that can guide therapists during this phase:

1. the advanced rehabilitation is individualized: the knowledge of the patient's vocational and avocational activities is important in the progress of the training;

2. the usage and operation of a tool, or interaction with an object, such as a carpenter's tool, a musical instrument, a cooking utensil, or a machine;

3. the achievement of complex tasks, requiring bimanual movements: treatment activities in this phase are less static and generally challenge the therapist to take the patient out of the clinic setting;

4. the use of the chosen and bought prosthesis;

5. the patient has to complete a final exam: several patients have completed carpentry projects, leather belt or wallet projects [92].

Chapter 3

The Electromyographic Signal

Since one of the goals of this thesis is the design of a system able to associate a predefined set of hand motion patterns to particular features of the correspondent EMG signals, a detailed study about this biologic signal is performed in this chapter. Moreover, the most commonly used methods for the analysis of the EMG signal are presented, since some of them are implemented in the current work.

3.1 Electromyographic Signal Genesis

The most elementary functional unit of the muscle is the *motor unit*, which is composed by an α-motoneuron and by the correspondent muscle fibers innervated by the axon fibrils of the motoneuron.
As discussed in Chapter 1, the movement is planned by the brain after the integration of all the sensory information. Hereafter the motor command is generated and transmitted to the muscles by means of the spinal motor neurons (α-motoneuron). Once the muscle fibers receive this command they execute the mechanic contraction.
During the contraction phase, under normal circumstances, an action potential propagates along the α-motoneuron and activates all its branches, which, in turn, activate all the muscle fibers of the *motor unit* (MU). When the post-synaptic membrane of the muscle fiber is depolarized, the depolarization spreads in both directions. The membrane depolarization, which is accompanied by a movement of ions, generates a magnetic field in the neighborhood of the muscle fibers.

An electrode located in this area will detect the potential, whose temporal excursion is known as *action potential*. In human muscles, the amplitude of the action potential is directly proportional to the diameter of the muscle fiber, inversely proportional to the distance between the muscle fiber and the electrode position and depends on the filtering properties of the electrode as well.
The temporal interval between the generation and the detection of the action potential is directly proportional to the length of the nervous branches and to the distance between the motor unit and the sampling area. Actually its duration depends on the speed of conduction of the fiber which is 3-6 m/s.

3.1.1 Motor Unit Action Potential

At the electrode surface it is presented the spatio-temporal sum of different signals generated by the depolarization of different fibers belonging to the single motor unit. This signal is called motor unit action potential (MUAP). The activation times of fibers belonging to the same motor unit are different each other, mainly for two reasons:

- variable delay dependent on the length and section of the axon innervating a single muscle fiber; which, actually, is fixed for each fiber;
- delay introduced by the discharge of acetylcholine in the neuromuscular junctions. In fact, since this type of discharge process is random, also the excitement of each fiber of a motor unit is a random function of time.

In Figure 3.1 a trifasic MUAP is represented. It is the result of a sampling carried out by placing surface electrodes parallel to the muscle fibers, in order for each action potential to be biphasic. The sign of the phases depends on the state of the membrane during the depolarization, in relation with the electrode.
Inside the detection area of the electrodes, there are contributions from other motor units, thus many MUAPs are sampled. These can have similar amplitude and shape, if every muscle fiber belonging to the respective motor unit has the same distance from the detection zone. Depending on the electrode used, there are variations on the shape, phase and duration of MUAPs. The amplitude and shape of a MUAP are, therefore, function of the geometrical arrangement of the motor unit, of the muscular tissue and of the properties of the electrodes applied. In a normal muscle, for example, the peak to peak

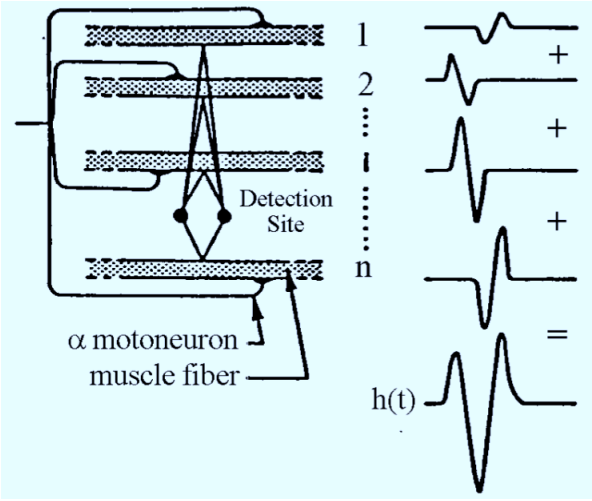

Figure 3.1: Generation of the MUAP [14].

amplitude of a MUAP, detected with a needle electrode, varies from 5 mV to 500 microvolts.
Since muscles can be quite heterogeneous, with respect to the fiber disposition. The location of the electrodes relative to the muscle will affect the EMG amplitude. An EMG signal collected from part of the muscle is thus not necessarily representative for the muscle as a whole.

3.1.2 Motor Unit Action Potential Train

A sequence of MUAPs, generated by the same motor unit, gives rise to the Motor Unit Action Potential Train (MUAPT). This series of signals can be described completely by its IPI (interpulse interval), which is regarded as a Gaussian random variable, and by the waveform of the MUAPs composing the train.

3.1.3 Multipath Interference: Surface EMG

The muscle tension gives rise to an electrical signal at the skin surface. This surface signal is composed by the sum of impulses produced by irregular discharges of the motor units (Figure 3.2).
Experimental observations revealed an inverse power relation between signal amplitude and the motor unit's depth, especially because the contribution of the *traveling wave* of the motor unit potential falls off rapidly with electrode-source distance. Accordingly, *active MUs close to the electrodes*

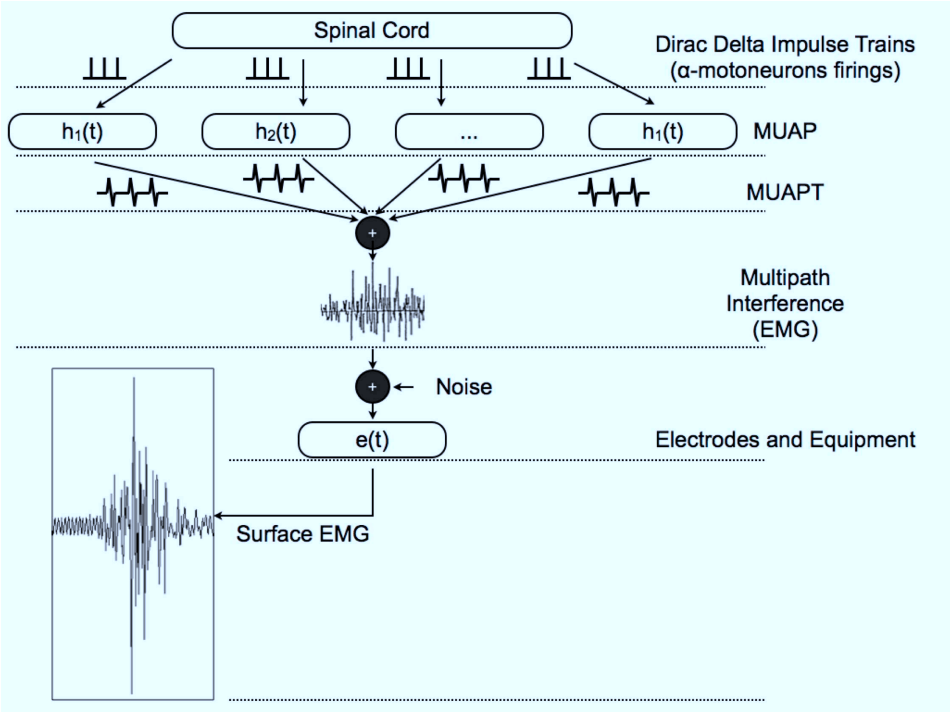

Figure 3.2: Generation of the sEMG signal

will dominate the EMG signal [17].
Given the definitions made in the previous sections, is now possible to define the surface EMG ("multipath interference") as the spatial and temporal interaction of the MUAPTs generated by all the active motor units in the area nearby the electrode.
Detected by surface electrodes, the electromyographic signal has to be considered as a stochastic precess. Therefore the analysis approach that are commonly applied are mean, variance, root mean square, autocorrelation, power spectral density, mean frequency, median frequency, Skewness, Curtosi and many others [34].

3.1.4 Signal Contamination

The pure EMG signal, given by the spatial and temporal interaction of the MUAPT of all the motor unit of the muscle, is impossible to obtain. Mainly three types of contamination can affect the surface EMG signal:

1. movement of electrodes, cables and connectors, arising from the motion of the subject. In principle, movements will cause signal contributions at relatively low frequencies (lower than 10 Hz);

2. cross-talk, which refers to a signal contribution originating from other muscles, can interfere with the EMG signal of the muscle under investigation;

3. external sources may cause deterministic contaminations of varying frequency content (best known is the 50 or 60 Hz interference from the electric mains).

At low contraction levels, the noise contribution in the signal can be relatively large and limit the precision of EMG amplitude estimates. Contamination of the EMG signal can be reduced by filtering techniques.

3.2 Electrodes

3.2.1 Configurations

The electromyographic signal can be detected with different types of electrodes, and amplified in various ways. The electrodes can be divided into two main classes, the depth and surface electrodes. Normally the second type is chosen because it is a noninvasive and painless approach.
From the point of view of the signal amplification, there are two possible configurations:

- monopolar configuration: the muscle potential is detected by one electrode, which has another electrode as a reference. The problem in this case is the low spatial resolution, in fact every electric potential between the detecting and the reference electrodes are sampled and amplified. This means that unwanted signals, like the ones coming from other muscles or the ones from the capacitive coupling with the line voltage, are also gathered;

- bipolar configuration: the spatial resolution is increased and the noise reduction is improved. This configuration is normally connected to an operational amplifier, having as inputs the two signals. Therefore the difference between two monopolar signals is amplified, and the information common to both electrodes is removed. Thereby, a large part of the unwanted noise and of the cross-talk, which are normally common to both electrodes, is eliminated [17][34].

Figure 3.3: Bipolar electrodes by Ottobock

Such factors as electrode size, electrode positioning and interelectrode distance over a particular site can affect the detected EMG signal and hence should be held constant across experimental conditions. For example, a smaller interelectrode spacing shifts the bandwidth to higher frequencies and lowers the amplitude of the signal.
Regardless of the optimal detection surface geometry, however, only closely spaced electrodes and differential amplification can yield spatially selective surface EMG recordings.

3.2.2 Electrodes size

Surface electrodes are available in a variety of sizes. Electrodes with small detection surfaces and housings allow closer interelectrode spacing and consequently higher selectivity.
On the other hand, the larger the size of the detection surfaces, the larger the amplitude of the signal that will be detected and the smaller the electrical noise that will be generated at the skin detection-surface interface.

3.2.3 Electrodes placement

Specification of surface electrode placements over target muscle groups is important to ensure that findings are comparable across individuals, sessions or laboratories. Electrodes should be placed proximal and orientated parallel to voltage gradients of interest and, simultaneously, be placed distal and

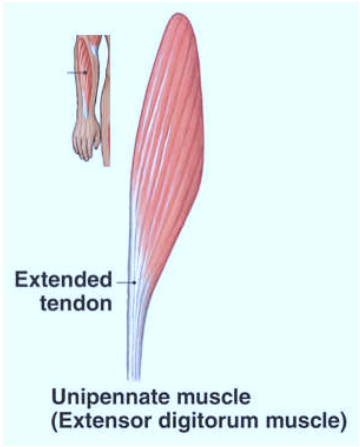

Figure 3.4: The extensor digitorum muscle: a pennate muscle [15].

orientated perpendicular to voltage gradients of extraneous signal sources. Particular attention has to be paid to the muscles of the forearm. An important example is the extensor digitorum: this muscle is unipennate, which means that all muscle cells are on the same side of the tendon. Pennate muscles have one or more tendons that run through the body, and fascicles form an oblique angle to the tendon. This kind of muscle has more fibers than a parallel one, thus generates more tension than a parallel muscle of the same size.
According to these considerations it is reasonable to position the two electrodes (bipolar) along the forearm, in a slightly oblique fashion. In this way the bipolar electrodes are parallel to the fibers and to the voltage gradients of interest.
Successful implementation of this principle is limited by the underlying anatomy, the magnitude of interfering signals and the availability of reliable anatomical landmarks. Moreover, it was shown that muscle fiber orientation changes during isometric contractions with increasing force [18][17].

3.3 Bandwidth, Filtering and Nonstationarity

The primary energy in the bipolar recorded surface EMG signal lies between approximately 10 and 200 Hz:

- between 10 and 30 Hz: primarily due to the firing rates of motor units;

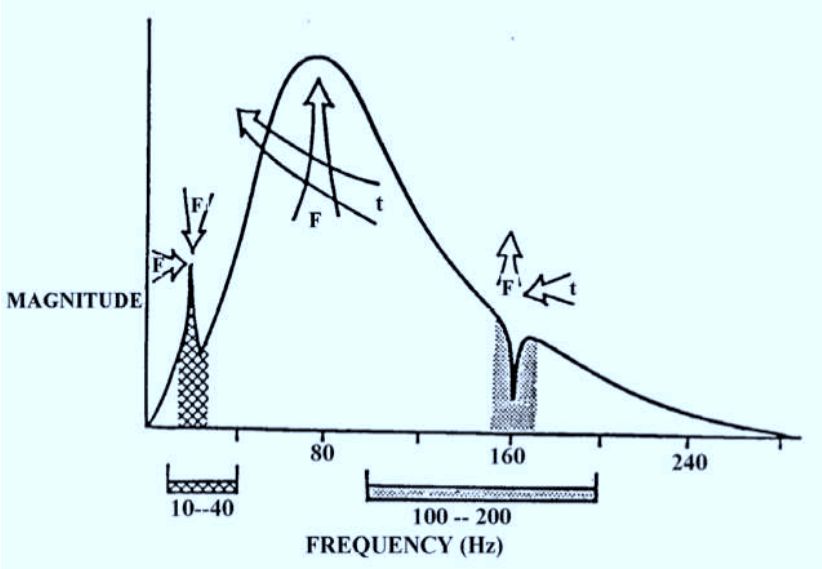

Figure 3.5: Qualitative evolution of the sEMG spectrum, depending on the force and duration of the contraction. The arrows show the direction of the modification of portion of the spectrum depending on the force or time increment [14].

- beyond 30 Hz: due to the shapes of the aggregated motor unit action potentials. This part of the spectrum depends on shape and disposition of the electrodes, distance between fibers and muscle fatigue [18].

The spectral characteristics of the EMG signal make it impossible to eliminate the 50/60 Hz noise: this would reduce a significant portion of the target signal. On the other hand, given that the frequency domain of the sEMG signal ranges between 10 and 500 Hz, it is possible to eliminate artifacts and low-frequency components using a high-pass filter with a cutoff frequency of 10 Hz.
Mainly three physiological parameters can influence the spectrum of the sEMG signal:

1. the muscle tension level (fatigue): in particular it has been noted that while contractions are performed along the time, the spectrum shifts towards the low-frequencies and increments its amplitude (Figure 3.5);

2. the muscle fibre length: at a lengthening of the muscle fibers corresponds a decrease of the mean frequency of the spectrum;

3. the speed of propagation along the fibers and the action potential duration: at longer MUAPs corresponds a shift towards the low frequencies [14].

As stated in the first point of the list above, muscle fatigue has a dominant role in altering the EMG signal, in particular its spectrum varies in time. A signal with this characteristic is referred to as non-stationary.

3.4 Rectification

The rectification (Figure 3.6b) of the sEMG signal represents its absolute value, therefore it is never negative and is characterized by a mean different from zero. Rectification can be done electronically in real-time and is mainly used as an intermediate step before other processes like averaging, linear envelope, root mean square and integration.

3.5 Linear envelope and Muscle Force

The relationship between EMG amplitude and muscle force is not necessarily linear, though linear models are often inevitably used and provide, in many cases, a reasonable description of the relationship.
The application of a low-pass filter (cutoff 2-3 Hz) to the rectification of the signal, produces the linear envelope, which can be considered as a moving average, inasmuch it follows the trend of the rectified EMG signal. The filtering can be done electronically but adds a delay.
This "smooth" signal provides a quite close proceeding of the force developed by the considered muscle (Figure 3.6c) [34].

3.6 Normalization

The EMG amplitude is often normalized to a 0-100% range through dividing the instantaneous amplitude by the value obtained when performing a maximum voluntary contraction (MVC). The corresponding EMG amplitude is then expressed as a percentage of maximum voluntary excitation (%MVE), or, more often used but less accurate, as a percentage of maximum voluntary contraction (%MVC). This normalization procedure is used to reduce between subject variability in the EMG amplitude associated with for example differences in thickness of subcutaneous tissue, but is also necessary to convert EMG amplitude to an estimate of muscle activation. Unfortunately, a true maximal voluntary activation is difficult to obtain even after

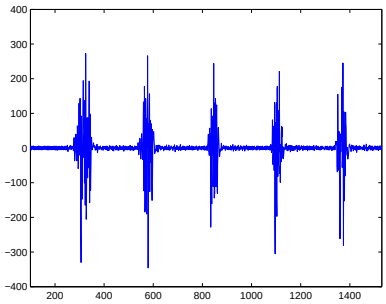

(a) Surface EMG signal.

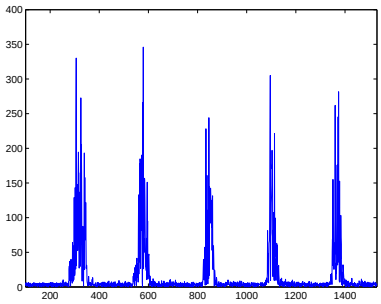

(b) Rectified sEMG

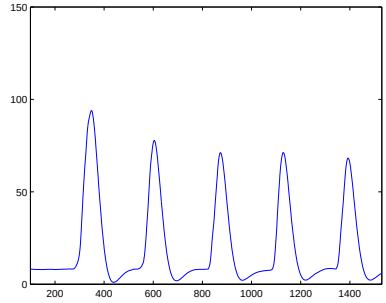

(c) Linear envelope of the sEMG: the filter used to obtain the envelope is a second order low-pass filter with a cutoff frequency of 2 Hz

Figure 3.6

training. Consequently the reliability of the MVE is relatively low. Underestimation of the true MVE is a potential and significant source of error. This is even more likely to be the case in special populations like patients in view of pain-related inhibition and in the elderly where maximum acti-

vation has also been found to be more difficult to achieve. Normalization in such cases may even cause true differences in muscle activation to disappear. Therefore, it is often advised to use well-defined, sub-maximal contractions for the purpose of EMG normalization [17].

Chapter 4

The Project

At this point a basic knowledge about the EMG signal and its analysis methods has been provided. This is very useful since some of the methods presented in the previous chapter are applied in the project implementation. As already mentioned, the system that we implemented aims at associating particular hand motion patterns to some features of the correspondent EMG signal. In this way it is able to understand, from the forearm muscle contractions, the movement that the robotic prosthesis has to perform according to the amputee's will.
This chapter presents the movements that the system is able to recognize, a simple abstract model of the prosthesis to control, the possible application of the classifier on a high level controller, the analysis methods applied to the EMG signal and, eventually, the actual implementation of the entire project.

4.1 Hand Movements To Classify

The first step in order to design an useful classification algorithm is the study of the target movements that a prosthetic hand has to accomplish, based on the needing of the amputees. To do that it is important to understand how the motions of the real hand can be classified from a functional and engineering point of view.

4.1.1 Grasp Taxonomies

There are different ways to interpret the concept of taxonomy when related to the prehensile abilities of the human hand. In this scope, many researchers presented different kinds of classifications, each of which has its own logic:

- the appearance of the grasp: cylindrical, fingertip, hook, palmar, spherical and lateral. Even during the course of a single task with a single object, the hand adopts different grips to adjust to changing force and torque conditions. This suggests that grasps should be first categorized according to function instead of appearance;
- the contact areas involved: a scheme in which grasps are divided into *power grasps and precision grasps*. Power grasps are distinguished by large areas of contact between the grasped object and the surfaces of the fingers and palm and by little or no ability to impart motions with the fingers. Where considerations of sensitivity and dexterity predominate a precision grasp is chosen. In precision grasps, the object is held with the tips of the fingers and thumb.
- task requirements and object shape: starting from the macro-categories of power and precision grasps, a hierarchical tree was developed.

Of these different approaches the one that best fit our needs is of course the one which considers the function of the grasps. The first researcher who succesfully theorized a taxonomy based on the function approach was Cutkosky [93]. He found 16 different types of grasps organized in the following way: moving from left to right the grasp becomes less powerful and the grasped object becomes smaller (Figure 4.1). The heavy wrap grips are the most powerful and least dexterous, while the tripod and the thumb-index finger grips are the most precise. However, the trend is not strictly followed.
An effective way to extend the grasp taxonomy is to consider grasps in terms of "virtual fingers" that do not necessarily have a one-to-one correspondence with fingers of the human hand. Iberall argues that in most grasps the object is held between two virtual fingers and that the type of opposition (for example, trapping an object between the fingers and the palm, or between the pads of the thumb and the index finger) is of central importance. Therefore three basic type of grasps are recognized:

1. encompassing grasps: grasps with palm opposition (grasps 1-4 and 11 in the Cutkosky's taxonomy);
2. lateral grasps: grasps with side opposition (the lateral pinch, grasp 16, is a grasp with side opposition in the Cutkosky's taxonomy);
3. precision grasps: grasps with pad opposition (the precision grasps on the right-hand side of the Cutkosky's taxonomy display pad opposition) [93].

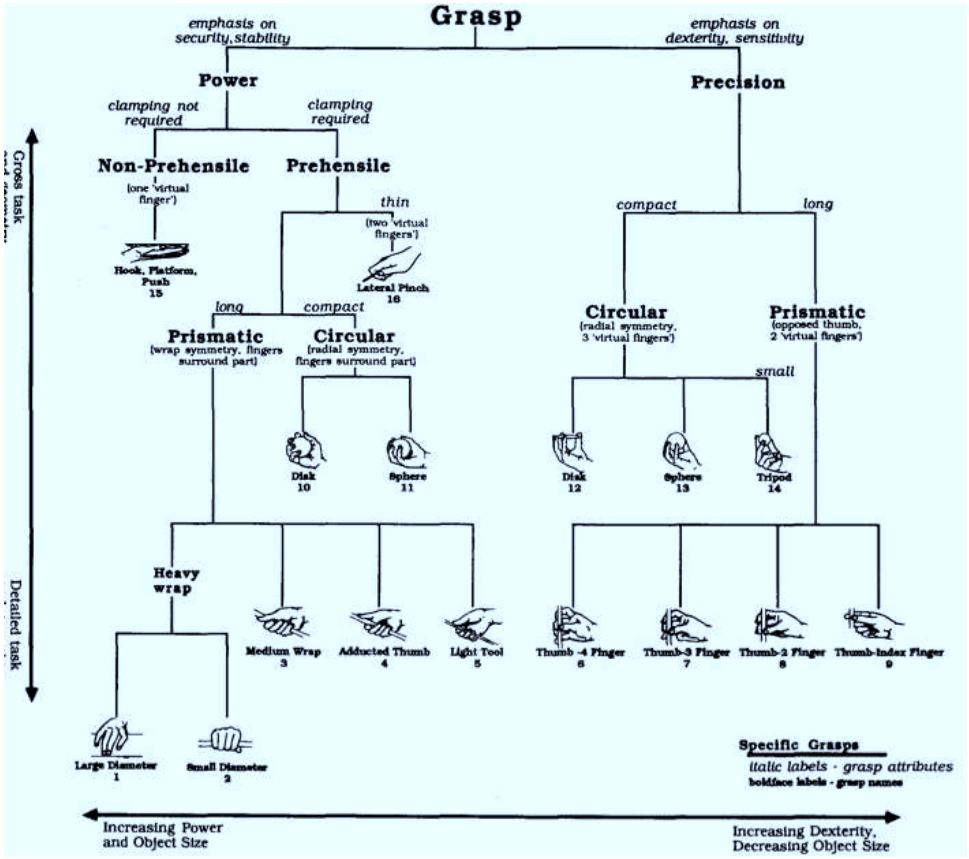

Figure 4.1: The Cutkosky's Taxonomy [93].

A more recent study tried to improve the previous works [94]. A total of 33 different grasps were identified and arranged in a taxonomy which differs from the previously presented ones. The position of the thumb was introduced as additional attribute, which can be either abducted or adducted. Depending on the need for precision, the taxonomy offers a second level of classification which includes only 17 grasp types. The taxonomy should cover the whole range of static grasping patterns, which will serve as a basis for further studies on human grasping.
Being the Cutkosky's taxonomy the most accepted and settled, it will be adopted in order to make comparisons between the characteristics of the real human hand and the artificial device, in the next phases of the thesis.

4.1.2 Target Movements

Since a prosthetic hand is not able to reproduce all the possible functions of a real hand, it is important to chose the motion patterns that seem to be the most useful in a person's life (Figure 4.2):

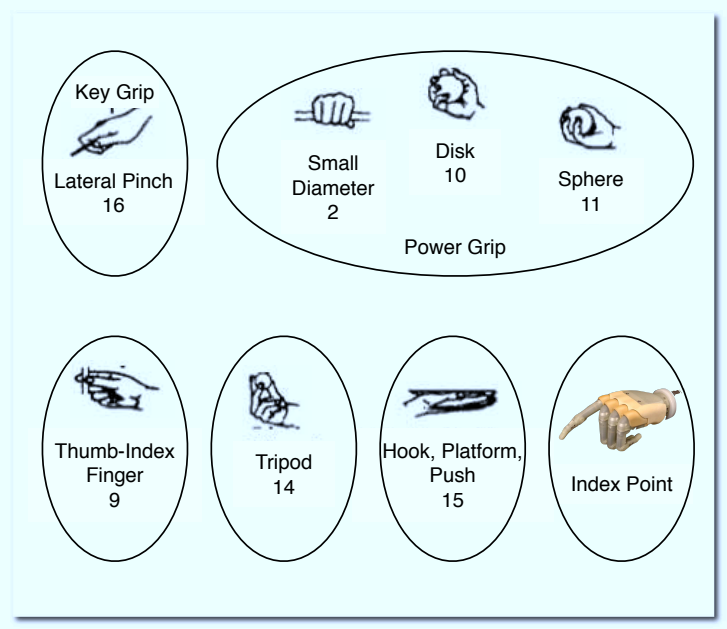

Figure 4.2: Grip patterns of the prosthesis.

- Key Grip: the thumb closes down onto the side of the index finger. It is the Lateral Pinch (Number 16) in the Cutkosky's taxonomy. This grip is useful to hold objects with the shape of a compact disc;
- Power Grip: all fingers and the thumb close down together to create a full-wrap grip. It can be associated to different grasps in the Cutkosky's taxonomy: Small Diameter (Number 2), Disk (Number 10) and Sphere (Number 11). This grip is useful to hold a can of drink whilst opening the ring-pull and, for example, for carrying shopping bags.
- Precision Grip: where the index finger and thumb meet, in order to

pick-up small objects and to hold objects when performing finer control tasks. It can be associated to the grasp Thumb-Index Finger (Number 9) in the Cutkosky's taxonomy.

- Tripod Grip: where the thumb meets the index and the middle fingers. It is associated to the Tripod Grasp (Number 14) in the Cutkosky's taxonomy.
- Platform: where the hand is completely open and holds an object without clamping. It is associated to the Hook, Platform, Push Grasp (Number 15) in the Cutkosky's taxonomy. It is useful to hold a plate.
- Index Point: the thumb and fingers close, but the index finger remains extended. It is useful for operating computer keyboards, telephone dial pads, ATM cash machines and a host of other everyday requirements.

In order to obtain the complex patterns aforementioned, it is necessary to put together more than one basic hand movement. These simpler motion patterns are the ones that are recognized by the classifier designed in the present work and are in order:

1. hand closing;
2. hand opening;
3. wrist extension;
4. wrist flexion;
5. thumb abduction;
6. thumb opposition;
7. index extension.

By the concatenation of the basic movements presented in the previous list, a high level controller is able to create a more complex motion pattern. Before abstractly showing the job of the high level controller, it is necessary to think about a possible model of prosthesis on which the classifier will run. Indeed the physical structure of the device, the number of DoF, the number of actuators and the type of sensors endowed are key factors for the design of the mapping between the motion recognized by the system and the actual movement performed by the prosthesis.

4.2 The Prosthesis Model

A possible model of a prosthesis able to perform the complex motion patterns described in the previous section, could be an underactuated device which has to be endowed with:

- 3 degrees of freedom per finger (total of 12), thumb excluded, of which just the metacarpophalangeal joint is actuated;
- thumb abduction/opposition and thumb flexion/extension (total of 2 DoF), both actuated. This way the thumb can't flex the phalanges;
- 1 actuated degree of freedom for the wrist flexion/extension;

Torque is transmitted from the DC motor in the metacarpophalangeal joint to the fingertips, by means of a system of tendons and pulleys. The current system is not able to detect the velocity of the movement from the EMG signal, therefore the fingers of the prosthesis move at a constant speed.
Another important feature of the device would be the presence of *sensors* on the fingertips and encoders in the motors. In this way it would be possible to detect contacts with objects and to compute the position of each joint of the fingers. In Chapter 2 are presented all kinds of sensors applicable to the real prosthetic hand.
The control of the prosthetic hand is done by means of a hierarchical method. The first and higher level is the one under the patient's will, while the low level is managed by the prosthesis controller.
The *low level control* relies on proprioceptive and exteroceptive sensors, which provide the prosthesis microprocessor with a lot of useful information during the grasp planning phase. This means that the user is not required to pay attention on every detail of the grasp phase, like fingertips pressure and force, while he just has to provide high level commands. In this thesis the low level control is not detailed, but in Chapter 2 are discussed useful examples of valid applications, like the SAMS and the MANUS system.
The sensory system could also be used to provide the patient with a sort of feedback. In particular the vibrotactile one, which conveys information to the user about the force extent of his grasp. This topic is discussed in the section "Bidirectional Interfaces" in Chapter 2.

4.3 The High Level Controller

Once the model of the prosthesis has been introduced, it is time to create the abstract mapping between the seven basic movements recognized by the classifier and the complex patterns taken from the Cutkosky's taxonomy. This mapping has to be performed by a high level controller, which, in this thesis is presented from a logical and abstract point of view, since our goal is to motivate the choice of the seven movements, rather than implementing a controller.
The high level controller does not have to bother with grasping details like force and pressure at the fingertips, which are delegated to the low level controller. Rather it has to manage the single basic movements from an abstract point of view and, strarting from a given sequence of these movements, to generate one of the complex motion patterns described above.
Therefore the first task that the high level control has to achieve is to create the following commands:

1. hand closing detected: all the DC motors in the metacarpophalangeal joint, plus the flexion/extension DC motor of the thumb start to flex the fingers;

2. hand opening detected: all the DC motors in the metacarpophalangeal joint, plus the flexion/extension DC motor of the thumb start to extend the fingers;

3. wrist extension detected: the single motor in the wrist performs the extension;

4. wrist flexion detected: the single motor in the wrist performs the flexion;

5. thumb abduction detected: if the hand is in the *"opened"* configuration, then the thumb can be abducted by its abduction/opposition DC motor ;

6. thumb opposition detected: if the hand is in the *"opened"* configuration, then the thumb can be opposed by its abduction/opposition DC motor;

7. index extension detected: flexion/extension DC motor of the index finger starts to extend, while all the other flexion/extension DC motors in the fingers, thumb included, start to flex.

Hereafter, from different concatenations of these basic movements the high level controller has to produce different complex motion patterns. The whole process is described in Figure 4.3 for the wrist control, which is independent from the control of the fingers described in Figure 4.4. It is important to notice that none of the commands in the previous list consider the actual details about the gripping phase, which is delegated to the low level control system.

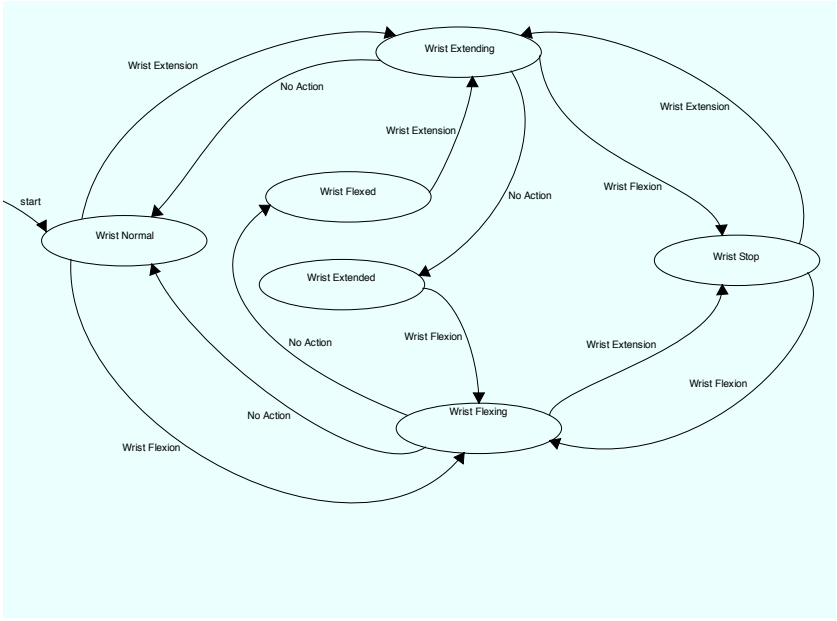

Figure 4.3: Wrist state diagram. Two of the motion patterns detected by the classifier are the state transitions of the diagram: wrist extend and flex.

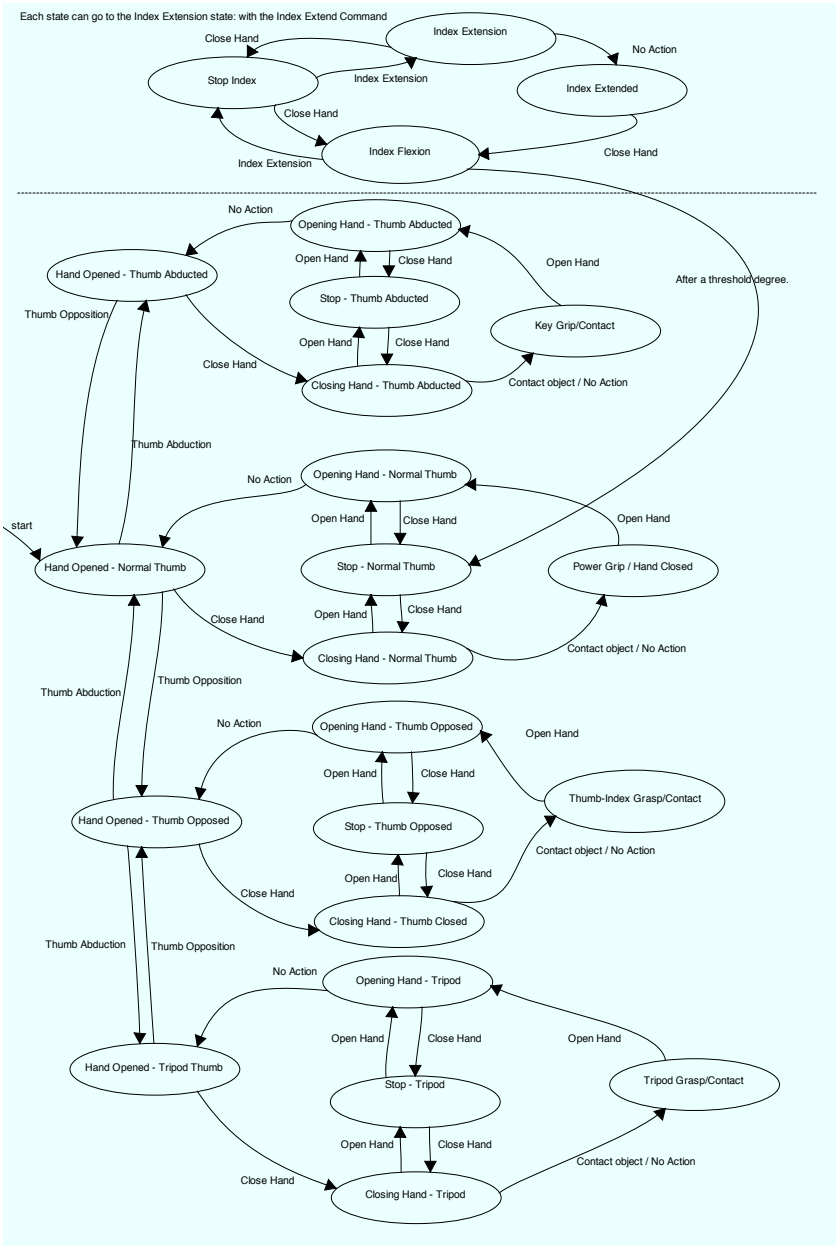

Figure 4.4: Hand state diagram. Five of the motion patterns detected by the classifier are the state transitions of the diagram: hand open and close, thumb opposition and abduction and index extension.

Some noteworthy considerations have to be made:

1. all the states under the dotted line of Figure 4.4 can go to the state "Index extension";
2. the motion patterns detected by the classifier are the state transitions of the diagrams.
3. the transition "Object contact" is related to the information coming from the sensory system;
4. the wrist control is independent from the hand control;
5. the "Platform grip" corresponds to the "Hand opened - Thumb abducted" state.

The next step is to understand how to recognize the seven basic movements from the contraction of the forearm muscles.

4.4 Classification of the EMG signal

4.4.1 Instrumentation

The instrumentation used during the work development is composed by the electromyography board, 7 electrodes by Tesmed, a MacBook 2.2 GHz Intel Core 2 Duo with 4 GB of memory. Being this thesis a preliminary study about the EMG signal and its analysis, the decision was to focus our attention on the principles underlying this subject, delegating every implementation detail of the prosthesis control system to future works. Therefore the classifying system has been entirely implemented on the Matlab 2008a platform.
The main hardware device involved in the project is, of course, the electromyography board. This is the module which receives the signals coming from the electrodes applied to the human skin, and after a series of operations, returns to the microcontroller (in our case a computer) the EMG signal to work with.
The main components of the board, designed at Politecnico di Milano, are going to be described (Figure 4.5 and Figure 4.6). The device is endowed with 3 bipolar channels, plus a reference electrode. This means that the total amount of electrodes in input is 7.
The INA modules can acquire and amplify differential signals covered by high noise, thanks to the series of two buffers and an operational amplifier. The amplification is adjustable in the range 200 - 2000.

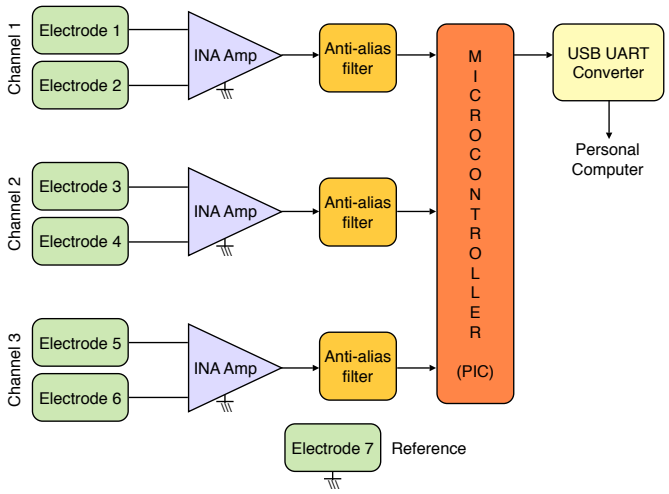

Figure 4.5: EMG board abstract diagram.

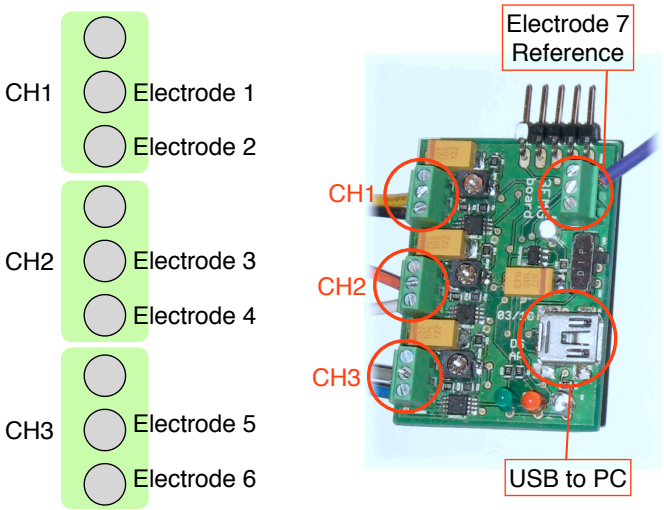

Figure 4.6: The actual EMG board. Electrode inputs and channels are represented.

The anti-aliasing filer is a Sullen-Key, double pole, low-pass filter with a cutoff frequency of 150 Hz, and with a further amplification of 2. This is

done because, as stated in Chapter 3, the dominant bandwidth of the EMG signal is in the range 20-150 Hz: the goal of the board is not to acquire the whole harmonics of the signal, rather just the single events of contraction and relaxation.
The analog data are then fed into a microcontroller PIC16F688, endowed with a 10 bit ADC, which converts the signals in digital and send them to the computer through a serial protocol USART. To allow the conversion from the standard RS232 to the standard USB, more adaptable to a PC, it was used a FT232RL module. The sampling rate of the board is of 270 Samples/Second.
A driver, able to understand the EMG board output, is the first product of this thesis: it is a C script, based on the Standard POSIX, which receives the string outputted by the EMG board and parses it, in order to divide the three channels, which are saved into different files.

4.4.2 Electrodes Configuration

In Chapter 3 the EMG genesis has been discussed in detail, as well as the best electrode configuration to use in the acquisition phase. The considerations made at that point, led to the decision of applying the couple of electrodes along the muscle fibers.
For future compatibility with other works on this subject, the actual configuration of the electrodes is presented, so that future results can be comparable with ours:

- Channel 1: is applied along the Extensor Carpi Ulnaris muscle, in particular, Electrode 1 is proximal, while Electrode 2 is distal;
- Channel 2: is applied along the Extensor Digitorum Communis muscle, in particular, Electrode 3 is distal and Electrode 4 is proximal;
- Channel 3: is applied to along the Front Forearm muscles, in particular, Electrode 5 is proximal and Electrode 6 is distal
- Electrode 7: is the reference electrode and has to be placed in a position without any muscular contraction. The choice made in this work is to apply it to the elbow skin.

For all the channels described above, the two electrodes have to be placed the nearest possible. But they mustn't be in contact, otherwise the signal acquisition turns out to be totally meaningless.

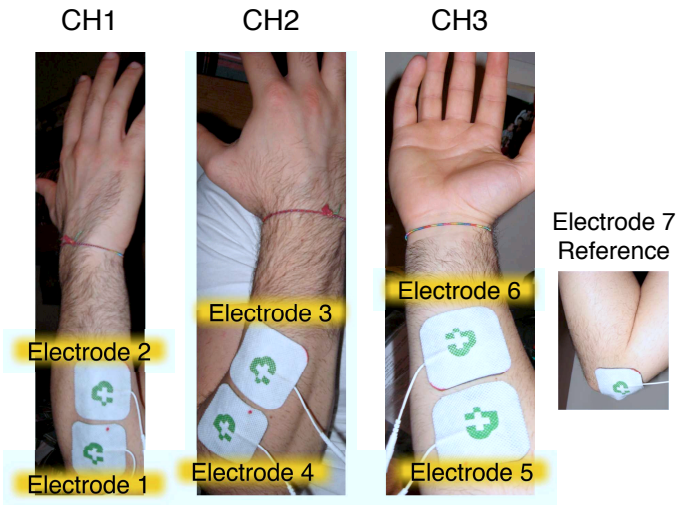

Figure 4.7: Electrode configuration

The choice of the target muscles is not specific, rather the most visible and powerful muscles of the forearm are chosen. Therefore the terminology used previously is just to help visualize the configuration of the electrodes. Indeed, these have such a big surface, that they are able to detect also the contractions of other muscles than the one mentioned in the list above. Even if single muscle contractions can't be detected, extensor and flexor muscles are all respectively in the posterior and anterior side of the forearm. Therefore we expect Channel 1 and Channel 2 to detect stronger signals when extension movements are performed and Channel 3 to detect more accurately the flexion movements.

4.4.3 The System Structure

The first module of the software system (Figure 4.8) is the *segmentation module*, which receives the digital signal from the EMG board. Its job is to understand when a contraction starts and ends in order to divide the signal in many bursts, each related to a specific contraction. The divided bursts are then analyzed by the *feature extractor*. As stated in the previous chapter the EMG signal is quite difficult to analyze because of its non-stationary and stochastic nature. This issue and the one of the feature extraction are solved by the application of the Wavelet Analysis (WA), whose result

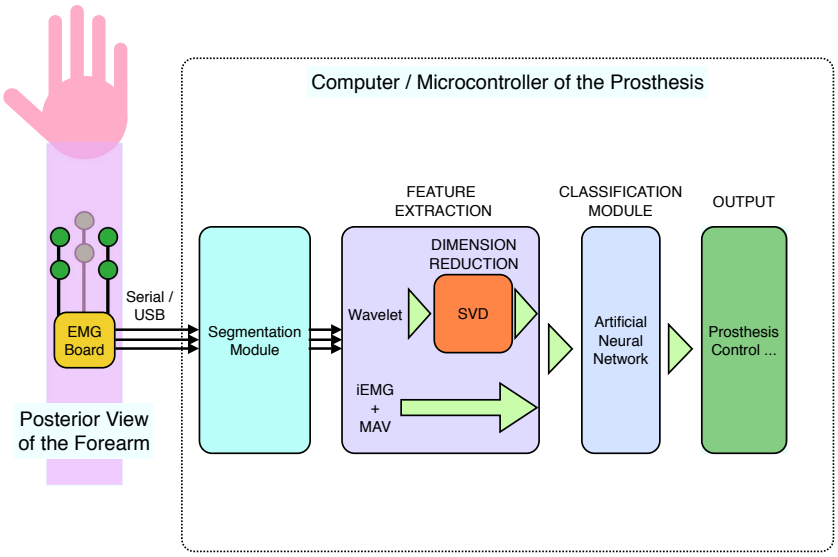

Figure 4.8: A simple view of the system structure

is, then, reduced in dimensionality using the Singular Value Decomposition (SVD). To the aforementioned features are added the integral EMG (iEMG) and the mean absolute value (MAV) of each burst. Eventually, an Artificial Neural Network is trained to associate the incoming feature vectors to the relative hand movements.

4.4.3.1 Segmentation Module

The raw signal received by the *segmentation module*, has to be split into different bursts, each one corresponding to the muscles contraction produced by a single hand movement.
Before starting the detailed discussion about the segmentation module, it is important to notice that in this subsection, the term *training signal* is used to address a kind of signal composed by the repetition of many bursts of the same type of movement. As the name itself suggests, it is used in the training phase of the classifier. The segmentation module is quite complex because of different reasons:

1. the digital signal is highly variable and can also be negative (Figure 4.9);

2. the signal varies at a high frequency (Figure 4.9);

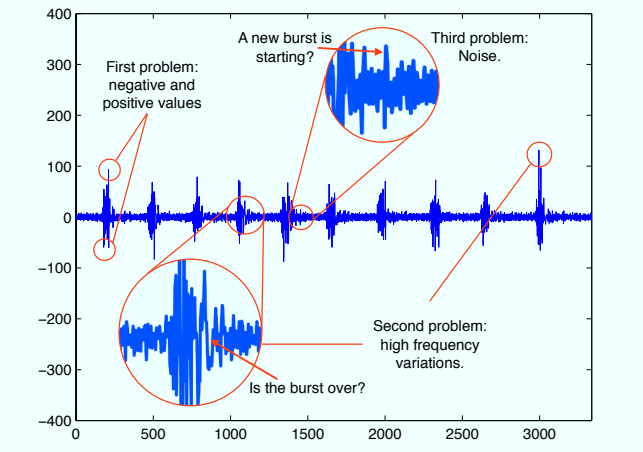

Figure 4.9: The first three problems related to the signal segmentation. The signal in figure is a training signal for the thumb abduction. In particular 10 contractions are performed.

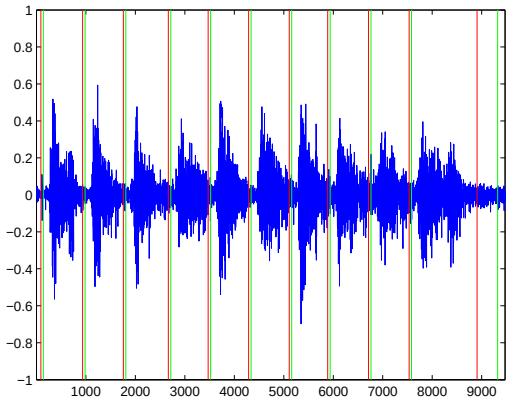

Figure 4.10: The last burst seems to be composed by two different bursts.

3. sometimes the signal is very low, or covered by high noise (Figure 4.9);

4. if the burst is too long, sometimes, it seems to be composed by two different bursts (Figure 4.10).

For all the reasons mentioned above, at this stage it is impossible to use a single threshold value to discriminate the start and the end of a burst. These issues are solved applying two methods in succession: rectification

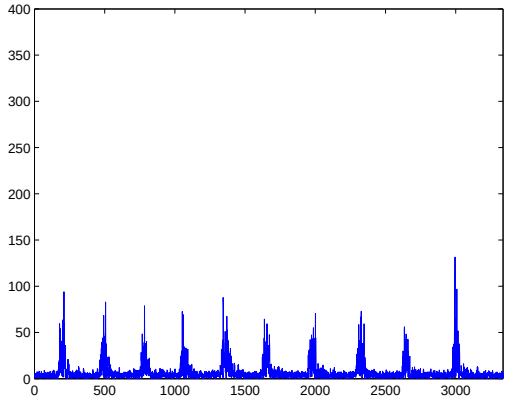

Figure 4.11: The rectification of the original signal in Figure 4.9

and linear enveloping.

Rectification: the absolute value of the incoming signal is computed in order to obtain the rectified version. This is never negative, therefore the first problem is solved. Moreover the mean of the rectified signal is no more negative (mean absolute value), which is very useful to extract information (Figure 4.11).

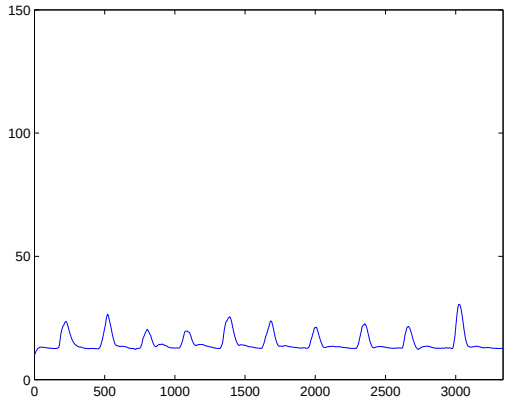

Figure 4.12: Linear envelope of the rectified signal in Figure 4.11

Linear envelope: the rectified raw signal is then filtered with a low-pass filter, characterized by a cutoff frequency of 2Hz. This means that just the slower harmonics are returned, which represent the contour of the rectified signal. This contour is called *linear envelope* (Figure 4.12) and, by construction, its frequency is very low, which solves the second and third problems. The fourth is addressed by another method discussed later in this section. At this stage the signal is ready for the segmentation.

Segmentation: this method is based on the moving average of the signal. The main idea of the algorithm is that whenever the signal (blue line in Figure 4.13) overcomes its own moving average (yellow line in in Figure 4.13), the contraction is detected. Then the algorithm waits for a certain amount of time (1 second), before closing the burst. If at this time the level of the envelope is high enough, the closing is delayed of a little amount of time (0.2 second).
When the end of the burst is reached, the segmentation module is ready to receive another burst. It is important to notice that the *delay feature* of

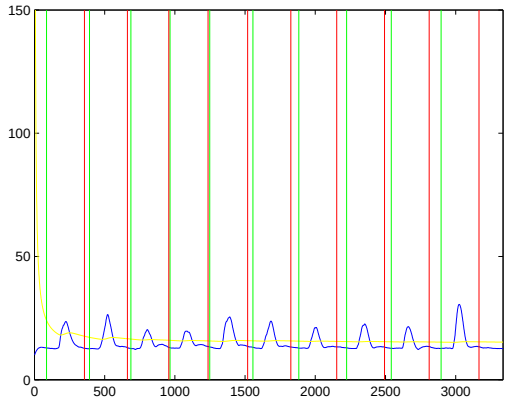

Figure 4.13: The moving average is the yellow line. The green line is the one relative to the start of the burst while the red one is relative to the end. In this example it is represented the second channel signal, relative to thumb abductions. The red and green lines are obtained using the algorithm designed by Brandon Kuczenski for Kensington Labs.

the segmentation algorithm is able to solve the fourth problem mentioned previously.
Actually, the threshold is not the real moving average: as it is possible to see from the yellow line in Figure 4.13, the starting value of the threshold is

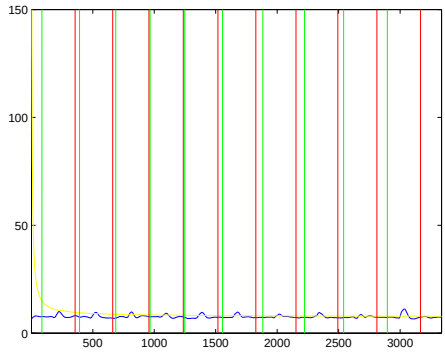

(a) Channel 1

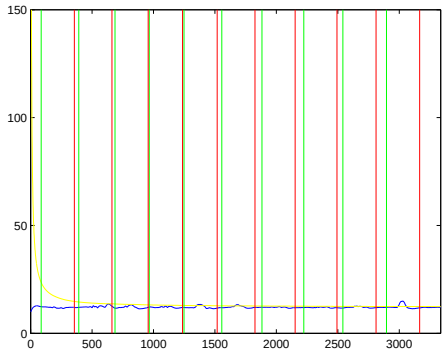

(b) Channel 3

Figure 4.14: First and third channels (second channel is in Figure 4.13) relative to the thumb abduction: they are characterized by a very small amplitude, thus it is difficult to detect the bursts from these signals. The segmentation of both the envelopes is done using the information contained in Channel 2.

very high, in order to avoid unwanted burst detection at the very beginning of the train. Then, after few fractions of a second, it meets the real moving average of the signal.

The system is endowed with three channels, therefore the algorithm has to deal with three linear envelopes at a time. The characteristics of the signals coming from the three distinct channels are heterogeneous: for example a contraction that is well sensed by a couple of electrodes, could be invisible to another couple applied in the opposed position (Figure 4.14). It is not possible to independently segment signals relative to different channels, because in this way, bursts happening at the same time would be divided in different ways.

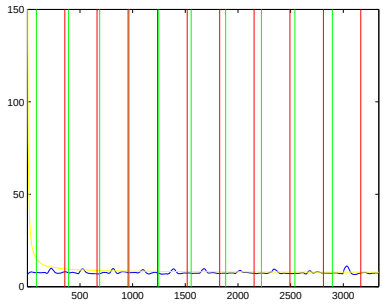

(a) Channel 1

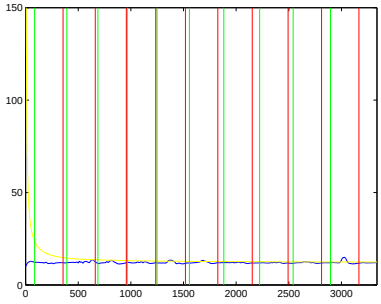

(b) Channel 2

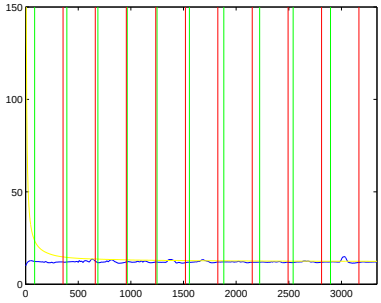

(c) Channel 3

Figure 4.15: Segmentation of the training signals coming from the three channels (thumb abduction).

The solution to this problem is that, at a given burst, the channel with the highest envelope value is the one which dominates the others, deciding the burst segmentation. When the current burst is closed, the highest value is reset, in the way that another channel can take the lead for the next burst detection.

In the example in Figure 4.14, Channel 2 dominates the other two channels for all the bursts, because this particular signal train is a training signal made just of thumb abductions. During a normal acquisition, channels exchange their roles.
The last step in the segmentation module is the high-pass filtering of the original signal. The cutoff frequency of 10 Hz allows the system to reduce the contribution of the low-frequency noise, generated by the movement of electrodes, cables and connectors, arising from the motion of the user. The final result of the segmentation module is shown in Figure 4.15. From now on, the term *burst* will be used to describe each segmented part of the *signal* relative to a muscle contraction, while the terms *signal* or *train* will be used to describe the whole train of *bursts*.

4.4.3.2 Feature Extraction

The feature extraction module has the role of identifying particular numeric parameters from the single signal burst. Such parameters are called *features*, and the whole set of features is called *feature vector*. This vector is much smaller in dimension compared to the original signal burst vector, and contains its significant and representing data. Reducing the signal burst to its feature vector is a necessary preprocessing in order to diminish the complexity of the classification.
In Chapter 2, the state of the art approach to this problem has been discussed in detail: many methods, both temporal and spectral, are available to achieve the feature extraction.

The temporal approach is mainly based on such parameters like mean absolute value, mean absolute value slope, number of zero crossings, slope sign changes, and waveform length.
The above temporal characterizations doesn't help much for the hand motion recognition, particularly in the discrimination of six synergetic grasp [76]. An exception is the first parameter, the mean absolute value, which can be loosely related to the signal's energy. As will be shown in the next chapter, this attribute helps the training for a successful classification of prehensile motions.
After these considerations and empiric evaluations, the decision for our project was to take as temporal features the mean absolute value (MAV) and the integral EMG (iEMG), which are, respectively, the mean value and the integral of the rectified burst.

The spectral approach: as stated above, the EMG signal is non-stationary, this means that its frequencies vary along the time. In Figure

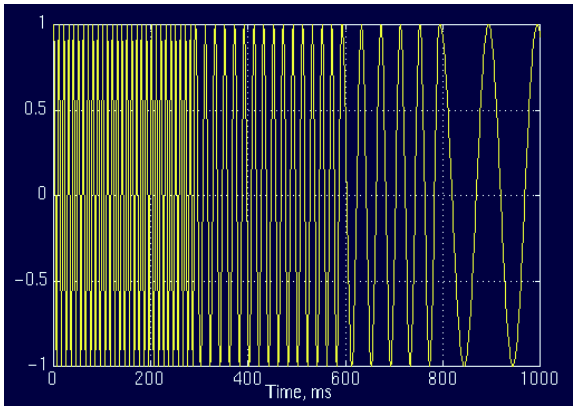

Figure 4.16: Example of a non-stationary signal. In particular the interval 0 to 300 ms has a 100 Hz sinusoid, the interval 300 to 600 ms has a 50 Hz sinusoid, the interval 600 to 800 ms has a 25 Hz sinusoid, and finally the interval 800 to 1000 ms has a 10 Hz sinusoid.

4.16 it is represented a non-stationary signal: four different frequency components at four different time intervals are distinguishable. In particular the interval 0 to 300 ms has a 100 Hz sinusoid, the interval 300 to 600 ms has a 50 Hz sinusoid, the interval 600 to 800 ms has a 25 Hz sinusoid, and finally the interval 800 to 1000 ms has a 10 Hz sinusoid.
The *spectral approach* aims at extracting parameters related to the spectral power of the signal, therefore such methods make massive use of the Fourier transform. This type of transform is not able to catch the distinction between the time intervals at which the frequency components are located, but returns all the spectral components of the signal, like they would occur at the same time. Hence, in this field of application, the Fourier analysis turned out to be poor of information.
When the time localization of the spectral components is needed, a transform giving the *time-frequency representation* has to be used.
The introduction of the short time Fourier Transform (STFT) solves the time-frequency issues. In STFT, the signal is divided into small enough portions, which can be assumed to be stationary. For this purpose, a win-

dow function is chosen. The width of this window must be equal to the portion of the signal where its stationarity is valid.
The STFT is unfortunately affected by resolution issues, mainly this means that at a narrow windowing corresponds a good time resolution and a poor frequency resolution, while at a wide windowing corresponds a good frequency resolution and a poor time resolution (Figure 4.17). Poor frequency

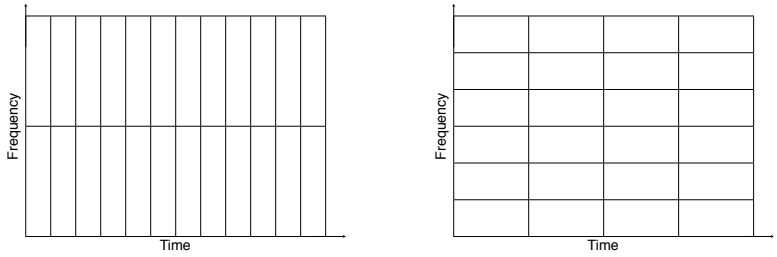

(a) High time resolution (b) High frequency resolution

Figure 4.17: If the time resolution is high, consequently the frequency resolution is poor 4.17a. On the other hand, if the frequency resolution is high, consequently the time resolution is poor 4.17b.

resolution means that the frequency peaks cover a range of frequencies, instead of a single frequency value.
The resolution issue is finally solved by the design of a new mathematical method, the Wavelet Transform. Literature considers the Wavelet Transform as one of the best methods to accomplish the time-frequency analysis, since it was designed on purpose to solve, to a certain extent (Heisenberg uncertainty principle), the resolution dilemma. [95].

The Wavelet Transform: the term wavelet means *little wave*. The adjective *little* refers to the fact that the entire transformation process is based on single wave, finite in length, the *mother wavelet*.
The basic idea underlying wavelet analysis consists of expressing a signal as a linear combination of a particular set of functions, obtained by shifting and scaling the mother wavelet. The decomposition of the signal into the basis of wavelet functions implies the computation of the inner products between the signal and the basis functions, leading to a set of coefficients called wavelet coefficients.
The wavelet analysis can be divided in two major categories: the Continuous Wavelet Transform (CWT) and the Discrete Wavelet Transform (DWT). Since DWT is used for data compression while CWT for signal analysis, this

subsection focuses on the latter. From now on, *wavelet analysis* and CWT will be used as synonyms.
A detailed analysis of the continuous wavelet transform has to be done, in order to understand its advantages with respect to the STFT. The actual role of the mother wavelet is to act as a prototype of windowing functions in the entire transformation process of the signal (x). That means that all the other window functions (wavelet) are computed starting from the mother wavelet (ψ), which is modified by changing two parameters:

- scale (σ): represents the dilatation of the wavelet. This parameter is not just a factor of enlargement of the wavelet, instead it also brings information about its frequency. To a high scale ($\sigma > 1$) corresponds a low frequency: just imagine to stretch the wavelet along time, obtaining a slowly varying wave. On the other hand, to a low scale ($\sigma = 1$) corresponds a high frequency: just imagine to compress the wavelet obtaining a wave varying faster in time;

- translation (τ): represents the time at which the wavelet starts.

After the definition of the main concepts, it is now possible to describe the transformation algorithm (Figure 4.18), based on the Formula 4.1.

$$CWT_x^{\psi}(\tau, \sigma) = \frac{1}{\sqrt{|\sigma|}} \int x(t)\, \psi\left(\frac{t-\tau}{\sigma}\right) dt \tag{4.1}$$

The main goal is to fill in a translation-scale table, with the coefficient of "similarity" between the signal and the wavelet at a given translation time(τ) and scale(σ), computed with the Formula 4.1:

1. the wavelet is placed at ($\tau = 0$) and ($\sigma = 1$);

2. the signal and the wavelet are multiplied and then integrated over time. Obviously, the product is nonzero only where the signal falls in the region of support of the wavelet, and it is zero elsewhere;

3. the result of the integration is then multiplied by the constant number $1/\sqrt{\sigma}$. This multiplication is for energy normalization purposes so that the transformed signal will have the same energy at every scale;

4. the final result is the value of the transformation for ($\tau = 0$) and ($\sigma = 1$). This is the wavelet coefficient in position ($\tau = 0$, $\sigma = 1$) in the translation-scale table;

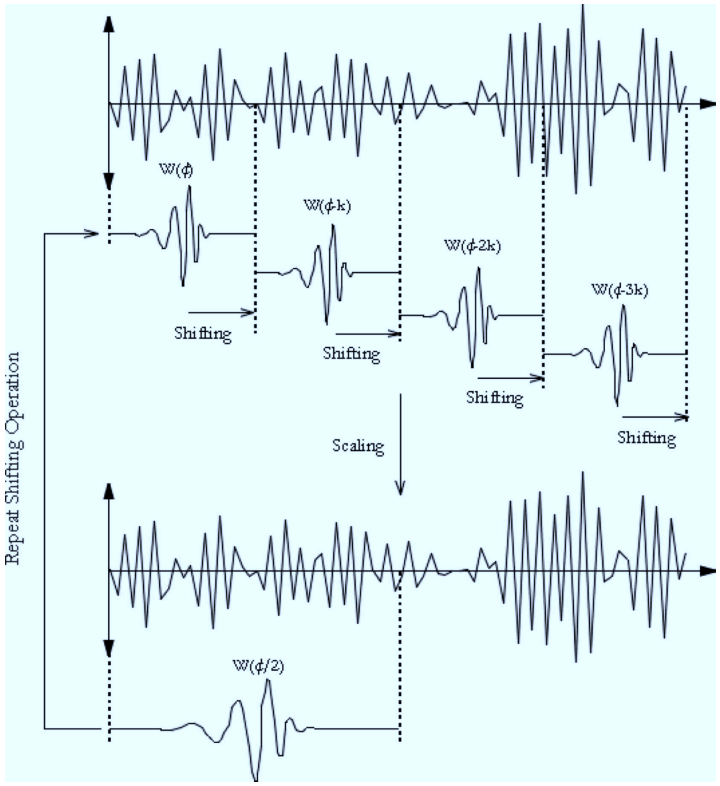

Figure 4.18: Wavelet shifting (τ) and scaling (σ) procedure [96]

5. the wavelet, keeping $\sigma = 1$, is then shifted of a sufficiently small step size ($\tau = \tau + \epsilon$);

6. the previous steps are repeated until the end of the signal;

7. the first row of the translation-scale plane is complete;

8. the scale is increased of a a sufficiently small step size ($\sigma = \sigma + \epsilon$). Coefficients are computed for all the values of τ and σ (inside a predefined range) as described in the previous points.

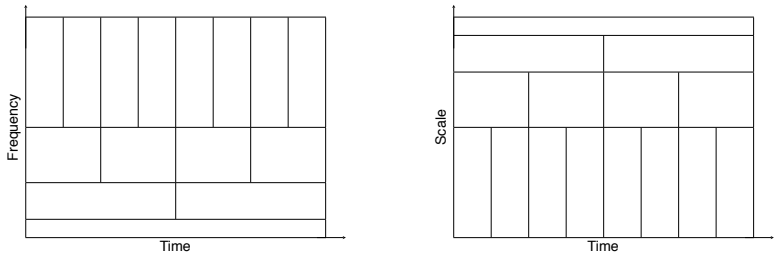

(a) Time-Frequency resolution. (b) Time-Scale resolution

Figure 4.19: Resolution given by the Wavelet Transform.

Unlike the STFT which has a constant resolution at all times and frequencies, the wavelet transform has a good time and poor frequency resolution at high frequencies, and good frequency and poor time resolution at low frequencies (compare figures 4.17 with Figure 4.19a). Recalling the relation between scale and frequency, lower scales (higher frequencies) have low scale resolution which corresponds to poorer frequency resolution. Vice versa, higher scales correspond to high scale and frequency resolutions (Figure 4.19).
The meaning of Figure 4.19a is that high frequency components can be located better in time than low frequency ones. On the contrary, low frequency components can be located better in frequency compared with high frequency components.
This approach makes sense especially when the signal has high frequency components for short durations and low frequency components for long durations, which is the case of the most signals of physical nature, especially the transient ones [96][95][97].
According to empiric observations and results obtained in other works, the mother wavelet we chose for our analysis was the Morlet (Figure 4.20) [78].
The problem of the Wavelet Transform is that the amount of data returned from the algorithm is too large to be inputted into an Artificial Neural Network. In our case, computing the CWT of a single burst composed by 270 samples, produces a matrix of size 5X270. This is composed of five rows because of the empirical choice to make the scale vary between 1 and 5, which produces the best tradeoff between performance and computation speed.
At this stage, our feature vector is composed by 2 temporal parameters, namely the MAV and the iEMG plus an entire matrix of size 5X270. Therefore before using a classifier, like an Artificial Neural Network, a dimension-

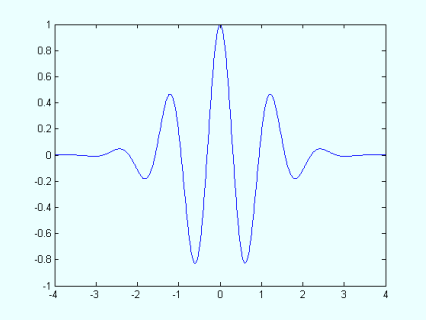

Figure 4.20: Morlet mother wavelet.

ality reduction of the feature vector is needed.

4.4.3.3 Dimensionality Reduction of Feature Vectors

The dimensionality reduction of the matrix obtained applying the Wavelet Transform, is achieved by a powerful method called Singular Value Decomposition (SVD). This method is used to factorize a whatsoever m-by-n matrix M into three different matrices:

$$M = U\Sigma V^T \tag{4.2}$$

Let's consider a 2X2 geometric example in which an orthogonal grid is transformed into another orthogonal grid. Normally there are no reasons for which the orthonormality would hold. We are looking for a special set up for which the M matrix brings from an orthonormal to another orthonormal space [98]. The basis of the grid on the left in Figure 4.21 are orthogonal unit vectors v_1 and v_2 (orthonormal) and if they are correctly chosen, then, after the transformation, the vectors Mv_1 and Mv_2 become orthogonal.
The next step, is to describe the vectors Mv_1 and Mv_2 as a stretched version of particular unit vectors u_1 and u_2, in order to achieve the orthonormality also in the transformed space:

$$Mv_1 = \sigma_1 u_1 \qquad Mv_2 = \sigma_2 u_2 \tag{4.3}$$

The extent of the grid stretching in those particular directions is given by σ_1 and σ_2, which are called the singular values of M.
Considering again the formula $M = U\Sigma V^T$, U is a matrix whose columns are the vectors u_1 and u_2, Σ is a diagonal matrix whose entries are σ_1 and σ_2, and V is a matrix whose columns are v_1 and v_2.

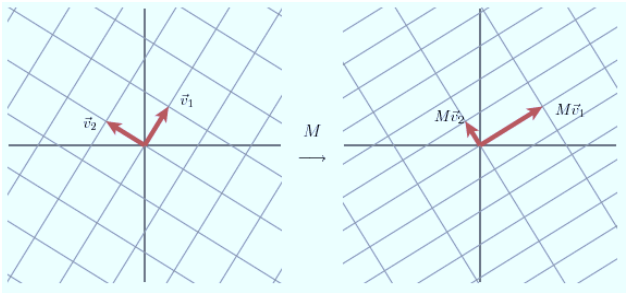

Figure 4.21: Transformation from an orthogonal grid to another one [99].

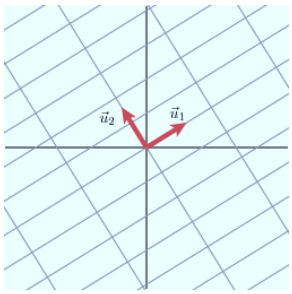

Figure 4.22: Representation of the unit vectors of Mv_1 and Mv_2. They are an orthonormal basis of the co-domain in Figure 4.21 [99].

The previous intuitive explanation of the SVD shows how to decompose the matrix M into the product of three matrices: V describes an orthonormal basis in the domain (left part in Figure 4.21), U describes an orthonormal basis in the co-domain (Figure 4.22), and Σ describes how much the vectors in V are stretched to give the vectors in U [99]. Another property is that the rank of M equals the rank of Σ.
Singular Value Decomposition is applied in many fields because of its ductility: it can be used for the compression of large amount of data, noise reduction, matrix approximation, to execute the principal component analysis, signal processing, pattern recognition and many other tasks.

For example let's consider a noise reduction problem, in which the SVD applied to a matrix M returned a Σ of rank 15. The diagonal values are the following: $\sigma_1 = 14.15; \sigma_2 = 4.67; \sigma_3 = 3.00; \sigma_4 = 0.21; \sigma_5 = 0.19; ...; \sigma_{15} = 0.05$. It is easy to see that the first three σ are the biggest in the list. Therefore the original matrix, that should be constructed considering the original rank of the matrix (15), using the formula $M = U\Sigma V^T$, can actually be approximated in this way:

$$M \approx u_1\sigma 1 v_1^T + u_2\sigma_2 v_2^T + u_3\sigma_3 v_3^T \tag{4.4}$$

The result of this approximation is shown in Figure 4.23.

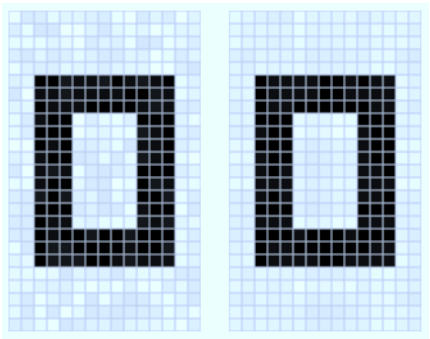

Figure 4.23: Noise reduction with SVD. On the left the noisy image, on the right the improved one [99].

For our purpose, namely the feature extraction, it is exploited a particular property of the SVD: if the diagonal entries of Σ are disposed in descending order, Σ itself is uniquely determined by M. Therefore by simply applying the SVD to the Wavelet Coefficient matrix and extracting the σ_i, it is possible to obtain a small set of values representing, at some extent, the original Wavelet Coefficient matrix . In order to understand the importance of the dimensionality reduction, the Wavelet Coefficient matrix goes from a size of 5X270 to a size of 5X1.

4.4.3.4 The Feature Vector

The feature vector representing a single burst is composed by 2 temporal parameters, the iEMG and the MAV, and by 5 time-frequency parameters

obtained by the synergy of the Wavelet Transform and the SVD methods, for a total of 7 features. This feature vector is, however, related to a single burst, coming from a single channel. Therefore, considering that the channels of the EMG board are three, the total amount of features per movement is 21.

4.4.3.5 Classification

A classifier is a black box model, trained to learn associations between a specified set of input-output pairs. Actually, what happens is that each training sample is labeled by a human, according to its corresponding abstract class (supervised learning). Then the training phase is carried on in the way that the classifier has to learn how to associate each training input to its label, otherwise called *target output*.
After being trained, the classifier is able to predict the class of membership of a whatsoever *unlabeled* input taken from a test set.
There are several techniques used in supervised learning: Linear Classifiers, k-Nearest Neighbors, Support Vector Machines and Artificial Neural Networks. The choice in this thesis has been to use Artificial Neural Networks, because of their massive application in classification and pattern recognition problems. Moreover, after an exploratory phase, the SVM was found difficult to set up: the performances of this classifier highly rely on the SVM kernel function, which has to be carefully selected.
An Artificial Neural Network consists of a topology graph of neurons, each of which computes the function (called *activation function*) of the inputs and sends the result in output. The inputs and outputs are weighed by weights w_{ij} and shifted by bias factor specific to each neuron. It has been shown that for certain neural network topologies, with the right set of weights and biases, any continuous function can be accurately approximated.
The learning problem consists of finding the optimal combination of weights w_{ij} so that the network output approximates a given target output as closely as possible. To achieve this goal, the training algorithm tries to minimize the difference between the target output (t) and the real current output (o). More precisely, we want to minimize the error function of the network, defined as

$$E = \frac{1}{2}\sum_{i=1}^{p}|o_i - t_i|^2 \tag{4.5}$$

In the equation 4.5, the value p represents the number of pairs (o,t) composing the training set.
The most common way to minimize the error, is the application of the classic *backpropagation algorithm*. But since another method, the Levenberg-

Marquardt(LM) algorithm, appears to be the fastest method for training moderate-sized feedforward neural networks (up to several hundred weights), the final decision has been to choose the latter [100]. The LM algorithm is a member of the family of the nonlinear least squares algorithms [101][102][103]. In the scope of this thesis, a two-layer feedforward neural network has been designed and trained with the EMG feature vectors. The single hidden layer

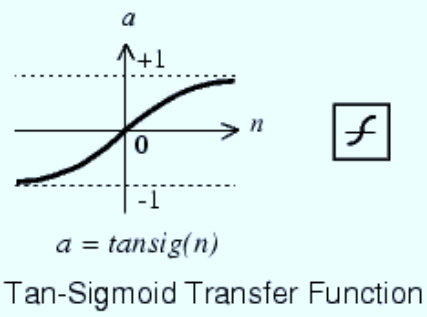

Figure 4.24: Tan-Sigmoid activation function.

is composed by 35 neurons, characterized by a Tan-Sigmoid activation function. Instead, the output layer is composed by just 7 output neurons, one for each movement to classify. The network outputs are linear, thus binary encoding is needed in order to bring compact information. For example if the first neuron output is the nearest to 1, then all the other outputs are manually set to 0. The resulting binary string, in this particular case, represents the event "Hand closed" ([1 0 0 0 0 0 0]). Each of the seven movement described previously in this chapter has its own binary encoding.

4.4.4 Training Procedure

The training procedure for the current work is divided into three steps, namely the acquisition procedure, the signal preprocessing and the network training (Figure 4.25).

4.4.4.1 Acquisition Procedure

The acquisition procedure has been found empirically, in particular it was chosen the minimum amount of movements to perform, still giving high performances:

1. acquire one train of 10 bursts for the movement “Hand close”;
2. make the muscle relax for few seconds (it is also possible to shift the electrodes just a bit, to achieve “cross-session” robustness);
3. repeat the previous two steps other two times;
4. once 3 trains of a given movement are acquired, take one minute for resting and change the type of movement;
5. repeat the previous steps for all the 7 movements.

The previous procedure generates a signal *training set* made up by 21 signals, not yet segmented, nor processed.

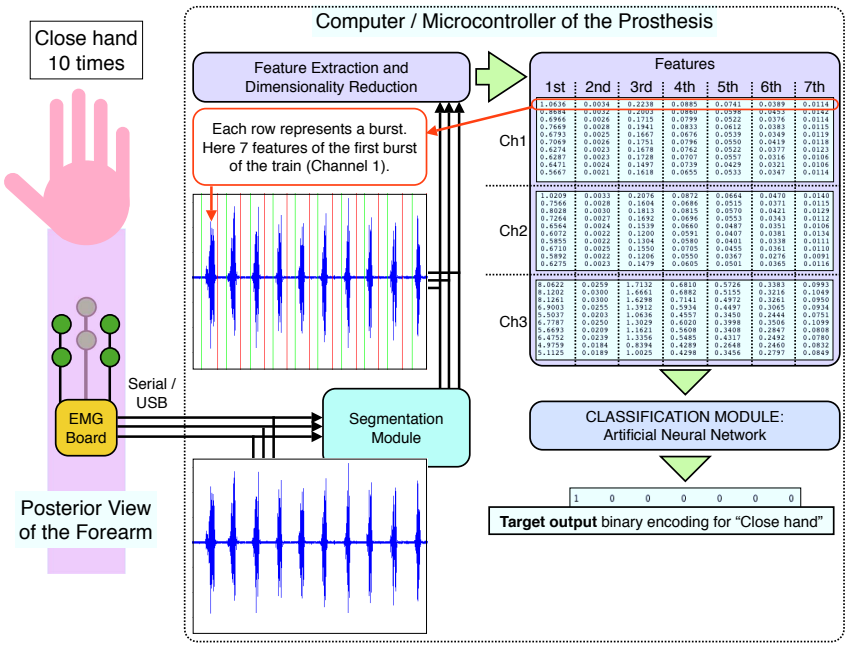

Figure 4.25: Detailed system structure. The incoming bursts train, composed by 10 “Close Hand” contractions, is segmented by the segmentation module. Then, for each burst, the corresponding feature vector is computed and, together with the target output ([1 0 0 0 0 0 0]), is inputted in the Artificial Neural Network. This is a schematic representation, therefore the actual training is performed on 3 trains of 10 burst for all the 7 movements.

4.4.4.2 Signal Preprocessing

This step has been carefully described in all its components, in the previous subsection. The signals composing the training set are first segmented and then the single bursts are processed with the temporal analysis, the Wavelet Transform and the SVD to extract the feature vectors. The real training set is, therefore, composed by 3 (trains) X 10 (bursts) X 7 (movements) feature vectors, for a total of 210.

4.4.4.3 Network Training

The *training set* previously obtained, is divided into three subsets:

- Training Set: is composed by the 3/5 of the whole set.
- Validation Set: is composed by 1/5 of the whole set. During the training, this set is used for cross-validation, a technique for assessing how the results of the network will generalize to an independent data set.
- Test Set: is composed by 1/5 of the whole set. After the training, it is used to test the performances of the network.

These data are then used to train the Artificial Neural Network, whose performances have been recorded and will be presented in the next chapter.

4.4.5 Motion Recognition

Once the system has been trained, it is able to recognize the movements performed by the user, and send the action to perform to the high level prosthesis controller.
In this subsection we consider the example of 7 consecutive movements:

1. hand closing ([1 0 0 0 0 0 0]);
2. hand opening ([0 1 0 0 0 0 0]);
3. wrist extension ([0 0 1 0 0 0 0]);
4. wrist flexion ([0 0 0 1 0 0 0]);
5. thumb abduction ([0 0 0 0 1 0 0]);
6. thumb opposition ([0 0 0 0 0 1 0]);
7. index extension ([0 0 0 0 0 0 1]).

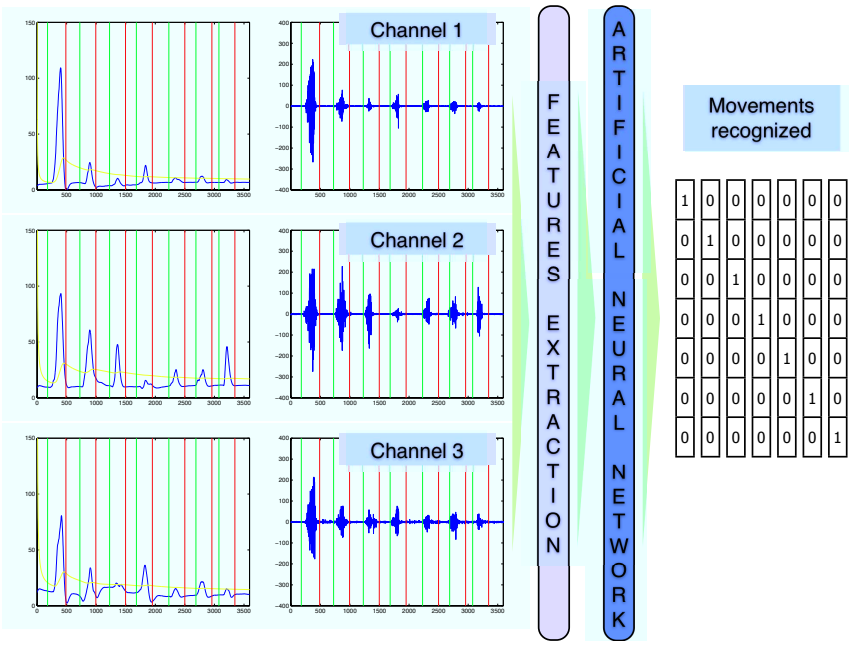

Figure 4.26: Abstract view of the recognition phase. 7 Movements are performed and each contraction burst is detected by all the three channels. The vectors at the output of the ANN represent the binary encoding of each recognized movement.

In the brackets it is shown the binary encoding of the each motion.
The three channels of the system detect a signal each, generated by the muscle contractions of the seven consecutive movements.
Each signal is composed by the bursts relative to each movement, which are segmented using the method described above. It is noteworthy to make a consideration about the segmentation: the level of the linear envelopes are different in each channel, therefore if they were segmented separately they would have had different durations for each contraction. The system, instead, dynamically adapts to envelope level variations, in particular the channel with the highest level of linear envelope is taken as the leading one, during the segmentation. For example, the first burst is recognized by Channel 1, while the last burst is recognized by Channel 2.
After the segmentation, feature vectors are extracted from each burst and inputted into the trained Artificial Neural Network, which recognizes each

movement performed (Figure 4.26).

4.4.6 Matlab Implementation

The complete implemented code is presented in Appendix A, while its structure is discussed in this subsection, also with the aid of Figure 4.27.

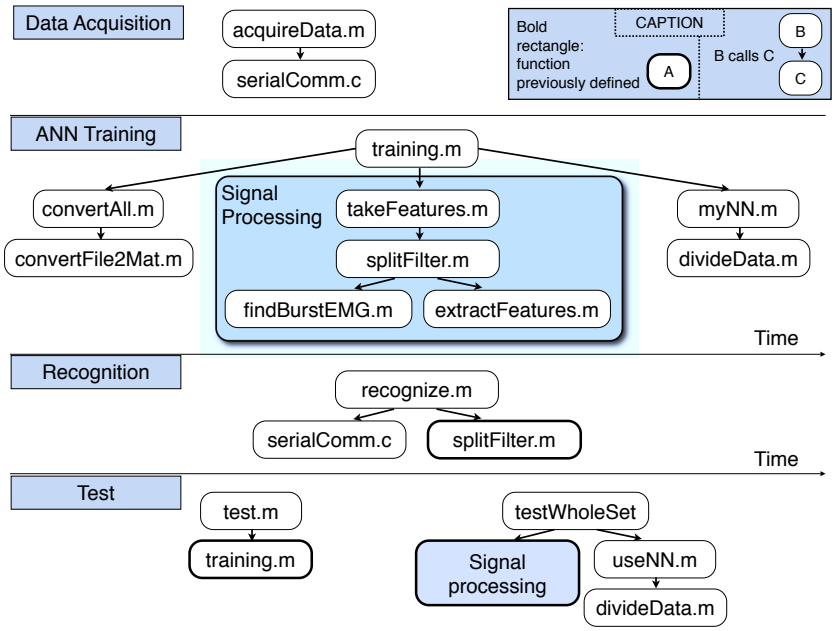

Figure 4.27: Abstract representation of the implementation of the project. The meaning of the arrows is that the function above calls the function below. The bold rectangle is used to represent that the function has already been defined along the graph. When a function calls more than one subfunction the calling order is from left to right (as the Time arrow shows).

Acquisition Implementation: the function *acquireData.m* calls the application "serialComm", written in C, to acquire data from the EMG board and to save them into text files. These data are the ones used during the network training. The files generated by the script are divided into folders relative to the person on which the acquisition is performed. Moreover,

the algorithm allows to chose a whatsoever number of motion patterns to classify (in this work this number is set to 7);

Signal Processing Implementation: this module is composed by several functions: first of all, *convertAll.m* is called in order to translate all the text files, previously generated, into Matlab files.
Then, *takeFeatures.m* is called to extract the feature vectors from all the acquired signals. To accomplish this task *takeFeatures.m* has to iteratively call the function *splitFilter.m*, which is applied to each signal.
In turn, *splitFilter.m* computes the linear envelope of one signal, composed by many bursts of contraction, on which is applied the function *findBurstEMG.m* for the segmentation. Once the system has found the division of all the bursts, they are processed by a high pass filter and then, on each one it is called *extractFeatures.m*. This function is useful for the task of extracting the feature vector from a burst, which is accomplished by applying the Wavelet Transform, the SVD and the Temporal Analysis. The Wavelet Transform is computed using the method *cwt()* taken from the Matlab Wavelet Toolbox, while the SVD is obtained calling the Matlab built-in function *svd()*.

Neural Network Training Implementation: the method *training.m* applies the functions described above in order to compute the training set to use for the training of an ANN. The actual implementation of the ANN and its training are accomplished by means of the function *myNN.m*, which in turn shows the performances of this process and returns the trained ANN. In order to divide the training set into the Training, Validation and Test sets, *myNN.m* calls *divideData.m*.

Motion Recognition Implementation: once the ANN has been trained it is possible to use it for the recognition of the gestures of the hand. In particular, this is done by applying the function *recognize.m*, which acquires new data from the EMG board, calling the application "serialComm". Then *splitFiler.m* is used to extract, from all the bursts in the signal, the feature vectors, which are inputted into the already trained Artificial Neural Network for the motion recognition.

Test Implementation: two methods have been implemented in order to study the performances of the system. The first is *testNet.m* which calls *training.m* more than one time and computes the overall performances.

The second algorithm is *testWholeSet.m*, which tests the performances of the trained network on data that can be different from the one acquired for the training. This new set could be in another folder, belonging to a person different from the one on whom the network was trained. In this way it is possible to execute *"cross-person"* and *"cross-session"* tests, which are very useful for further analysis. The algorithm uses the same files as *training.m*, except the one called *useNN.m*, which doesn't train a new ANN but simply uses the already trained one.

Chapter 5

Results

This chapter shows how the designed system is able to adapt to different situations. In particular, it has been tested on four different persons, each one with specific body characteristics. In this way it was possible to draw some conclusions about the goodness of the classifier and the procedures to follow in order to reach good performances. Moreover, factors influencing the acquisition and the analysis of the EMG signal, like subject's fatigue, concentration and motivation, as well as the electrodes placement, are discussed.

5.1 Test Procedure

Each subject was asked to execute a large amount of movements, as described in the previous chapter, in order to train his own Artificial Neural Network. The execution of these movements requires *high concentration*, because it is very likely to make unwanted contractions while performing a specific task. For this reason the patients are asked to think about, in case of real amputees, or actually perform, in case of sound subjects, a specific motion pattern at their best during the acquisition phase. The following is an empirically drawn procedure, explaining how to perform specific hand gestures in order to obtain great performances from the classifier training. It is included in the chapter of the results because it was obtained after a long period of experimental tries:

- *Close hand (CH)*: the patient has to contract the muscles related to the "hand closing" in a way that he can see their contraction. The latter has to be a bit more than impulsive (0.6 s) and requires a normal/high force level. Each movement is separated from the next one by a relax period of almost one second. Moreover, if he patient

wants to perform a "close hand" after another "close hand" contraction, he doesn't have to open the hand back between the two movements, but just relax the muscles. This prevents the system to detect an unwanted "open hand" between the two actions. It is also important that during the hand closing the patient doesn't flex the wrist.

- *Open hand (OH)*: the patient has to execute the "hand opening" in a way that he can clearly see the posterior forearm contracting. As in the previous case, the contraction has to be a bit more than impulsive (0.6 s) and requires a normal/high force level. Each movement is separated from the next one by a relax period of almost one second. Moreover, if he patient wants to perform a "open hand" after another "open hand" contraction, he doesn't have to close the hand back between the two movements, but just relax the muscles. This prevents the system to detect an unwanted "close hand" between the two actions. Eventually, it is important that during the hand opening the patient doesn't extend the wrist.

- *Wrist extension (WE)*: this movement is similar to the one performed during an acceleration on a motorbike. The force exerted has to be more natural, as well as the duration, which can be a bit smaller (0.5 s) than before, as in a normal wrist extension. The relax period is the same as all the other movements (1s). Moreover, if he patient wants to perform a "wrist extension" after another "wrist extension" contraction, he doesn't have to flex the wrist back between the two movements, but just relax the muscles. This prevents the system to detect an unwanted "wrist flexion" between the two actions. This type of movement requires a high concentration, in particular for sound people, because it is important that the fingers are not moved during its execution.

- *Wrist flexion (WF)*: this movement is like the "wrist extension", but in the opposite direction. The force exerted has to be natural, and the duration of the contraction is around 0.6 s. The relax period is the same as all the other movements (1s). Moreover, if he patient wants to perform a "wrist flexion" after another "wrist flexion" contraction, he doesn't have to extend the wrist back between the two movements, but just relax the muscles. This prevents the system to detect an unwanted "wrist extension" between the two actions. The same considerations hold here as for the wrist extension about

the finger movement.

- *Thumb abduction (TA)*: this movement is like the "Thumb Up" sign. A sound subject can check if the movement is executed correctly by looking if the thumb tendon stiffens. The force exerted has to be natural, and the duration of the contraction is around 0.6 s. The relax period is the same as all the other movements (1s). Moreover, if he patient wants to perform a "thumb abduction" after another "thumb abduction" contraction, he doesn't have to oppose the thumb back between the two movements, but just relax the muscles. This prevents the system to detect an unwanted "thumb opposition" between the two actions.

- *Thumb opposition (TO)*: this movement is like pushing the thumb against the palm for half a second (0.6 s). The force exerted has to be a bit larger than the normal one, so that the EMG board can detect the low EMG signal generated. The relax period is the same as all the other movements (1s). Moreover, if he patient wants to perform a "thumb opposition" after another "thumb opposition" contraction, he doesn't have to abduct the thumb back between the two movements, but just relax the muscles. This prevents the system to detect an unwanted "thumb abduction" between the two actions.

- *Index extension (IE)*: this movement is composed by the extension of both the index and middle finger, which generates an higher EMG signal than the single index extension. It requires high concentrations, because the extension of these fingers usually extends also other fingers in the hand. The contraction lasts a bit less (0.5 s) than in other movements and its force has to be as normal as possible, always reminding that the EMG signal has to be strong enough to be detected.

5.2 Subjects

The test phase was performed on four sound subjects with different physical structures. A deep characterization is important to understand in which cases and for which reasons the system works well or less well. In particular, we investigate how different features of the forearm and different lifestyles can influence the signal acquisition and analysis. In the following list the muscle tone scale ranges from 0, corresponding to hypotonia, to 5, corresponding to hypertonia:

- Subject A (A)
  - Gender: Male
  - Age: 23
  - Height: 1.73 m
  - Weight: 71 Kg

  Subject A does a sedentary job, he usually carries bags and weights but doesn't go to the gym. His muscle tone can be located in 3, moreover the volume between the forearm muscles and the skin is small. These features allow a good signal acquisition, in which the EMG signal overcomes the noise and can be highly recognizable, even in the small contractions related to the thumb movements.

- Subject B (B)
  - Gender: Male
  - Age: 50
  - Height: 1.73 m
  - Weight: 95 Kg

  Subject B has a lifestyle similar to subject A.

- Subject C (C)
  - Gender: Male
  - Age: 15
  - Height: 1.83 m
  - Weight: 110 Kg

  Subject C does a sedentary job and, due to the young age, his muscle structure still has to consolidate. His muscle tone can be located in 2 and the volume between the forearm muscles and the skin is large, given height and weight. These features make the signal acquisition more difficult, in particular for movements generated by the contraction of weaker muscles, like the thumb abduction and opposition.

- Subject D (D)

- Gender: Female
- Age: 46
- Height: 1.68 m
- Weight: 87 Kg

Subject D does a sedentary job and rarely carries weights. Her muscle tone can be located in 1 and the volume between the forearm muscles and the skin is large, given height and weight. These features make the signal acquisition almost impossible for movements generated by the contraction of weaker muscles.

5.3 System performances

The system has to be customized on each patient, therefore every person who is subject to the analysis has to perform his own movements.
Subject A and subject B performed the procedures mentioned above and in the previous chapter, without changing the position of the electrodes, to produce 3 trains of 10 contractions each for all the 7 movement patterns. These data are randomly divided into three sets: 3/5 for Training, 1/5 for Validation and 1/5 for Test. The first two are used to train the network, while the third to test its performances.

Subject A	CH	OH	WE	WF	TA	TO	IE	Perf.
Total Movements	6	6	6	6	6	6	6	
Total Errors	0	0	0	0	0	0	0	100%

Table 5.1: "Training performances" of the network, obtained running the script training.m *with folder* A_normal_1 *as input .*

Subject B	CH	OH	WE	WF	TA	TO	IE	Perf.
Total Movements	6	6	6	6	6	6	6	
Total Errors	0	0	0	0	0	0	0	100%

Table 5.2: "Training performances" of the network, obtained running the script training.m *with folder* B *as input.*

This means that for each type of movement the test set is composed by 6 bursts of contraction. The best result that can be obtained after the training of the network is shown in Table 5.1 and Table 5.2.
The captions of each table say what scripts are run on which folders of the documentation in order to obtain the results.
In the examples above are presented the best performances obtainable, given a random division of the training set, but when this set is divided in another way, it is possible to notice slight changes in performance. This highlights the importance of an average performance value, which is obtained running the training algorithm more than one time on different networks and with different commutations of the training data.
All the results are memorized and used to compute an average performance. Using the script *testNet.m*, different Artificial Neural Network have been trained 20 times on different random commutations of the training data, and tested with the respective Test Set, leading to the results in Table 5.3 and Table 5.4.

Subject A	CH	OH	WE	WF	TA	TO	IE	Perf.
Total Movements	120	120	120	120	120	120	120	
Total Errors	1	5	0	1	6	3	9	97%

Table 5.3: Average "training performances" of the network, obtained running the script testNet.m *with folder* A_normal_1 *as input.*

Subject B	CH	OH	WE	WF	TA	TO	IE	Perf.
Total Movements	120	120	120	120	120	120	120	
Total Errors	1	6	4	0	7	2	2	97.4%

Table 5.4: Average "training performances" of the network, obtained running the script testNet.m *with folder* B *as input.*

An Artificial Neural Network trained following the previous procedure, with a "training performance" of 100% is a good network but still imperfect. Indeed, what has been shown so far, highly relies on the particular acquisition set, leading to many errors when the system has to recognize movements acquired in different times.
An example is proposed in Table 5.5, in which are shown the results of

a "recognition test". An Artificial Neural Network trained with 100% of "training performance" on data coming from Subject A, has been applied on a "recognition set" (never seen before by the ANN and acquired in a different moment) composed by 10 bursts for each movement type, with a result of 95.7%, which is bad compared to the 100% obtained in the training. Moreover, the procedure is too dependent on the electrode placement, therefore, when the electrodes are placed on a slightly different position the performance lowers down even more.

Subject A	CH	OH	WE	WF	TA	TO	IE	Perf.
Total Movements	10	10	10	10	10	10	10	
Total Errors	0	0	0	0	0	0	3	95.7%

Table 5.5: Results of the recognition phase, obtained running the script testWholeSet *with these inputs: folder* A_sess_ind_ts1 *and an Artificial Neural Network trained with 100 % performance on folder* A_normal_2.

5.4 Generalization and Session Independence

From session to session, it is impossible to place electrodes at the exact same position. Therefore it is important to achieve a sort of Session Independence, which allows the system to react well even to different electrode configurations.
Few days after the first acquisition phase, Subject A was asked to repeat the procedure. In this case the electrodes were put on a slightly different position of the forearm.
Moreover the contractions exerted by the subject were quite different in force and pattern, compared with the ones of the first acquisition session, because he couldn't remember the exact way he performed them the first time.

Subject A	CH	OH	WE	WF	TA	TO	IE	Perf.
Total Movements	10	10	10	10	10	10	10	
Total Errors	0	0	0	0	0	0	1	98.6%

Table 5.6: Results of the recognition phase, obtained running the script testWholeSet *with these inputs: folder* A_sess_ind_ts1 *and an Artificial Neural Network trained with 100 % performance on folder* A_sess_ind.

Data from the first and the second sessions were, then, merged together in a unique training set, which was used to train an Artificial Neural Network with a "training performances" of 100%. After the training, this network has been tested on the same "recognition set" that gave the results in Table 5.5 in the previous example, producing the results in Table 5.6.
The ANN is now more stable and can recognize 69 movements on 70, which is a very high rate. From these results we can draw important conclusions: the slight change in force exerted and in motion execution, helped the system to generalize the training. Which means that now the ANN is able recognize a hand gesture even if executed in different ways.
It is also important to mention that if the number of movement patterns to recognize is diminished to 6, eliminating the index extension, the performance of the classification ranges between the 99% and 100%. While if we also eliminate the thumb opposition, we obtain a stable performance of 100%.
Another experiment is presented in order to show how the session independence is improved.

Subject A	CH	OH	WE	WF	TA	TO	IE	Perf.
Total Movements	10	10	10	10	10	10	10	
Total Errors	0	1	3	0	0	3	0	90%

Table 5.7: Results of the recognition phase, obtained running the script testWholeSet *with these inputs: folder* A_sess_ind_new_ts *and an Artificial Neural Network trained on folder* A_normal_2.

Subject A	CH	OH	WE	WF	TA	TO	IE	Perf.
Total Movements	10	10	10	10	10	10	10	
Total Errors	0	2	1	0	1	0	0	94.3%

Table 5.8: Results of the recognition phase, obtained running the script testWholeSet *with these inputs: folder* A_sess_ind_new_ts *and an Artificial Neural Network trained on folder* A_sess_ind.

Two networks that have been presented previously are compared. In particular, the first is the one trained not to be session independent, which

recognized just the 95.7% of the movements (Table 5.5). The second is the one trained to be session independent, which had a performance of 98.6% (Table 5.6).
These two networks have been tested on a completely new "recognition set", acquired with a different configuration of electrodes than the one used to acquire the training data of the two networks. Table 5.7 and Table 5.8 show how badly the first network reacts to the new electrode configuration, compared to the session independent ANN .
Even if the second network performed better than the first, its performance still decreased if compared with the 98.6% obtained with the previous "recognition set". However this isn't a problem, since the actual prosthesis are attached to the human forearm in a way that the electrodes are always placed in the same position.

5.5 Patient's Fatigue and Concentration

Muscle fatigue is another important aspect of the EMG signal analysis. As stated in the previous chapter, the signal varies its frequency components in time and this issue can be solved thanks to the Wavelet Analysis.

Subject A	CH	OH	WE	WF	TA	TO	IE	Perf.
Total Movements	20	20	20	20	20	20	20	
Total Errors	0	0	0	0	3	0	1	97.1%

Table 5.9: Results of the recognition phase, obtained running the script testWholeSet *with these inputs: folder* A_sess_ind_ts2 *and an Artificial Neural Network trained with 100 % performance on folder* A_sess_ind.

Subject A	CH	OH	WE	WF	TA	TO	IE	Perf.
Total Movements	30	30	30	30	30	30	30	
Total Errors	0	2	0	0	9	0	1	94.3%

Table 5.10: Results of the recognition phase, obtained running the script testWholeSet *with these inputs: folder* A_sess_ind_ts3 *and an Artificial Neural Network trained with 100 % performance on folder* A_sess_ind.

Unfortunately we still can see from some experiments that executing new movements with very little relax time can lead to bad performances.
The example in Table 5.9 shows how the performances in Table 5.6 are reduced, by adding to the "recognition set" other ten contractions for each movement type, and get even worse when other 10 bursts are added (Table (5.10).
The fact of performing so many muscle contractions in such a small time leads to a level of muscle fatigue that is difficult to face even with the Wavelet Analysis. What is comforting is that, normally a person doesn't perform a total of 210 consecutive movements in a time range of 10 minutes.
It is also important to mention that Subject A realized that his concentration decreased from session to session, given the fact that he was bored and tired. This highlights how the patient's motivation is a key factor in the whole training process, which can lead to great or very bad results.

5.6 Signal attenuation and filtering

Tests made on Subject C and Subject D gave different results than before, in particular the system is able to recognize the first five movements with the same performances, but unfortunately when it comes to the thumb opposition and the index extension it doesn't work anymore. This is due to the fact that Subject C and D have more volume between the forearm muscles and the skin. Moreover their muscles are less trained than the ones of Subject A and Subject B.
The volume conductor properties largely determine the features of the detected surface EMG signals, in terms of their signal amplitude and also in terms of frequency content. Other experimental observations confirm an inverse power relation between signal amplitude and the MU's depth, especially because the contribution of the traveling wave of the MUAP falls off rapidly with electrode-source distance. In general, it is assumed that the biological tissue acts as a temporal low-pass filter. Indeed, the tissue has a "blurring" effect on a MUAP by widening its traveling waves [17].
The Wavelet Analysis solved the issue related to the frequency component modification, but it couldn't overcome the problems related to the signal amplitude. Indeed, the first five movements, are well recognized by the system because they are produced by strong muscles, while thumb abduction and index extension are not even segmented, since they are invisible also to the human eye.
The results obtained by the tests performed on Subject C and D suggest

that a patient with a similar body structure, will have to attend physiotherapy and electrostimulation sessions to improve the muscle tone, before training their own Artificial Neural Network.

5.7 Patient's Motivation

From the tests performed on Subject C it was also possible to reinforce some considerations made previously about the patient's motivation. Indeed, given the young age of Subject C, it was more difficult to make him concentrate and motivate, in particular after the first failures obtained from the thumb abduction and index extension. This suggests that, in particular with young patient, it is important to develop a more attractive system, which would support the patient with games based on the electromyography analysis. An inspiring system could be the Otto Bock MyoBoy software, which has been discussed in Chapter 2.

5.8 Patient's Training

Other conclusion can be drawn from the test phase of this work, in particular it has been noticed how important is the training of the patient in order to exert the right muscles contractions. In fact, when the acquisition phase is concluded and the Artificial Neural Network is trained, the system is able to recognize particular muscle contractions. This means that if the network is trained to recognize the wrist extension, but then the patient, not concentrated or badly trained, contracts also the muscles which extend the fingers, the system will likely recognize an "open hand". Therefore an amputee has to continuously exercise his abilities, even after the first phase in which he learns how to use the prosthesis. This is important in order not to "forget" how to execute the muscle contractions in the right way.
Moreover, an amputee cannot see his own hand when performing a movement, this produces new difficulties also in the acquisition phase: if the trainer says to the patient to close his hand, there is no way that they can see if the contraction has been performed correctly. This means that a new software has to be designed in order to overcome this problem. The main idea would be to train an Artificial Neural Network on data coming from a large amount of people. This would produce a network with low performances if we consider its application to a real prosthesis, but which would still give an idea of the movement performed by the amputee.

Chapter 6

Conclusions and Future Directions

In this work we establish the basis for the design of a our own brand new prosthesis, since the whole prosthetic control relies on the EMG signal analysis. The performances (98.6%) that the system is able to achieve are really promising, considering that it is able to recognize seven motion patterns with the use of just three channels. These seven basic patterns could be fed into a high level controller, able to produce six different complex movements, like *key, power, precision, tripod grips*, plus *platform grasp* and *index point*. In this way the dexterity and the reliability of the hand are improved with respect to previous works on the subject. Moreover we were able to investigate the influence that factors like electrode displacement, fatigue, body structure, concentration, motivation and the training of the patient can influence the whole system.

Of course, for the patient's sake the reliability and the recognition rate of such a product should be of 100%. This goal is reachable just if the patient is well trained, motivated and concentrated. This means that he needs a trainer who helps him to overcome both the psychological and technical issues related to the acquisition phase and to the training phase. Moreover, people are different from each other, therefore, it is important to draw customized approaches for each patient, in order to reach great results.

Learning to use such a system is like learning to drive, at the beginning it is quite difficult, because of the lack of sensibility of the feet when approaching to the pedals. But after some sessions of training, a person becomes able to master the control of his car. The trainer of an amputee is more or less like a driving instructor, who explains to his "student" how to perform certain tasks and corrects him in case of mistake.

This thesis is just the top of the iceberg, since many aspects of the EMG controlled prosthesis still has to be accounted. The future directions are mainly of three types, the first is related to the prosthesis design, the second concerns the patient support, while the third is about the improvement of the current work.

- The prosthesis design:
  - substitute the personal computer with a portable microcontroller;
  - translate the Matlab code into a language which can be run on the portable device;
  - design a model of the hand following the specifications presented in this thesis;
  - model a system able to provide the vibrotactile feedback to the patient (discussed in Chapter 2).
- The support to the patient:
  - design a graphical software, which can support the patient during the acquisition and the training. This tool would be useful to help the trainer and the amputee to understand when a movement has been correctly performed. The abstract specifications of such a tool are described at the end of Chapter 5.
  - design of a graphical software, which could motivate the patient during his training phase. This means that patients, in particular young people, could play with games based on the EMG analysis, in order to improve their muscle ability without getting bored.
- The improvement of the current work:
  - acquire data from as many people as possible, in order to improve the knowledge about the EMG signal and its analysis and make more precise statistic evaluations.

The dream of designing a biomimetic prosthesis, as similar as possible to the real hand is close to being considered utopia. But what engineers and

biologists can do, is to try their best to design a prosthetic hand which can help amputees to come back, at some extent, to their normal life.
This thesis tried to give some hints to achieve this important goal, from the control of the prosthesis to the support of the patient.

Bibliography

[1] Matteo Arvetti. *Studio di segnali mioelettrici per pilotare una protesi robotica per un arto superiore*. PhD thesis, Politecnico di Milano.

[2] www.medterms.com.

[3] L. M. Smurr, K. Gulick, K. Yancosek, and Oren Ganz. A method for measuring and recording joint function. *Journal of Bone & Joint Surgery*, 18:455–465, 1936.

[4] Henry Gray. *Anatomy of the Human Body*. 20 edition, 1918.

[5] Christian Cipriani. *Control Developments for Prosthetic and Cybernetic Hands*. PhD thesis, Scuola Superiore di Studi Universitari e di Perfezionamento Sant'Anna, Pisa, Italy.

[6] anatomy.med.umich.edu (musculoskeletal system).

[7] O. Hauger, C.B. Chung, N. Lektrakul, M.J. Botte, D. Trudell, R.D. Boutin, and D. Resnick. Pulley system in the fingers: Normal anatomy and simulated lesions in cadavers at mr imaging, ct, and us with and without contrast material distention of the tendon sheath. *Radiology*, 217:201–212, 2000.

[8] C.L. Taylor and R.J. Schwarz. The anatomy and mechanics of the human hand. *Orthotics and Prosthetics Library*, 2(2):22–35, 1955.

[9] Bradon J Wilhelmi. Hand anatomy. *Emedicine*, Clinical procedures - Anatomy, 2009.

[10] D. Purves, G.J. Augustine, D. Fitzpatrick, L.C. Katz, AS LaMantia, and S.M. McNamara, J.O.; Williams. *Neuroscience*. 2001.

[11] http://www.in.pi.cnr.it.

[12] A. R. Moller. *Sensory systems: anatomy and physiology*. 16 edition, 2003.

[13] thebrain.mcgill.ca.

[14] Marcello Bracale. Elettromiografia, 2002.

[15] The muscular system skeletal muscle tissue and muscle organization, chapter 9, part iii - http://www.elcamino.edu/.

[16] E. Henneman. The size-principle: a deterministic output emerges from a set of probabilistic connections. *J, exp. Biol*, 115:105–112, 1985.

[17] D. Staudenmann, K. Roeleveld, D.F. Stegeman, and J.H. van Dieen. Methodological aspects of semg recordings for force estimation - a tutorial and review. *Journal of Electromyography and Kinesiology*, 20:375–387, 2010.

[18] L. G. Tassinary, J. T. Cacioppo, and E. J. Vanman. *Handbook of Psychophysiology*. 16 edition, 2007.

[19] D.G. Allen, G.D. Lamb, and H. Westerblad. Skeletal muscle fatigue: Cellular mechanisms. *Physiol Rev*, 88:287–332, 2008.

[20] Maurizio Marchetti and Paolo Pillastrini. *Neurofisiologia del movimento: anatomia, biomeccanica, chinesiologia, clinica*. 1997.

[21] S. G. Millstein, H. Heger, and G. A. Hunter. Prosthetic use in adult upper limb amputees: a comparison of the body powered and electrically powered prostheses. *Prosthetics and Orthotics International*, 10:27–34, 1986.

[22] Ellen J. MacKenzie. Limb amputation and limb deficiency: epidemiology and recent trends in the united states. *Southern Medical Journal*, August(1), 2002.

[23] K. Ziegler-Graham, E.J. MacKenzie, P.L. Ephraim, T.G. Travison, and R. Brookmeyer. Estimating the prevalence of limb loss in the united states: 2005 to 2050. *Arch Phys Med Rehabil*, 89(3):422–9, 2008.

[24] National center for health statistics. Current estimates from the national health interview survey, 1996. *Vital and Health Statistics*, 10(200), 1996.

[25] Ruth M. Morris. Therapeutic influences on the upper-limb amputee. *The Academy Today*, 2008.

[26] J. J. Nicholas, L. R. Robinson, R. Schulz, C. Blair, R. Aliota, and G. Hairston. Problems experienced and perceived by prosthetic patients. *Journal of Prosthetics and Orthotics*, 5(1):16–19, 1993.

[27] Christopher Lake. Effects of prosthetic training on upper-extremity prosthesis use. *Journal of Prosthetics and Orthotics*, 9(1):3–9, 1997.

[28] Brian M Kelly. Upper limb prosthetics. *eMedicine Specialties*, Physical Medicine and Rehabilitation Articles(Prosthetics: http://emedicine.medscape.com/article/317234-overview), 2009.

[29] Scott G. Edwards. Wrist and forearm amputations. *eMedicine Specialties*, Orthopedic Surgery(Hand and Upper Extremity: http://emedicine.medscape.com/article/1245535-overview), 2008.

[30] Douglas G. Smith. Atlas of Amputation and Limb Deficiencies.

[31] B. C. Lawrence, B Radocy, and Marschall P. D. Spectron 12 cable for upper-limb prostheses. *Journal of Prosthetics and Orthotics*, 3(3):130–141, 1991.

[32] L. E. Carlson, B. D. Veatch, and D. D. Frey. Prosthetic use in adult upper limb amputees: a comparison of the body powered and electrically powered prostheses. *Journal of Prosthetics and Orthotics*, 7(3):96–99, 1995.

[33] R. Mazet, C.L. Taylor, and Bechtol C. O. Upper-extremity amputation surgery and prosthetic prescription. *The journal of bone and joint surgery*, 38:1185–1198, 1956.

[34] G. C. Santambrogio, A. Aliverti, G. Andreoni, and C. Gabardi. *Analisi Motoria: Esercizi Svolti e Commentati*. Progetto Leonardo, Bologna, 1996.

[35] J. C. K. Lai, M. P. Schoen, A. Perez Gracia, D. S. Naidu, and S. W. Leung. Prosthetic devices: challenges and implications of robotic implants and biological interfaces. *Proceedings of the Institution of Mechanical Engineers, Part H: Journal of Engineering in Medicine*, 221(2 / 2007):173–183, 2006.

[36] Jingdong Zhao, Zongwu Xie, Li Jiang, Hegao Ca, Hong Liu, and Gerd Hirzinger. Levenberg-marquardt based neural network control for a five-fingered prosthetic hand. *Proc. 2005 IEEE International Conference on Robotics and Automation, Barcelona*, pages 4482–4487, 2005.

[37] Carl D. Brenner. *Prosthetic Principles*. Atlas of Limb Prosthetics: Surgical, Prosthetic, and Rehabilitation Principles.

[38] A. Davalli and R. Sacchetti. Protesi per arto superiore. Technical report, Inail Centro Protesi.

[39] D. J. Atkins, D. C. Y. Heard, and W. H. Donovan. Epidemiologic overview of lndividuals with upper-limb loss and their reported research priorities. *Journal of Prosthetics and Orthotics*, 8(1):2–11, 1996.

[40] Judith Davidson. A survey of the satisfaction of upper limb amputees with their prostheses, their lifestyles, and their abilities. *Journal of Hand Therapy*, 15:62–70, 2002.

[41] C. Cipriani, C. Antfolk, C. Balkenius, B. Rosen, G. Lundborg, M.C. Carrozza, and F. Sebelius. A novel concept for a prosthetic hand with a bidirectional interface: A feasibility study. *IEEE Transactions on Biomedical Engineering*, 56(11), 2009.

[42] Claudio Castellini and Patrick van der Smagt. Surface emg in advanced hand prosthetics. *Biol Cybern*, (100), 2008.

[43] M. C. Carrozza, B. Massa, S. Micera, R. Lazzarini, M. Zecca, and P. Dario. The development of a novel prosthetic handÑongoing research and preliminary results. *IEEE/Asme Transaction on Mechatronics*, 7(2), 2002.

[44] TouchBionics. iLimb. *http://www.touchbionics.com/i-LIMB/*.

[45] J.M. Herrmann, A. Biess, F. Worgotter, and Otto Bock HealthCare GmbH. Control of multi-joint multi-sensor hand prostheses. *Bfnt-Goettingen*.

[46] RSLSteeper. Bebionic pre-launch world premier.

[47] C. Cipriani, F. Zaccone, S. Micera, and M.C. Carrozza. On the shared control of an emg-controlled prosthetic hand: Analysis of user-prosthesis interaction. *IEEE Transactions on Robotics*, 24(1), 2008.

[48] M. Bergamasco and S. Scattareggia Marchese. The machanical design of the marcus prosthetic hand. *Proceedings of IEEE International Workshop on Robot and Human Communication*, pages 95–100, 1995.

[49] D.P.J. Cotton, A. Cranny, P.H. Chappell, and N.M. Whiteand S.P. Beeby. Control strategies for a multiple degree of freedom prosthetic

hand. *The Journal of the Institute of Measurement and Control*, 40:24–27, 2007.

[50] C.M. Light and P.H. Chappell. Development of a lightweight and adaptable multiple-axis hand prosthesis. *Medical Engineering & Physics*, 22:679–684, 2001.

[51] J.L. Pons, E. Rocon, R. Ceres, D. Reynaerts, B. Saro, S. Levin, and W. Van Moorleghem. The manus-hand dextrous robotics upper limb prosthesis: Mechanical and manipulation aspects. *Autonomous Robots*, 16:143–163, 2004.

[52] K.B. Fite, T.J. Withrow, K.W. Wait, and M. Goldfarb. A gas-actuated anthropomorphic transhumeral prosthesis. *IEEE International Conference on Robotics and Automation*, 2007.

[53] S. Schulz, C. Pylatiuk, and G. Bretthauer. A new ultralight anthropomorphic hand. *Proceedings of the 2001 IEEE International Conference on Robotics & Automation*, 2001.

[54] A. Cranny, D.P.J. Cotton, P.H. Chappell, S.P. Beeby, and N.M White. Thick-film force, slip and temperature sensors for a prosthetic hand. *Measurement science and technology*, 16:931–941, 2005.

[55] C.M. Light, P.H. Chappell, B. Hudgins, and K. Engelhart. Intelligent multifunction myoelectric control of hand prostheses. *Journal of Medical Engineering & Technology*, 2002.

[56] P.J. Kyberd and P.H. Chappell. The southampton hand: An intelligent myoelectric prosthesis. *Journal of Rehabilitation Research and Development*, 31(4):326–334, 1994.

[57] P.J. Kyberd, O.E. Holland, P.H. Chappell, S. Smith, R. Tregidgo, P.J Bagwell, and M. Snaith. Marcus: a two degree of freedom hand prosthesis with hierarchical grip control. *IEEE Transactions on Rehabilitation Engineering*, 3(1), 1995.

[58] C. Pylatiuk, S. Mounier, A. Kargov, S. Schulz, and G. Bretthauer. Progress in the development of a multifunctional hand prosthesis. *Proc. IEEE EMBS Int. Conf., San Francisco, CA,*, 2004.

[59] P. J. Kyberd, N. Mustapha, F. Carnegie, and P. H. Chappell. Clinical experience with a hierarchically controlled myoelectric hand prosthesis with vibro-tactile feedback. *Prosthetics and Orthotics International*, 1993.

[60] M. C. Carrozza, G. Cappiello, S. Micera, B. B. Edin, L. Beccai, and C. Cipriani. Design of a cybernetic hand for perception and action. *Biol. Cybern.*, 2006.

[61] A.H. Arieta, H. Yokoi, T. Arai, and W. Yu. Study on the effects of electrical stimulation on the pattern recognition for an emg prosthetic application. *Proceedings of the 27th IEEE annual conference of the Engineering in Medicine and Biology Society*, pages 6919–6912, 2005.

[62] A. Chatterjee, P. Chaubey, J. Martin, and N.V. Thakor. Quantifying prosthesis control improvements using a vibrotactile representation of grip force. *Region 5 Conference, 2008 IEEE*, pages 1–5, 2008.

[63] X. Jia, M. A. Koenig, X. Zhang, J. Zhang, T. Chen, and Z. Chen. Residual motor signal in long-term human severed peripheral nerves and feasibility of neural signal controlled artificial limb. *The Journal of Hand Surgery*, 2007.

[64] G. S. Dhillon and K. W. Horch. Direct neural sensory feedback and control of a prosthetic arm. *IEEE Trans. Neural Syst. Rehabil. Eng.*, 2005.

[65] T.A. Kuiken, L.A. Miller, R.D. Lipschutz, B.A. Lock, K. Stubblefield, P.D. Marasco, P. Zhou, and G.A. Dumanian. Targeted reinnervation for enhanced prosthetic arm function in a woman with a proximal amputation: a case study. *Lancet*, 2007.

[66] Childress D.S. Historical aspects of powered-limb prostheses. *Clin Pros and Orth*, 9(1):2–13, 1985.

[67] P. Parker, J.A. Stuller, and R.N. Scott. Signal processing for the multistate myoelectric channel. *Proceedings of the IEEE*, 1977.

[68] N. Hogan and R.W. Mann. Myoelectric signal processing: Optimal estimation applied to electromyography-part i: Derivation of the optimal myoprocessor. *IEEE Transactions on Biomedical Engineering*, 1980.

[69] D. Graupe and W.K. Cline. Functional separation of emg signals via arma identification methods for prosthesis control purposes. *IEEE Transactions on Systems, Man, and Cybernetics*, 1975.

[70] P. Parker, K. Englehart, and B. Hudgins. Myoelectric signal processing for control of powered limb prostheses. *Journal of Electromyography and Kinesiology*, 2006.

[71] B. Hudgins, P. Parker, and R.N. Scott. A new strategy for. multifunction myoelectric control. *IEEE Transactions on Biomedical Engineering*, 1993.

[72] G.N Saridis and T. Gootee. Emg pattern analysis and classification for a prosthetic arm. *IEEE Transactions on Biomedical Engineering*, 1982.

[73] P.C. Doershuk, D.E. Gustafson, and A.S. Willsky. Upper extremity limb function discrimination using emg signal analysis. *IEEE Transactions on Biomedical Engineering*, 1983.

[74] P.C. Doershuk, D.E. Gustafson, and A.S. Willsky. Upper extremity limb function discrimination using emg signal analysis. *IEEE Transactions on Biomedical Engineering*, 1983.

[75] P.C. Doershuk, D.E. Gustafson, and A.S. Willsky. Upper extremity limb function discrimination using emg signal analysis. *IEEE Transactions on Biomedical Engineering*, 1983.

[76] S. Du and M. Vuskovic. Temporal vs. spectral approach to feature extraction from prehensile emg signals. *Information Reuse and Integration*, 2004.

[77] Xiao wen Zhang, Yu pu Yang, Xiao ming Xu, Tian pei Hu, Zhong hua Gao, Jian Zhang, Tong yi Chen, , and Zhong wei Chen. Clinical detection and movement recognition of neuro signals. *J Zhejiang Univ Sci B.*, 2005.

[78] J. Rafiee, M.A. Rafiee, N. Prause, and M.P. Schoen. Biorobotics: Optimized biosignal classification using mother wavelet matrix. *IEEE 35th Annual Northeast Bioengineering Conference, Harvard-MIT Division of Health Sciences and Technology, Cambridge, MA, USA*, 2009.

[79] Xiaodong Zhang, Weifeng Diao, and Zhiqiang Cheng. *Digital Human Modeling - Wavelet Transform and Singular Value Decomposition of EEG Signal for Pattern Recognition of Complicated Hand Activities.* 2007.

[80] S. Bitzer and Patrick van der Smagt. Learning emg control of a robotic hand: Towards active prostheses. *Proceedings of the 2006 IEEE International Conference on Robotics and Automation*, pages 2819–2823, 2006.

[81] C. Castellini, Patrick van der Smagt, G. Sandini, and G. Hirzinger. A novel emg motion pattern classifier based on wavelet transform and nonlinearity analysis method. *Proceedings of the 2006 IEEE International Conference on Robotics and Biomimetics*, pages 1494–1499, 2006.

[82] Yi-Hung Liu, Han-Pang Huang, and Chang-Hsin Weng. Recognition of electromyographic signals using cascaded kernel learning machine. *IEEE/ASME Transactions on Mechatronics*, 12(3):253–264, 2007.

[83] Jun-Uk Chu, Inhyuk Moon, Yun-Jung Lee, Shin-Ki Kim, and Mu-Seong Mun. A supervised feature-projection-based real-time emg pattern recognition for multifunction myoelectric hand control. *IEEE/ASME Transactions on Mechatronics*, 12(3):282–290, 2007.

[84] G.R. Naik, D.K. Kumar, H. Weghorn, and M. Palaniswami. Subtle hand gesture identification for hci using temporal decorrelation source separation bss of surface emg. *9th Biennial Conference of the Australian Pattern Recognition Society on Digital Image Computing Techniques and Applications*, 2007.

[85] S. Maier and Patrick van der Smagt. Surface emg suffices to classify the motion of each finger independently. *Proceedings of MOVIC 2008, 9th International Conference on Motion and Vibration Control*, 2008.

[86] A. Kiso and H. Seki. Human forearm motion discrimination based on myoelectric signal by fuzzy inference. *IEEE 11th International Conference on Rehabilitation Robotics*, pages 295–299, 2009.

[87] M. Hioki and H. Kawasaki. Estimation of finger joint angles from semg using a recurrent neural network with time-delayed input vectors. *IEEE 11th International Conference on Rehabilitation Robotics*, pages 289–294, 2009.

[88] C. Castellini and Patrick van der Smagt. Surface emg in advanced hand prosthetics. *Biol Cybern*, 2009.

[89] C. Castellini, Patrick van der Smagt, G. Sandini, and G. Hirzinger. Surface emg for force control of mechanical hands. *IEEE International Conference on Robotics and Automation*, pages 725–730, 2008.

[90] COL Geoffrey Ling M.D. Ph.D.: Program Manager. Revolutionizing prosthetics. Technical report, Defense Science Office - http://www.darpa.mil.

[91] R. Weir, M. Mitchell, S. Clark, G. Puchhammer, K. Kelley, M. Haslinger, N. Kumar2, R. Hofbauer, Kuschnigg P., V. Cornelius, M. Eder, and R. Grausenburger. New multifunctional prosthetic arm and hand systems. *Proceedings of the 29th Annual International Conference of the IEEE EMBS*, 2007.

[92] L. M. Smurr, K. Gulick, K. Yancosek, and Oren Ganz. Managing the upper extremity amputee: A protocol for success. *Journal of Hand Therapy*, 21:160–176, 2008.

[93] Mark R. Cutkosky. On grasp choice, grasp models, and the design of hands for manufacturing tasks. *IEEE Transactions On Robotics and Automation*, 5(3):269–279, 1989.

[94] T. Feix, R. Pawlik, H.B. Schmiedmayer, J. Romero, and D. Kragic. The generation of a comprehensive grasp taxonomy. *http://web.student.tuwien.ac.at*, 2008.

[95] http://users.rowan.edu/ polikar/wavelets/wttutorial.html.

[96] http://www.wavelet.org/tutorial/wbasic.htm.

[97] D. Moshou, I. Hostens, G. Papaioannou, and H. Ramon. Wavelets and self-organizing maps in electromyogram (emg) analysis. 2000.

[98] MIT lecture by professor Strang Gilbert: http://ocw.mit.edu/ OcwWeb/Mathematics/18-06Spring-2005/VideoLectures/detail/lecture29.htm.

[99] David Austin. We recommend a singular value decomposition. *American Mathematical Socitey*, 2010.

[100] MathWorks. *Neural Network Toolbox Documentation.*

[101] K. Madsen, H.B. Nielsen, and O. Tingleff. *Methods for non-linear least squares problems.* 2004.

[102] R. Rojas. *Neural Networks.* Springer-Verlag, 1996.

[103] Symon Hayjin. *Neural Networks.* Pearson Education, 2005.

[104] D. Dumitru and D.L. Jewett. Far-field potentials. *Muscle and Nerve*, 16(3):237–254, 2004.

Appendix A

The Implementation of the Project

The following Matlab scripts were included with the use of Florian Knorn's M-code LaTeX Package.

A.1 Data Acquisition

acquireData.m :

```
%% AcquireData
% This function is used to acquire the data from the EMG board.
% It calls an external application written in C, which starts
% the communication with the board and saves the signals into
% different folders.
% This script actually load the data stored into the folders
% created by the C application.
%
% By Giuseppe Lisi for Politecnico di Milano
% beppelisi@gmail.com
% 8 June 2010

%% Inputs
%
% np: is the new folder in which we want to save the acquired
% data. Usually it is the name of the person.
%
% mov: is the name of the movement.
%
% id: is the movement id (for example the ID of the Close Hand
```

```
% is 1)
%
% prog: is the progressive number of a given movement (at the
% first acquisition of a Close Hand the prog is 1, at the
% second acquisition of the Close Hand is 2 and so on )

%% Outputs
%%
function acquireData(np,mov,id,prog)
close all;

%calls the external application serialComm, which creates a new
%folder and store the acquired data inside (txt files).
comm=['./serialComm ' np ' ' mov ' ' sprintf('%d',id) ' ' prog]
[status,result] = unix(comm,'-echo');
c = cell(1, 4);

%the txt files saved by the external application are loaded by
%the script.

file=['/Users/giuseppelisi/University/Thesis/Matlab/'...
    'FilesNewEmg/serial/' np '/ch1/' sprintf('%d',id)...
    '-' prog '-' mov '.txt'];

fid = fopen(file);
c{1,1} = fscanf(fid, '%d', [1 inf])';

fclose(fid);


file=['/Users/giuseppelisi/University/Thesis/Matlab/'...
    'FilesNewEmg/serial/' np '/ch2/' sprintf('%d',id)...
    '-' prog '-' mov '.txt'];

fid = fopen(file);
c{1,2} = fscanf(fid, '%d', [1 inf])';

fclose(fid);


file=['/Users/giuseppelisi/University/Thesis/Matlab/'...
    'FilesNewEmg/serial/' np '/ch3/' sprintf('%d',id)...
    '-' prog '-' mov '.txt'];

fid = fopen(file);
c{1,3} = fscanf(fid, '%d', [1 inf])';

fclose(fid);

```

```
70 c{1,4}=id;
71
72 % useful to see if the signal has been segmented well.
73 f=splitFilter(c,1,1,0,1,np,1,1);
74
75
76 end
```

A.2 Artificial Neural Network Training

training.m :

```
1  %% Training
2  % This function is used to train a network on data contained
3  % inside a folder. This data are the EMG signals acquired
4  % from a single person using three different channels.
5  %
6  % By Giuseppe Lisi for Politecnico di Milano
7  % beppelisi@gmail.com
8  % 8 June 2010
9
10 %% Inputs
11 % debug=1: to pause the segmentation phase and plot the
12 % figures of each segemented signal. Debug mode
13 %
14 % np: (name of the person) is the name of the folder in
15 % which are contained the training data.
16 %
17 % plotting=1: to save the figures of the segmented
18 % signals inside the 'img' folder contained inside the np
19 % folder. 'img' is automatically created.
20 %
21 % ch2=1: if the second channel is used.
22 %
23 % ch3=1: if the third channel is used.
24 %% Outputs
25 %
26 % net: is the trained artificial neural network
27 %
28 % mov: is the vector containing the number of movement
29 % performed during the test phase
30 %
31 % err: is the vector containing the errors during the test
32 % phase
33 %
```

```
34 % perf: is the training performance achived
35 %%
36 function [net,mov,err,perf]=training(debug,np,plotting,ch2,ch3)
37 close all;
38 clc;
39
40 % converts data: txt -> matlab
41 disp('Converting in matlab format')
42 [c movNum]=convertAll(debug,np,plotting);
43
44 % extracts the feature vectors from all the signals contained
45 % in the np folder.
46 f=takeFeatures(c,debug,plotting,np,ch2,ch3);
47
48 if ¬isempty(f{1,1})
49 %trains an artificial neural network
50 [net,mov,err,perf]=myNN(f,movNum);
51 else
52     net=1;
53     mov=1;
54     err=1;
55     perf=1;
56 end
57
58
59 end
```

convertAll.m :

```
1  %% Convert All
2  % This function converts all the txt files into the matlab
3  % format.
4  % Future users have to replace
5  % /Users/giuseppelisi/University/...
6  %   Thesis/Matlab/FilesNewEmg/serial/
7  % with their own favourite folder
8  % Remember that this code is run on a uinix based machine,
9  % therefore it is
10 % important to modify some OS oriented commands.
11 %
12 % By Giuseppe Lisi for Politecnico di Milano
13 % beppelisi@gmail.com
14 % 8 June 2010
15
16 %% Inputs
17 % debug=1: to pause the segmentation phase and plot the figures
```

```
% of each segemented signal. Debug mode
%
% np: is the name of the folder in which are contained the
% training data.
%
% plotting=1: to save the figures of the segmented signals
% inside the 'img' folder contained inside the np folder. 'img'
% is automatically created.
%
%% Outputs
% c: is the cell array containing the converted data.
%%
function [c movNumber]=convertAll(debug,np,plotting)

file=['/Users/giuseppelisi/University/Thesis/'...
    'Matlab/FilesNewEmg/serial/' np '/ch1/*.txt'];
d = dir(file);

fileIndex = find(¬[d.isdir]);
len=length(fileIndex);
c = cell(len, 4);
movNumber=1;
movId=[];
movKey=[];



for i = 1:length(fileIndex)

fileName = d(fileIndex(i)).name;
movement=sscanf(fileName,'%d%*s');
f=['/Users/giuseppelisi/University/Thesis/Matlab/'...
    'FilesNewEmg/serial/' np '/ch1/' fileName];
data=convertFile2MAT(f);
c{i,1}=data;
f=['/Users/giuseppelisi/University/Thesis/Matlab/'...
    'FilesNewEmg/serial/' np '/ch2/' fileName];
data=convertFile2MAT(f);
c{i,2}=data;
f=['/Users/giuseppelisi/University/Thesis/Matlab/'...
    'FilesNewEmg/serial/' np '/ch3/' fileName];
data=convertFile2MAT(f);
c{i,3}=data;

pos=find(movId==movement);
if(isempty(pos))
% here the movement IDs are mapped into a key ID in order to
% make it possible to use data ordered whith different IDs
% inside the folder
```

```
67      movId=[movId movement];
68      movKey=[movKey movNumber];
69      c{i,4}=movNumber;
70      movNumber=movNumber+1;
71  else
72      c{i,4}=movKey(pos);
73  end
74  end
75  movId
76  movKey
77  movNumber=movNumber-1;
78
79  end
```

convertFile2MAT.m :

```
1  %% ConvertFile2Mat
2  % This function converts each single txt file in matlab format
3  %
4  % By Giuseppe Lisi for Politecnico di Milano
5  % beppelisi@gmail.com
6  % 8 June 2010
7  %% Inputs
8  % file: is the file to convert
9  %% Outputs
10 % a: is the converted matlab file
11 %%
12 function a=convertFile2MAT(file)
13
14 fid = fopen(file);
15 a = fscanf(fid, '%d', [1 inf])';
16 fclose(fid);
17
18
19 end
```

takeFeatures.m :

```
1  %% TakeFeatures
2  % This function extracts the feature vectors from all the
3  % signals contained in the np folder.
4  %
```

```
% By Giuseppe Lisi for Politecnico di Milano
% beppelisi@gmail.com
% 8 June 2010

%% Inputs
% c: is the cell array containing all the singals converted in
% matlab format.
%
% debug=1: to pause the segmentation phase and plot the figures
% of each segemented signal. Debug mode
%
% np: (name of the person) is the name of the folder in which
% are contained the training data.
%
% plotting=1: to save the figures of the segmented signals
% inside the 'img' folder contained inside the np folder.
% 'img' is automatically created.
%
% ch2=1: if the second channel is used.
%
% ch3=1: if the third channel is used.
%% Outputs
% feat: is the cell array containing the feature vectors and
% the corresponding target vecors of the signals.
%%
function feat=takeFeatures(c,debug,plotting,np,ch2,ch3)
nsamp=size(c);
nsamp=nsamp(1);
feat = cell(nsamp, 2);

for i=1:nsamp
   % each signal in the cell array is segmented and filtered
   f=splitFilter(c,debug,0,plotting,i,np,ch2,ch3);
   feat{i,1}=f;
   feat{i,2}=c{i,4};
end

end
```

splitFilter.m :

```
%% Split Filter
% This script is used to split the incoming signal and to
% filter it.
%
% By Giuseppe Lisi for Politecnico di Milano
```

```
6  % beppelisi@gmail.com
7  % 8 June 2010
8  %% Inputs
9  % c: is the cell array containing all the signals in matlab
10 % format.
11 %
12 % debug=1: to pause the segmentation phase and plot the figures
13 % of each segemented signal. Debug mode
14 %
15 % acq=1: if the script is used during the acquisition phase
16 %
17 % np: (name of the person) is the name of the folder in which
18 % are contained the training data.
19 %
20 % i: is the index representing the current single signal to
21 % process.
22 %
23 % plotting=1: to save the figures of the segmented signals
24 % inside the 'img'folder contained inside the np folder.
25 % 'img' is automatically created.
26 %
27 % ch2=1: if the second channel is used.
28 %
29 % ch3=1: if the third channel is used.
30 %% Outputs
31 % f: is the cell array containing all the feature vector
32 % related to the signal contained in c at the position i.
33 %%
34 function f=splitFilter(c,debug,acq,plotting,i,np,ch2,ch3)
35
36 c1=c{i,1};
37 c2=c{i,2};
38 c3=c{i,3};
39 nsamp=c{i,4};
40
41 % Rectification
42 y1=abs(c1-512);
43 y2=abs(c2-512);
44 y3=abs(c3-512);
45
46 f=[];
47 f1=[];
48 f2=[];
49 f3=[];
50
51 %Linear envelope
52 if(length(y1)≠1)
53
54     freqCamp=270; %sampling frequency
```

```
55      cutOffFreq=2; %cutoff frequency of the low-pass filter
56      nyquistFreq=cutOffFreq/(freqCamp/2);
57      [b,a]=butter(2,nyquistFreq);
58      %filt is the envelope of the rectified signal
59      filt1=filter(b,a,y1);
60      filt1=filt1(50:length(filt1));
61
62
63      filt2=filter(b,a,y2);
64      filt2=filt2(50:length(filt2));
65
66
67      filt3=filter(b,a,y3);
68      filt3=filt3(50:length(filt3));
69
70
71
72      % find the edges of each burst
73      [firstDiv,secondDiv]...
74          =findBurstEMG(filt1,filt2,filt3,debug,ch2,ch3);
75
76
77      %Filtering above 10 Hz
78      cutoffF1=10;
79      nyquistF=cutoffF1/(freqCamp/2);
80      [num,den] = butter(2,nyquistF,'high');
81      filtS=filter(num,den,c1);
82      filtSign=filtS(50:length(filtS));
83
84      filtS2=filter(num,den,c2);
85      filtSign2=filtS2(50:length(filtS2));
86
87      filtS3=filter(num,den,c3);
88      filtSign3=filtS3(50:length(filtS3));
89
90      % the feature extraction is not performed during the
91      % acquisition phase.
92      if(¬acq)
93
94      for j=1:length(firstDiv)
95          f1(j,:)=...
96            extractFeatures(filtSign(firstDiv(j):secondDiv(j)));
97      end
98
99
100     if ch2
101     for j=1:length(firstDiv)
102         f2(j,:)=...
103           extractFeatures(filtSign2(firstDiv(j):secondDiv(j)));
```

```
104     end
105     end
106
107     if ch3
108     for j=1:length(firstDiv)
109         f3(j,:)=...
110           extractFeatures(filtSign3(firstDiv(j):secondDiv(j)));
111     end
112     end
113
114     if(¬isempty(firstDiv))
115
116     f=[f1 f2 f3];
117     end
118
119     end
120
121     sum1=filt1(1)*100;
122     sum2=filt2(1)*100;
123     sum3=filt3(1)*100;
124     thr1(1)=sum1;
125     thr2(1)=sum2;
126     thr3(1)=sum3;
127      % computing the 'splitting threshold' in order to plot it
128     for i=2:length(filt1)
129         sum1=sum1+filt1(i);
130         thr1(i)=sum1/i;
131         sum2=sum2+filt2(i);
132         thr2(i)=sum2/i;
133         sum3=sum3+filt3(i);
134         thr3(i)=sum3/i;
135     end
136
137
138
139     if debug
140         % Plots the segmentation of the envelope of the first
141         % channel.
142         figure;
143         plot(1:length(filt1),filt1)
144         hold on;
145         plot(1:length(thr1),thr1,'y');
146         axis([1 length(filt1) 0 150]);
147         if(¬isempty(firstDiv))
148         vline(firstDiv,'g','');
149         vline(secondDiv,'r','');
150
151         end
152         % Plots the segmentation of the envelope of the second
```

```
153         % channel.
154         figure;
155         plot(1:length(filt2),filt2)
156         hold on;
157         plot(1:length(thr2),thr2,'y');
158         axis([0 length(filt2) 0 150]);
159         if(¬isempty(firstDiv))
160         vline(firstDiv,'g','');
161         vline(secondDiv,'r','');
162
163         end
164
165         % Plots the segmentation of the envelope of the third
166         % channel.
167         figure;
168         plot(1:length(filt3),filt3)
169         hold on;
170         plot(1:length(thr3),thr3,'y');
171         axis([0 length(filt3) 0 150]);
172         if(¬isempty(firstDiv))
173         vline(firstDiv,'g','');
174         vline(secondDiv,'r','');
175         end
176
177         % Plots the segmented and high-pass filtered signal of
178         % Channel 1.
179         figure;
180         plot(1:length(filtSign),filtSign);
181         axis([1 length(filtSign) -400 400]);
182         if(¬isempty(firstDiv))
183         vline(firstDiv,'g','');
184         vline(secondDiv,'r','');
185         end
186
187         % Plots the segmented and high-pass filtered signal of
188         % Channel 2.
189         if ch2
190         figure;
191         plot(1:length(filtSign2),filtSign2);
192         axis([0 length(filtSign2) -400 400]);
193         if(¬isempty(firstDiv))
194         vline(firstDiv,'g','');
195         vline(secondDiv,'r','');
196         end
197         end
198
199         % Plots the segmented and high-pass filtered signal of
200         % Channel 3.
201         if ch3
```

```
202         figure;
203         plot(1:length(filtSign3),filtSign3);
204         axis([0 length(filtSign3) -400 400]);
205         if(¬isempty(firstDiv))
206         vline(firstDiv,'g','');
207         vline(secondDiv,'r','');
208         end
209         end
210         numberOFMovements=length(firstDiv)
211         if(¬acq)
212         ginput(1);
213         close all;
214         end
215
216
217     end
218
219     % saving the figures of the fitered and segmented signal
220     % into the 'img' folder
221     if plotting
222         file2save=['/Users/giuseppelisi/University/Thesis/'...
223             'Matlab/FilesNewEmg/serial/' np '/ch1/img/image'...
224             sprintf('%d',nsamp) '_' sprintf('%d',i) '.eps'];
225         fig = figure('visible','off');
226         plot(1:length(filtSign),filtSign,'b');
227         axis([0 length(filtSign) -400 400]);
228         if(¬isempty(firstDiv))
229         vline(firstDiv,'g','');
230         vline(secondDiv,'r','');
231         end
232         saveas(fig,file2save,'eps');
233
234         if ch2
235         file2save=['/Users/giuseppelisi/University/Thesis/'...
236             'Matlab/FilesNewEmg/serial/' np '/ch2/img/image'...
237             sprintf('%d',nsamp) '_' sprintf('%d',i) '.eps'];
238         fig = figure('visible','off');
239         plot(1:length(filtSign2),filtSign2,'b');
240         axis([0 length(filtSign2) -400 400]);
241         if(¬isempty(firstDiv))
242         vline(firstDiv,'g','');
243         vline(secondDiv,'r','');
244         end
245         saveas(fig,file2save,'eps');
246         end
247
248
249         if ch3
250         file2save=['/Users/giuseppelisi/University/Thesis/'...
```

```
            'Matlab/FilesNewEmg/serial/' np '/ch3/img/image'...
            sprintf('%d',nsamp) '_' sprintf('%d',i) '.eps'];
        fig = figure('visible','off');
        plot(1:length(filtSign3),filtSign3);
        axis([0 length(filtSign3) -400 400]);
        if(¬isempty(firstDiv))
        vline(firstDiv,'g','');
        vline(secondDiv,'r','');
        end
        saveas(fig,file2save,'eps');
        end
    end



end
end
```

findBurstEMG.m :

```
%% FindBurstEMG
% Function to find the edges of each burst
%
% By Giuseppe Lisi for Politecnico di Milano
% beppelisi@gmail.com
% 8 June 2010
%% Inputs
% signal1: is the liear envelope of the signal coming from
% Channel 1.
%
% signal2: is the liear envelope of the signal coming from
% Channel 2.
%
% signal3: is the liear envelope of the signal coming from
% Channel 3.
%
% debug=1: to pause the segmentation phase and plot the figures
% of each segemented signal. Debug mode
%
% ch2=1: if the second channel is used.
%
% ch3=1: if the third channel is used.
%% Outputs
% secondDivision: vector containing all the ending edges of the
% bursts
%
```

```
27 % firstDivision: vector conaining all the starting edges of the
28 % bursts
29 %%
30 function [firstDivision,secondDivision]=...
31     findBurstEMG(signal1,signal2,signal3,debug,ch2,ch3)
32
33 ls=length(signal1); %length of the signal
34 firstDivision=[];
35 secondDivision=[];
36
37 %54 samples correspond to 0.2 seconds of signal(sampling rate
38 % 270Samp/Sec) normal burst duration corresponding to 1second
39 sampleDur=54*5;
40
41 %normal movement
42 delay=40;
43
44 %short movement
45 %delay=20;
46
47 %the lower level under which it is impossible to start a burst
48 cost=10;
49
50 %factor for which the initial part of the moving average is
51 %computed in order to avoid fake initial bursts
52 mult=30;
53
54
55 %once the burst has been detected its edges have to be shifted
56 %back of this value
57 back=100;
58
59 % contain the value of the next ending edge. Equal to 1 if the
60 % start still have to be found
61 next1=1;
62 next2=1;
63 next3=1;
64
65 %sum for the threshold computation.
66 sum1=signal1(1)*mult;
67 sum2=signal2(1)*mult;
68 sum3=signal3(1)*mult;
69
70 %threshold for the three channels
71 thr1(1)=sum1;
72 thr2(1)=sum2;
73 thr3(1)=sum3;
74
75 % records the highest value found so far in all the three
```

```
% channels
max=0;

%1 if first channel, 2 if second 3 if third
choice=0;

%restart=1 if the system is ready to detect a new burst
restart=0;

% empiric values for the decision to take about the burst
% start.
perc=22/100;
clos=1/20;

% burst edges detection
for i=2:ls

    sum1=sum1+signal1(i);
    thr1(i)=sum1/i;
    sum2=sum2+signal2(i);
    thr2(i)=sum2/i;
    sum3=sum3+signal3(i);
    thr3(i)=sum3/i;

    if(signal1(i)≥thr1(i)+perc*thr1(i) &&...
            next1==1 && i>restart && signal1(i)>cost)
        % prev contains the starting point of the edge.
        prev1=i;
        if(prev1-back>1)
            prev1=prev1-back;
            if(prev1+sampleDur<ls)
                next1=prev1+sampleDur;
            else
                next1=1;
            end
        else
            prev1=1;
            next1=1+sampleDur;
        end
    end

    if(i==next1)
        %if the signal is still high -> delay the closing
        %of the burst
        if(signal1(i)>thr1(i)-clos*thr1(i))
            if(next1+delay<ls)
                next1=next1+delay;
            else
                next1=ls;
```

```
125             end
126         else
127             if(choice==1)
128 
129                 firstDivision=[firstDivision prev1];
130                 secondDivision=[secondDivision next1];
131                 max=0;
132                 choice1=0;
133                 restart=next1+back;
134                 next1=1;
135                 next2=1;
136                 next3=1;
137             end
138         end
139     end
140 
141     if(ch2)
142         if(signal2(i)≥thr2(i)+perc*thr2(i) && next2==1 &&...
143                 i>restart && signal2(i)>cost)
144 
145             prev2=i;
146             if(prev2-back>1)
147                 prev2=prev2-back;
148 
149                 if(prev2+sampleDur<ls)
150                     next2=prev2+sampleDur;
151                 else
152                     next2=1;
153                 end
154             else
155                 prev2=1;
156                 next2=1+sampleDur;
157             end
158         end
159         if(i==next2)
160             %if the signal is still high delay -> the closing
161             %of the burst
162             if(signal2(i)>thr2(i)-clos*thr2(i))
163                 if(next2+delay<ls)
164                     next2=next2+delay;
165                 else
166                     next2=ls;
167                 end
168             else
169 
170                 if(choice==2)
171                     firstDivision=[firstDivision prev2];
172                     secondDivision=[secondDivision next2];
173                     max=0;
```

```
174                     choice2=0;
175                     restart=next2+back;
176                     next1=1;
177                     next2=1;
178                     next3=1;
179                 end
180             end
181         end
182     end
183
184     if(ch3)
185         if(signal3(i)≥thr3(i)+perc*thr3(i) && next3==1 &&...
186                 i>restart && signal3(i)>cost)
187
188             prev3=i;
189
190             if(prev3-back>1)
191                 prev3=prev3-back;
192                 if(prev3+sampleDur<ls)
193                     next3=prev3+sampleDur;
194                 else
195                     next3=1;
196                 end
197             else
198                 prev3=1;
199                 next3=1+sampleDur;
200             end
201         end
202
203         if(i==next3)
204             %if the signal is still high -> delay the
205             %closing of the burst
206             if(signal3(i)>thr3(i)-clos*thr3(i))
207                 if(next3+delay<ls)
208                     next3=next3+delay;
209                 else
210                     next3=ls;
211                 end
212             else
213
214                 if(choice==3)
215                     firstDivision=[firstDivision prev3];
216                     secondDivision=[secondDivision next3];
217                     max=0;
218                     choice3=0;
219                     restart=next3+back;
220                     next1=1;
221                     next2=1;
222                     next3=1;
```

```
223                 end
224             end
225         end
226     end
227
228     if signal1(i)>max && signal1(i)≥thr1(i)+perc*thr1(i)
229         max=signal1(i);
230         choice=1;
231     end
232     if signal2(i)>max && ch2 && signal2(i)≥thr2(i)+...
233             perc*thr2(i)
234         max=signal2(i);
235         choice=2;
236     end
237     if signal3(i)>max && ch3 && signal3(i)≥thr3(i)+...
238             perc*thr3(i)
239         max=signal3(i);
240         choice=3;
241     end
242 end
243
244
245 % if there a burst start has been detected, but not the end,
246 % eliminate the
247 % burst
248 if(¬isempty(firstDivision) && ...
249         length(firstDivision)>length(secondDivision))
250     firstDivision=firstDivision(1:length(secondDivision));
251 end
```

extractFeatures.m :

```
1  %% ExtractFeatures
2  %  this function extract the features from a given burst
3  %
4  %  Features:
5  %   - IEMG (Integral EMG)
6  %   - MAV (Absolute Mean Value)
7  %   - WAVELET COEFFICIENTS + SVD
8  %
9  % By Giuseppe Lisi for Politecnico di Milano
10 % beppelisi@gmail.com
11 % 8 June 2010
12
13 %% Inputs
14 %  data: is the vector representing a burst.
```

```
%% Outputs
% f: is the feature vector.
%%
function f=extractFeatures(data)
iemg=calculateIEMG(data);
mav=calculateMAV(data);
w=myWavelet(data);
f=[iemg mav];
f=cat(2,f,w');

% integral EMG
function iemg=calculateIEMG(data)
iemg=sum(abs(data));

% mean absolute value
function mav=calculateMAV(data)
mav=sum(abs(data))/length(data);

% Wavelet Coefficient + SVD
function w=myWavelet(data)

% computing the wavelet
c = cwt(data,1:5,'morl');

% reducing the dimensionality of the wavelet coefficient matrix
vector=svd(c);

w=vector;
```

myNN.m :

```
%% MyNN
% This function trains and simulates an artificial neural
% network
%
% By Giuseppe Lisi for Politecnico di Milano
% beppelisi@gmail.com
% 8 June 2010

%% Inputs
% feat: is the cell array containing the feature vectors
% and the
% corresponding target vecors of the signals.
%
% movNum: is the number of movement types (7 in this thesis)

```

```
%% Outputs
%
% net: is the trained artificial neural network
%
% movementDone: is the vector containing the number of movement
% performed during the
% test phase
%
% errorOnTheMovementDone: is the vector containing the errors
% during the test phase
%
% performance: is the training performance achived
%%
function ...
    [net,movementsDone,errorOnTheMovementsDone,performance]...
    =myNN(feat,movNum)

% divide the incoming data into Training, Validation and Test
% sets.
[p t vp vt tp tt]=divideData(feat,movNum,3/5,1/5,1/5);

% create the ANN
net=newff(p,t,35);

% modify some network parameters (values found empirically)
v.P=vp;
v.T=vt;
net.trainParam.mu=0.9;
net.trainParam.mu_dec=0.8;
net.trainParam.mu_inc=1.5;
net.trainParam.goal=0.001;

% train the ANN
net = train(net,p,t,{},{},v);

% simulate the network
out = sim(net,tp);


% computing the performances
lout=length(out(1,:));
for i=1:lout
    y(:,i)= ismember(out(:,i),max(out(:,i)));
end

error=zeros(1,movNum);
elements=zeros(1,movNum);
good=0;

```

```
65
66 ltp=length(tp(1,:));
67 for i=1:ltp
68     if(eq(tt(:,i),y(:,i)))
69         good=good+1;
70     else
71         error(logical(tt(:,i)))=error(logical(tt(:,i)))+1;
72     end
73     elements(logical(tt(:,i)))=elements(logical(tt(:,i)))+1;
74 end
75 movementsDone=elements
76 errorOnTheMovementsDone=error
77
78 performance=good/ltp*100
79 end
```

divideData.m :

```
1  %% DivideData
2  % Divides the data in 3 training sets: training, validation
3  % and testing
4  %
5  % By Giuseppe Lisi for Politecnico di Milano
6  % beppelisi@gmail.com
7  % 8 June 2010
8  %% Inputs
9  %
10 %   data: data to divide
11 %
12 %   movNum: numer of the movement types
13 %
14 %   pperf: percentage for the training set
15 %
16 %   vperc: percentage for the validation set
17 %
18 %   tperc: percentage for the test set
19
20 %% Outputs
21 %   p   training set
22 %   t   target of the training set
23 %   vp  validation set
24 %   vt  target for the validation set
25 %   tp  test set
26 %   tt  target of the test set
27
28 %%
```

```
function [p t vp vt tp tt]=...
    divideData(data,movNum,pperc,vperc,tperc)

f=cell(movNum,1);
targ=cell(movNum,1);
nsamp=size(data);
nsamp=nsamp(1);
base=zeros(1,movNum);

p=[];
t=[];
vp=[];
vt=[];
tp=[];
tt=[];


for i=1:nsamp

    f{data{i,2}}=[f{data{i,2}} data{i,1}'];
    nmov=size(data{i,1});
    nmov=nmov(1);
    for j=1:nmov
        base(data{i,2})=1;
        targ{data{i,2}}=[targ{data{i,2}} base'];
        base(data{i,2})=0;
    end

end

for i=1:movNum
    train=f{i};
    target=targ{i};
    sz=size(train);
    len=sz(2);
    per=randperm(len);
    traintemp=train(:,per);
    targettemp=target(:,per);
    trlen=floor(len*pperc);
    vallen=floor(len*vperc);
    testlen=floor(len*tperc);
    trlen=trlen+len-(trlen+vallen+testlen);

    trainingrange=1:trlen;
    validationrange=trlen+1:trlen+vallen;
    testrange=trlen+vallen+1:trlen+vallen+testlen;

    p=[p traintemp(:,trainingrange)];
    t=[t targettemp(:,trainingrange)];
```

```
78      vp=[vp traintemp(:,validationrange)];
79      vt=[vt targettemp(:,validationrange)];
80      tp=[tp traintemp(:,testrange)];
81      tt=[tt targettemp(:,testrange)];
82  end
83
84  end
```

A.3 Motion Recognition

recognize.m :

```
1  %% Recognize
2  % this script recognizes new movements, acquired at the moment.
3  % It uses a trained ANN
4  %
5  % By Giuseppe Lisi for Politecnico di Milano
6  % beppelisi@gmail.com
7  % 8 June 2010
8
9  %% Inputs
10 % net: is the trained ANN used for the recognition
11 %
12 % mov: is the number of movement types on which the ANN has
13 % been trained.
14
15 %% Outputs
16 %%
17 function recognize(net,ch2,ch3,mov)
18
19 close all;
20 comm=['./serialComm recognize 1 1 1']
21 [status,result] = unix(comm,'-echo');
22 c = cell(1, 4);
23
24 file=['/Users/giuseppelisi/University/Thesis/Matlab/'...
25     'FilesNewEmg/serial/recognize/ch1/1-1-1.txt'];
26
27 fid = fopen(file);
28 c{1,1} = fscanf(fid, '%d', [1 inf])';
29
30 fclose(fid);
31
32
33 file=['/Users/giuseppelisi/University/Thesis/Matlab/'...
```

```
34      'FilesNewEmg/serial/recognize/ch2/1-1-1.txt'];
35
36  fid = fopen(file);
37  c{1,2} = fscanf(fid, '%d', [1 inf])';
38
39  fclose(fid);
40
41
42  file=['/Users/giuseppelisi/University/Thesis/Matlab/'...
43      'FilesNewEmg/serial/recognize/ch3/1-1-1.txt'];
44
45  fid = fopen(file);
46  c{1,3} = fscanf(fid, '%d', [1 inf])';
47
48  fclose(fid);
49
50  c{1,4}=0;
51
52  % extract the feature vectors from the burst contained in the
53  % single signal
54  f=splitFilter(c,1,0,0,1,'recognize',ch2,ch3)'
55
56  % uses the ANN to reognize the movement performed.
57  if(¬isempty(f))
58      out = sim(net,f);
59
60
61  % performance evaluation, depending on the number of movements
62  % on which the ANN is trained
63      lout=length(out(1,:));
64      if mov==7
65        for i=1:lout
66          y= ismember(out(:,i),max(out(:,i)))'
67          if(eq(y,[1 0 0 0 0 0 0]))
68           [status,result] = unix('say close hand','-echo');
69          elseif (eq(y,[0 1 0 0 0 0 0]))
70           [status,result] = unix('say open hand','-echo');
71          elseif (eq(y,[0 0 1 0 0 0 0]))
72           [status,result] = unix('say wrist extension','-echo');
73          elseif (eq(y,[0 0 0 1 0 0 0]))
74           [status,result] = unix('say wrist flexion','-echo');
75          elseif (eq(y,[0 0 0 0 1 0 0]))
76           [status,result] = unix('say thumb abduction','-echo');
77          elseif (eq(y,[0 0 0 0 0 1 0]))
78          [status,result] = unix('say thumb opposition','-echo');
79          elseif (eq(y,[0 0 0 0 0 0 1]))
80           [status,result] = unix('say index extension','-echo');
81          end
82        end
```

```
83      end
84
85
86      if mov==6
87        for i=1:lout
88          y= ismember(out(:,i),max(out(:,i)))'
89          if(eq(y,[1 0 0 0 0 0]))
90           [status,result] = unix('say close hand','-echo');
91          elseif (eq(y,[0 1 0 0 0 0]))
92           [status,result] = unix('say open hand','-echo');
93          elseif (eq(y,[0 0 1 0 0 0]))
94           [status,result] = unix('say wrist extension','-echo');
95          elseif (eq(y,[0 0 0 1 0 0]))
96           [status,result] = unix('say wrist flexion','-echo');
97          elseif (eq(y,[0 0 0 0 1 0]))
98           [status,result] = unix('say thumb abduction','-echo');
99          elseif (eq(y,[0 0 0 0 0 1]))
100         [status,result] = unix('say thumb opposition','-echo');
101         end
102       end
103     end
104
105     if mov==5
106       for i=1:lout
107         y= ismember(out(:,i),max(out(:,i)))'
108         if(eq(y,[1 0 0 0 0]))
109          [status,result] = unix('say close hand','-echo');
110         elseif (eq(y,[0 1 0 0 0]))
111          [status,result] = unix('say open hand','-echo');
112         elseif (eq(y,[0 0 1 0 0]))
113          [status,result] = unix('say wrist extension','-echo');
114         elseif (eq(y,[0 0 0 1 0]))
115          [status,result] = unix('say wrist flexion','-echo');
116         elseif (eq(y,[0 0 0 0 1]))
117          [status,result] = unix('say thumb abduction','-echo');
118         end
119       end
120     end
121
122     if mov==4
123       for i=1:lout
124         y= ismember(out(:,i),max(out(:,i)))'
125         if(eq(y,[1 0 0 0]))
126          [status,result] = unix('say close hand','-echo');
127         elseif (eq(y,[0 1 0 0]))
128          [status,result] = unix('say open hand','-echo');
129         elseif (eq(y,[0 0 1 0]))
130          [status,result] = unix('say wrist extension','-echo');
131         elseif (eq(y,[0 0 0 1]))
```

```
132           [status,result] = unix('say wrist flexion','-echo');
133         end
134       end
135     end
136
137     if mov==3
138       for i=1:lout
139         y= ismember(out(:,i),max(out(:,i)))'
140         if(eq(y,[1 0 0]))
141           [status,result] = unix('say close hand','-echo');
142         elseif (eq(y,[0 1 0]))
143           [status,result] = unix('say open hand','-echo');
144         elseif (eq(y,[0 0 1]))
145           [status,result] = unix('say wrist extension','-echo');
146
147         end
148       end
149     end
150
151     if mov==2
152       for i=1:lout
153         y= ismember(out(:,i),max(out(:,i)))'
154         if(eq(y,[1 0]))
155           [status,result] = unix('say close hand','-echo');
156         elseif (eq(y,[0 1]))
157           [status,result] = unix('say open hand','-echo');
158         end
159       end
160     end
161
162 end
163 end
```

A.4 Test

testNet.m :

```
1 %% TestNet
2 % this function runs many times the training of different ANN,
3 % on different commutations of the training data. This is done
4 % in order to understand the average performances of the
5 % network.
6 %
7 % By Giuseppe Lisi for Politecnico di Milano
8 % beppelisi@gmail.com
```

```
% 8 June 2010

%% Inputs
%
% debug=1: to pause the segmentation phase and plot the figures
% of each segemented signal. Debug mode
%
% np: (name of the person) is the name of the folder in which
% are contained the training data.
%
% movNum: is the number of movement types on which the ANN is
% going to betrained
%
% ch2=1: if the second channel is used.
%
% ch3=1: if the third channel is used.
%
% rep: number of training repetitions.

%% Outputs
%%
function testNet(debug,np,movNum,ch2,ch3,rep)
%rep number of repetition
movSum=zeros(1,movNum);
errSum=zeros(1,movNum);
perform=0;


for i=1:rep

    [net,mov,err,perf]=training(debug,np,0,ch2,ch3);
    movSum=movSum+mov;
    errSum=errSum+err;
    perform=perform+perf;

end

movSum
errSum
stat=perform/rep
end
```

testWholeSet.m :

```
%% TestWholeSet
% This function is used to test a trained ANN on a whole data
```

```
3  %set, contained in the folder np.
4  %
5  % By Giuseppe Lisi for Politecnico di Milano
6  % beppelisi@gmail.com
7  % 8 June 2010
8  %% Inputs
9  %
10 % debug=1: to pause the segmentation phase and plot the figures
11 % of each segemented signal. Debug mode
12 %
13 % np: (name of the person) is the name of the folder in which
14 % are contained the training data.
15 %
16 % plotting=1: to save the figures of the segmented signals
17 % inside the 'img' folder contained inside the np folder. 'img'
18 % is automatically created.
19 %
20 % ch2=1: if the second channel is used.
21 %
22 % ch3=1: if the third channel is used.
23 %
24 % net: is the trained ANN tested with the data contained in np.
25 %% Outputs
26 %
27 % mov: is the vector containing the number of movement
28 % performed during the test phase
29 %
30 % err: is the vector containing the errors during the test
31 % phase
32 %
33 % perf: is the training performance achived
34 %%
35 function [mov,err,perf]=...
36     testWholeSet(debug,np,plotting,ch2,ch3,net)
37 close all;
38 clc;
39
40 % Converts data: txt -> matlab
41 disp('Converting in matlab format')
42 [c mov]=convertAll(debug,np,plotting);
43
44 % finds the size of the output vector
45 movNum=net.outputs{2}.processedSize;
46
47 % extract feature vectors from data contained in the np folder
48 f=takeFeatures(c,debug,plotting,np,ch2,ch3);
49
50 % uses the trained ANN
51 if ¬isempty(f{1,1})
```

```
52      [mov,err,perf]=useNN(f,movNum,net);
53  else
54      net=1;
55      mov=1;
56      err=1;
57      perf=1;
58  end
59
60  end
```

useNN.m :

```
1   %% UseNN
2   % this fucntion only uses an already trained ANN, and computes
3   % the performances.
4   % The difference with myNN is that useNN doens't train the ANN.
5   %
6   % By Giuseppe Lisi for Politecnico di Milano
7   % beppelisi@gmail.com
8   % 8 June 2010
9
10  %% Inputs
11  %
12  % feat: is the cell array containing the feature vectors and
13  % the corresponding target vecors of the signals.
14  %
15  % movNum: is the number of movement types on which the ANN is
16  % going to be trained.
17  %
18  % net: is the trained ANN tested with the data contained in
19  % feat.
20  %% Outputs
21  %
22  % movementDone: is the vector containing the number of movement
23  % performed during the test phase
24  %
25  % errorOnTheMovementDone: is the vector containing the errors
26  % during the test phase
27  %
28  % performance: is the training performance achived
29  %%
30  function [movementsDone,errorOnTheMovementsDone,performance]...
31      =useNN(feat,movNum,net)
32
33  [p t vp vt tp tt]=divideData(feat,movNum,0,0,1);
34
```

```
out = sim(net,tp);

lout=length(out(1,:));

for i=1:lout
    y(:,i)= ismember(out(:,i),max(out(:,i)));
end

error=zeros(1,movNum);
elements=zeros(1,movNum);
good=0;


ltp=length(tp(1,:));
for i=1:ltp
    if(eq(tt(:,i),y(:,i)))
        good=good+1;
    else
        error(logical(tt(:,i)))=error(logical(tt(:,i)))+1;
    end
    elements(logical(tt(:,i)))=elements(logical(tt(:,i)))+1;
end
movementsDone=elements
errorOnTheMovementsDone=error

performance=good/ltp*100
end
```

A.5 Serial Communication with the EMG Board

```
/*
% By Giuseppe Lisi for Politecnico di Milano
% beppelisi@gmail.com
% 8 June 2010
*/

#include <sys/time.h>
#include <sys/types.h>
#include <stdio.h>   /* Standard input/output definitions */
#include <string.h>  /* String function definitions */
#include <unistd.h>  /* UNIX standard function definitions */
#include <fcntl.h>   /* File control definitions */
#include <errno.h>   /* Error number definitions */
#include <termios.h> /* POSIX terminal control definitions*/
#include <stdlib.h>
```

```
16 #include <string.h>
17 #include <sys/types.h>
18 #include <sys/dir.h>
19
20 int open_input_source(char *);
21
22 void handle_input_from_source(int,FILE*,FILE*,FILE*,
23         FILE*,int*,int*,int*,char*);
24
25 void handle_input_from_source2(int,int,FILE*,FILE*,FILE*,
26         FILE*);
27
28 int MAX(int, int);
29
30 main(int argc, char* argv[]){
31
32     if (argc == 5) {
33
34         /*
35          fd1: input source 1 is for the standard input
36          fd2: input source 2 is for the EMG channel input
37          */
38         int    fd1, fd2;
39
40         /*destination files*/
41         FILE *df,*df1,*df2,*df3;
42
43          /* file descriptor set */
44         fd_set readfs;
45
46         /* maximum file desciptor used */
47         int    maxfd;
48
49          /* loop while TRUE */
50         int    loop=1;
51
52         int    res;
53         struct timeval Timeout;
54
55         /*line started*/
56         int ls=0;
57
58         int current=0;
59         char line[800];
60         int flagStart=0;
61         char * file;
62         int result_code;
63
64
```

```
65          chdir("serial");
66
67          mode_t process_mask = umask(0);
68
69          result_code = mkdir(argv[1], S_IRWXU | S_IRWXG |
70                  S_IRWXO);
71
72          chdir(argv[1]);
73          umask(process_mask);
74
75          file = malloc(sizeof(char) *
76                  ((strlen(argv[2])+strlen(argv[4])) + 6));
77
78          strcpy(file,argv[3]);
79          strcat(file,"-");
80          strcat(file,argv[4]);
81          strcat(file,"-");
82          strcat(file,argv[2]);
83          strcat(file,".txt");
84
85          /*
86           Creates the directories ch1, ch2 and ch3 with the
87           relative img folders
88           */
89
90          result_code =
91                  mkdir("ch1", S_IRWXU | S_IRWXG | S_IRWXO);
92
93          chdir("ch1");
94
95          result_code =
96                  mkdir("img", S_IRWXU | S_IRWXG | S_IRWXO);
97
98          umask(process_mask);
99          df1 = fopen(file, "w");
100
101         if(df1==NULL) {
102             printf
103     ("Error: can't create file for writing first channel.\n");
104             exit(0);
105         }
106
107         chdir("..");
108
109         result_code =
110                 mkdir("ch2", S_IRWXU | S_IRWXG | S_IRWXO);
111
112         chdir("ch2");
113
```

```
114         result_code =
115                 mkdir("img", S_IRWXU | S_IRWXG | S_IRWXO);
116 
117         umask(process_mask);
118         df2 = fopen(file, "w");
119 
120         if(df2==NULL) {
121             printf
122     ("Error: can't create file for writing second channel.\n");
123             exit(0);
124         }
125 
126         chdir("..");
127 
128         result_code =
129                 mkdir("ch3", S_IRWXU | S_IRWXG | S_IRWXO);
130 
131         chdir("ch3");
132 
133         result_code =
134                 mkdir("img", S_IRWXU | S_IRWXG | S_IRWXO);
135 
136         umask(process_mask);
137         df3 = fopen(file, "w");
138 
139         if(df3==NULL) {
140             printf
141     ("Error: can't create file for writing third channe.\n");
142             exit(0);
143         }
144 
145         /* SERIAL */
146         fd1 = open_input_source("/dev/tty.usbserial-A2003H2n");
147         if (fd1<0) exit(0);
148         fcntl(fd1, F_SETFL, 0);
149         struct termios options;
150 
151         /*
152          * Get the current options for the port
153          */
154 
155         tcgetattr(fd1, &options);
156 
157         /*
158          * Set the baud rates
159          */
160 
161         cfsetispeed(&options, B57600);
162         cfsetospeed(&options, B57600);
```

```
163
164         /*
165          * Enable the receiver and set local mode
166          */
167
168         options.c_cflag |= (CLOCAL | CREAD);
169
170         /*
171          * Set the new options for the port
172          */
173
174         tcsetattr(fd1, TCSANOW, &options);
175
176         /* STANDARD INPUT */
177         fd2 =0;
178         if (fd2<0) exit(0);
179
180         /* maximum bit entry (fd) to test */
181         maxfd = max (fd1, fd2)+1;
182
183
184         /* loop for input */
185         while (loop) {
186
187             // set timeout value within input loop
188             Timeout.tv_usec = 0;  // milliseconds
189             Timeout.tv_sec  = 3;  // seconds
190
191              /* set testing for source 1 */
192             FD_SET(fd1, &readfs);
193
194             /* set testing for source 2 */
195             FD_SET(fd2, &readfs);
196
197             /* block until input becomes available */
198             res = select(maxfd, &readfs, NULL, NULL, &Timeout);
199
200             //number of file descriptors with input = 0,
201             //timeout occurred.
202             if (res == 0) {
203                 printf("Timeout occured\n");
204                 exit(1);
205             }
206             /* input from source 1 available */
207             if (FD_ISSET(fd1, &readfs))
208              handle_input_from_source
209              (fd1,df,df1,df2,df3,&flagStart,&ls,&current,line);
210
211             /* input from source 2 available */
```

```
212             if (FD_ISSET(fd2, &readfs))
213              handle_input_from_source2(fd1,fd2,df,df1,df2,df3);
214         }
215     }
216
217     else{
218         printf("Provide in order:\n");
219         printf("1) the name of the person \n");
220         printf("2) the movement done \n");
221         printf("3) the wanted movement identificator(int)\n");
222         printf("4) the progressive number of the movement\n");
223
224     }
225 }
226
227 /*
228  */
229 int open_input_source(char * port)
230 {
231     int fd = 0;
232
233     /* open the device to be non-blocking (read will
234     return immediatly) */
235     fd = open(port, O_RDWR | O_NOCTTY | O_NONBLOCK);
236     if (fd <0) {
237         perror(port);
238         return -1;
239     }
240     else
241         return fd;
242 }
243
244 void handle_input_from_source(int fd,FILE *df,FILE *df1,
245     FILE *df2,FILE *df3,int *flagStart,int *ls,int *current,
246         char *line)
247 {
248     int res = 0, i;
249     char buf[255];
250     char ret='\r';
251     int d1,d2,d3;
252     res = read(fd,buf,255);
253     buf[res]=0;
254
255     /*Parsing of the data coming from the EMG board*/
256
257     for (i = 0; i < res; i++){
258
259         if(*flagStart==0 && buf[i]=='I'){
260             *flagStart=1;
```

```
261         }
262
263         if(*flagStart==1){
264             if(buf[i]=='D' && *ls==0){
265                 *ls=1;
266                 *current=0;
267
268             }
269             else if(*ls==1){
270                 line[*current]=buf[i];
271                 *current=*current+1;
272             }
273             if(buf[i]=='\r' && *ls==1){
274                 *ls=0;
275                 *current=0;
276
277                 sscanf(line,":%d %d %d",&d1,&d2,&d3);
278                 printf("%d %d %d\n",d1,d2,d3);
279
280
281                 fprintf(df1,"%d\r",d1);
282                 fprintf(df2,"%d\r",d2);
283                 fprintf(df3,"%d\r",d3);
284             }
285         }
286     }
287 }
288
289 void handle_input_from_source2
290     (int fd1,int fd2, FILE *df,FILE *df1,FILE *df2,FILE *df3)
291 {
292     fclose(df1);
293     fclose(df2);
294     fclose(df3);
295     close(fd1);
296     close(fd2);
297     exit(0);
298 }
299
300 int max(int i1, int i2)
301 {
302     if (i1 > i2)
303         return i1;
304     else
305         return i2;
306 }
```